Mathematics and Natural Sciences
Research and Theory

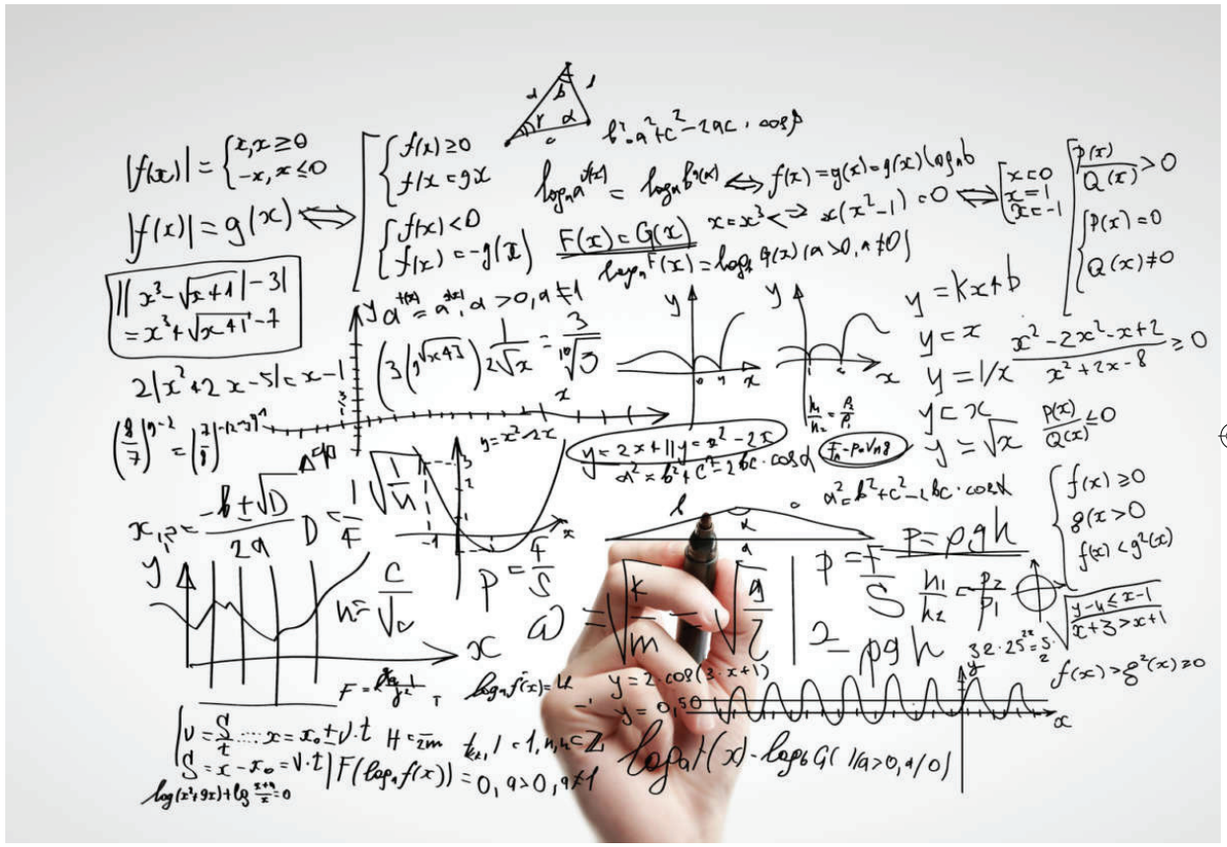

Editor
Prof. Dr. Rıdvan Karapınar

Natural Sciences

LIVRE DE LYON

Lyon 2021

ISBN: 978-2-38236-235-8

9 782382 362358

LIVRE DE LYON

livredelyon.com
livredelyon
livredelyon
livredelyon

MATHEMATICS AND NATURAL SCIENCES

Research and Theory

Editor

Prof. Dr. Rıdvan Karapınar

LIVRE DE LYON
Lyon 2021

Mathematics and Natural Sciences: Research and Theory

Editor •. Prof. Dr. Rıdvan Karapınar • Orcid: 0000-0002-4694-6876

Cover Design • Clarica Consulting

Book Layout • Mirajul Kayal

First Published • December 2021, Lyon

ISBN: 978-2-38236-235-8

Publisher • Livre de Lyon

Address • 37 rue marietton, 69009, Lyon France

website • http://www.livredelyon.com

e-mail • livredelyon@gmail.com

CONTENTS

Preface ***v***

CHAPTER 1 ***1***

FUMONISIN MYCOTOXINS: METABOLISM, TOXICITY, DETECTION AND PREVENTION / Fatma Aydinoglu

CHAPTER 2 ***21***

FIRST RECORD OF THE TWO SNAKES MICROBIOTA FROM ÇANAKKALE (TURKEY) / Nurcihan Hacıoğlu Doğru & Çiğdem Gül & Murat Tosunoğlu

CHAPTER 3 ***33***

DETERMINATION OF SOME NUTRIENT CONCENTRATIONS AND ANTIOXIDANT ENZYME ACTIVITIES OF NATURALLY GROWN SPINACH (Spinacia oleracea L.) PLANT IN FIELD CONDITIONS / Handan Sarac & Hasan Durukan & Ahmet Demirbas

CHAPTER 4 ***43***

OPTICAL PROPERTIES OF PDLC FILMS / Rıdvan KARAPINAR

CHAPTER 5 ***57***

THE EFFECT OF MOBILE PHASE pH ON CAPACITY FACTOR AND SELECTIVITY IN HIGH PERFORMANCE LIQUID CHROMATOGRAPHY / Murat Soyseven & Burcu Sezgin

CHAPTER 6 ***65***

DETERMINATION OF SUCRALOSE IN BEVERAGES BY HPLC-ELSD METHOD / Murat Soyseven & Burcu Sezgin

CHAPTER 7 ***77***

SYNTHESIS AND SPECTRAL CHARACTERIZATION OF THE BENZYLIDENEAMINO-PYRIMIDIN-2(1H)-ONE/-THIONE DERIVATIVES / Zülbiye Kökbudak & Halime Güzin Aslan

CHAPTER 8 ***85***

THE RELATIONSHIP BETWEEN GEOMETRIC DISTRIBUTION, MOMENT GENERATING FUNCTION AND PASCAL TRIANGLE APPROACH / Ege Kor & Sıddık Keskin

PREFACE

Research in mathematics and natural sciences covers various fields and forms the foundations of engineering. This book provides a concise, informative and current overview of some topics in the field of mathematics and natural sciences. In particular, the link between theory, research and practice is well developed in the individual chapters. In this book, the authors share their results with the scientific community. The selected articles have been reviewed and approved for publication by referees. It is hoped that this book will be of interest to academics and researchers in the fields of mathematics and natural sciences.

Editor

CHAPTER 1

FUMONISIN MYCOTOXINS: METABOLISM, TOXICITY, DETECTION AND PREVENTION

Fatma Aydinoglu

(Assoc. Prof. Dr.) Gebze Technical University, faydinoglu@gmail.com

Orcid: 0000-0002-9974-045X

1. Introduction

Fumonisins mycotoxins are a number of structurally related naturally occurring secondary metabolites which are produced by a wide variety of species of Fusarium fungi. They mainly are found in maize and maize-used products. In addition, their occurrence was also reported in wheat, rice, wine, black tea, nuts, and other food commodities (Martins et al., 2001; Marin et al., 2007; Zimmer et al., 2008; Logrieco et al., 2010; Zheng et al., 2020). Because the recent evidence has pointed out their adverse effects on animals and livestock health, leading to cancer and birth defects, there are growing concerns about the contamination of fumonisins of foods and feeds. Humans are under threat directly or indirectly due to the consumption of contaminated food. Therefore, it is crucial to develop management strategies employing reduced environmental risk against this pathogenic fungus to decrease fumonisin contamination. In this context, to avoid hazards of fumonisins, it must be recognized by humans and governmental authorities and need to make regulations keeping fumonisins in food with acceptable limits to protect the consumer. To this end, simple and accurate fumonisins detection methods must be improved in parallel to unraveling its metabolic pathway to facilitate manipulation of toxin production for safer plants (Visentin et al., 2012).

Fumonisin mycotoxins were first recognized in 1988 in a village of the Transkei region in South African, where esophageal cancer was the high incidence (Marasas et al., 1988a). The investigation revealed that the disease outbreak coincided with the consumption of beer brewed from moldy maize and sorghum contaminated by *Fusarium verticillioides*. The mycotoxins were initially isolated from maize cultures of *F. verticillioides* (formerly *F. moniliforme*) and named fumonisins (Gelderblom, 1988). Afterward, fumonisins have been characterized from other Fusarium species, such as *F. proliferatum, F. fujikuroi F. nygami* and *F. oxysporum* and *Alternaria alternata f. sp. Lycopersici, and Aspergillus niger* (Bezuidenhout et al., 1988; Musser et al., 1997; Sewram et al., 2005; Frisvad et al., 2007; Li et al., 2017). Among those species, *F. verticillioides* is the main producer of fumonisins due to its being the most common pathogen of maize plants. Besides producing fumonisins, it also causes

seedling blight, stalk, and ear rot disease which leads to growth inhibition even death of the plants. This pathogenic fungus leaves its spores on kernels which makes its maintenance over several generations. It also stores its mycotoxins in the kernel which is the main cause of contaminated food and feed (Munkvold, 2003). There are several studies that investigate the role of fumonisins in the pathogenicity process, but it was not clearly identified because of different and multiple modes of *F. verticillioides* infection depending on both fungus and plant growth and developmental stages. For example, experimental evidence has shown that fumonisins are not necessary or sufficient for the development of ear rot in maize (Desjardins et al., 2002). On the contrary, seedling blight symptoms are coincided with fumonisin production and decreased root weight, shortening, and exhibiting leaf abnormalities and leaf lesions (Glenn et al., 2008). Also, it was also detected that there is a correlation between the amount of fumonisin B1 in the root of maize seedling which was infected with *F. verticillioides* strains, and the formation of leaf lesions (Williams et al., 2007).

1.1. Metabolism of fumonisin mycotoxins and disruption of sphingolipid biosynthesis pathway by fumonisins

Fumonisin mycotoxins are natural metabolites that are produced by fungi primarily belonging to the Fusarium genus within the Nectriaceae family. These fungi locate around the rhizospheres and move into plants to live as saprophytes (Burgess et al., 1981). *F. verticillioides* is the most common pathogen of maize (*Zea mays*) as being the major fumonisin-producing fungus, predominantly produced at the pre-harvesting stage of plants (Kamle et al., 2019). Although fumonisins are not essential for fungal growth, they gain extra advantages to the fungus such as inhibiting the growth of their competitors and regulating the ecology around fungi (Calvo et al., 2002). They are compounds with low molecular weight (lower than 1000 Daltons) and have hydrophilic nature facilitating their dissolution in organic solvents (Alshannaq & Yu, 2017). These mycotoxins are thermally stable and corrosion resistant, making them difficult to eliminate during food and feed processing (Hartinger & Moll, 2011).

Fumonisin mycotoxins are the highly reduced form of polyketide derivatives with a carboxyl group at the terminal site, consisting of propane-1,2,3-tricarboxylic acid (TCA) which is included in ester formation together with the C14 and C15 hydroxyl groups (Voss et al., 2007). Recently, 28 different types of fumonisins are characterized, but the total number of them is not able to be completely determined yet. They are grouped into A-series (FAs), B-series (FBs), C-series (FCs), and P-series (FPs).

The fumonisin B-series (FBs), also named FB1, FB2 and FB3, include the most prevalent species and the major forms found in food and feed (Bartok et al., 2010). FB1 is the most abundant and toxic among fumonisins which are found in contaminated products with 70–80% occurrence. FB1 is founded as a diester of propane-1,2,3-tricarboxylic acid (TCA) and 2-amino-12,16-dimethyl-3,5,10,14,15-pentahydroxyeicosane, where the C14 and C15 have hydroxyl and carboxyl groups in TCA to form an ester (Soriano et al., 2005). FB2 is similar to FB1, but differs as being a C10-deoxy analog of FB1. FB3 is a C5-deoxy analogue of FB1. In addition to these, FB4 and FB6 were identified in *Aspergillus niger* (Mogensen et al., 2010). FB6

is an isomer of FB1, including different hydroxyl group attachments at C3, C4, and C5, unlike FB1 having the attached hydroxyl groups at C3, C5, and C10 positions.

The fumonisin A-series (FAs, *N*-acetyl analogs) have a similar structure as B-series but differ with possessing an acetylated C2 amino group. FAs are less known and relatively harmless compared to FBs. The fumonisin C-series (FCs, demethyl analogs), and the fumonisin P-series (FPs, *N*-3-hydroxypiridinium analogs) have been identified in the Fusarium culture. Compared to FBs and FCs possessing the free amino group at the C2 site, FPs have a 3-hydroxypyridinium moiety. FCs are yielded a C19 backbone by a condensation reaction of an acyl chain with glycine instead of alanine in FAs, FBs and FPs. It was reported that FCs and FPs displayed phytotoxic and cytotoxic effects in plants and cells (Abbas et al., 1998).

Because it is the most abundant and most toxic, the biosynthesis pathway of FB1 is the most studied among the others. According to pathway, FB1 synthesis initiates with a condensation reaction of nine acetates and two methyl units yielding a linear, 18-carbon-long polyketide (Huffman et al., 2010). This reaction is followed by a second condensation reaction of the alanine and linear polyketide, hydroxylation of the polyketide-alanine condensation product, C3 carbonyl reduction, C10 hydroxylation, C14/C15 esterification, and C5 hydroxylation. It was identified at least 17 genes functioning in this biosynthesis pathway which are designated as FUM genes which form a clustered constituting a 75-kb length of *F. verticillioides* DNA (Proctor et al., 2008).

FUM1, FUM8, and *FUM21* are the main players in the fumonisin biosynthesis pathway. *FUM1* encoding a polyketide synthase (PKS) operates the 18-carbon chain of FB backbone synthesis by using eight molecules of malonyl-CoA, two molecules of S-adenosyl methionine (SAM), and one molecule of acetyl-CoA (Huffman et al., 2010) (Figure 1). *FUM8* encodes class II α-aminotransferases homologous enzyme which condensates amino acids and acyl-CoA thioester releasing carbon dioxide. *FUM21* was predicted to encode a transcription factor from the binuclear zinc cluster class which regulates the expression of the other FUM genes. *FUM13* encodes an NADPH-dependent ketoreductase which catalyzes the reaction yielding a 3-hydroxy intermediate further hydroxylated to another intermediate by a P450-oxygenase-reductase enzyme encoded by *FUM6. FUM7, FUM10, FUM11*, and *FUM14* encode the enzymes catalyzing reactions yielding the tricarboxylic esters on C14 and C15 positions. The product of *FUM7, FUM10,* and *FUM14* make a nonribosomal peptide synthetase (NRPS)-like protein complex. Within this complex, *FUM7* encodes a reductase domain, *FUM10* is analogous to the adenylation domain, and *FUM14* encodes peptidyl carrier protein and condensation domain. *FUM14* directs the conversion of HFB1 (two hydroxyl groups are attached at C14 and C15) to FB1 where the acyl group was donated by the N-acetylcysteamine monothioester of tricarballylic acid. *FUM11* encodes a tricarboxylate transporter. FB4 was produced by esterification reaction at C14 and C15 and further converted to FB2, FB3, and FB1 by two different types of oxygenase enzymes. *FUM2* is predicted as a P450 monooxygenase. Because *FUM12* expresses only during FB2 and FB4 production, it was predicted as functioning in C10 hydroxylation. *FUM3* exhibits a C5 hydroxylase in the presence of 2-ketoglutarate which transforms FB3 to FB1. The other genes

located in FUM clusters such as *FUM15, FUM16, FUM17, FUM18, FUM19,* and *FUM20* were identified but their roles have not been understood yet.

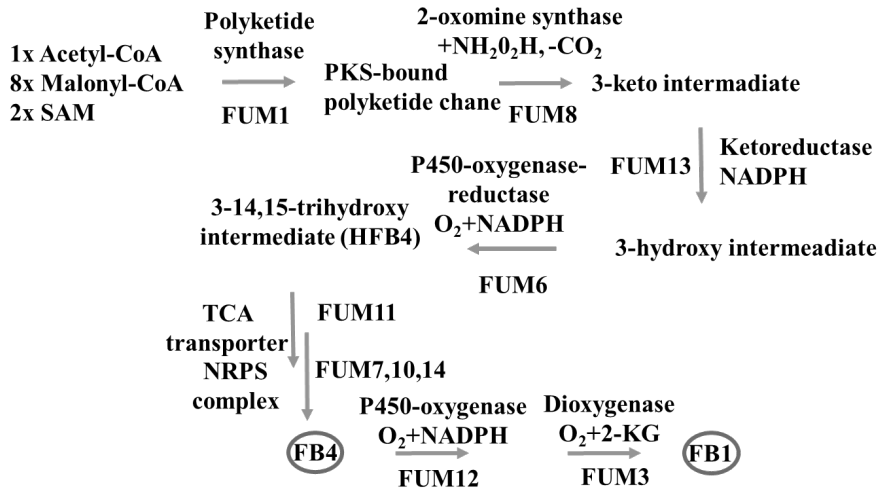

Figure 1. The schematic representation of fumonisin mycotoxins biosynthesis mechanism (Huffman et al., 2010). SAM: S-adenosyl methionine, TCA: propane-1,2,3-tricarboxylic acid, PKS: polyketide synthase, NRPS: nonribosomal peptide synthetase

It was also shown that epigenetic modification like histone deacetylation and acetylation is important in the fumonisin biosynthesis pathway which regulates the transcription of the genes functioning in the pathway (Gardner et al. 2016). Besides genetic and epigenetic regulations, the biosynthesis of fumonisins is also affected by environmental factors like temperature, water, pH, nutrients, and defense mechanism of plants. Fumonisins were shown to increase when plants suffer from drought stress and excessive insect damage (Parsons & Munkvold, 2010).

1.2. Disruption of sphingolipid biosynthesis by fumonisins

Fumonisins exhibit a similar chemical structure to sphingosine, which has a base with a long chain consisting of the backbone of cellular sphingolipids. Because of this similarity, fumonisins act as a competitive inhibitor of sphinganine and sphingosine N-acyltransferase (by other name ceramide synthase). N-acyltransferase is a key enzyme in the de novo biosynthesis pathway of sphingolipid, and operates the acylation of sphinganine (or sphingosine) derived from sphingolipid recycling (Norred et al., 1999).

The sphingolipids and ceramides biosynthesis pathway starts with a condensation reaction of serine and palmitoyl CoA which are catalyzed by serine palmitoyl CoA transferase (SPT) and yield sphinganine (Sa) (Merrill et al., 1996) (Figure 2). SPT composes of two subunits which are Sptlc1 and Sptlc2. Following to condensation

reaction, Sa is acylated by (dihydro) ceramide synthase (CerS1–6) yielding dihydroceramide (N-acylsphinganine). Dihydroceramide is reduced to form ceramide (N-acylsphingosine) by dihydroceramide desaturase (Des). Ceramide functions in activation of protein phosphatases and kinases, regulation of growth, differentiation and apoptosis. The yielded Sa from the condensation reaction can also be a substrate of sphingosine kinases (Sphk1, Sphk2), carrying out a phosphorylation reaction to form sphinganine-1-phosphate (Sa1P). Sphk 1 and Sphk2 are very similar but differ in subcellular localization and tissue distribution (Gardner et al., 2016). Sphk1 is mainly cytoplasmic and carries out cytoplasmic and extracellular Sa1P and S1P synthesis. Sphk2 is mainly nuclear causing inhibition of DNA synthesis and cell division and carrying out nuclear Sa1P and S1P synthesis. Sa1P is a bioactive signaling molecule. It is transferred to out of the cell by ABC transporters and interacts with G protein-coupled S1P receptors (S1Pr1–5) located on the cell surface. Sa1P can be also transported to the nucleus which acts as an inhibitor of histone deacetylases (HDACs). Sa1P can be recycled to Sa by dephosphorylation by sphingosine phosphate phosphatases (Sgpp) or by lipid phosphate phosphatases (Lpp). Ceramide can be converted to Sphingosine (So) via de-acylation by ceramidase. So can be also converted to ceramide with acylation reaction by CerS1–6. Sphk1 and Sphk2 can also phosphorylate So to form sphingosine-1-phosphate (S1P). S1P can also act on S1P receptors as being a kind of bioactive signaling molecule and inhibit HDACs.

Sphingolipids display essential roles in many cellular regulations such as cell morphology, membrane structure, the behavior of protein kinases and cell-surface proteins, enhancement of cellular and extracellular interaction, promotion of cell differentiation, regulation of growth factor levels and viability, apoptosis and cell carcinogenicity (Ahangarkani et al., 2014). Sphingolipids also role in many signal transduction pathways as secondary messengers.

Fumonisins are believed to cause toxicity by blocking N-acyltransferase causing a reduction of the production of ceramide and raising sphingoid bases, sphinganine (Sa) and sphingosine (So), and their phosphorylated metabolites, sphinganine-1-phosphate (Sa1P) (by other name dihydro-S1P) and sphingosine-1-phosphate (S1P) (Wang et al., 1991; Zitomer et al., 2009 Tafesse et al., 2015; Gardner et al., 2016;). This disruption of sphingolipid metabolism by fumonisin leading to cellular toxicity is the most agreed as the potential toxicity mechanism of fumonisin due to accumulation of sphingoid bases at toxic level. Because sphingolipid metabolism is important for the maintenance of membranes in all eukaryotic cells, the accumulated sphingoid bases both stimulate and inhibit cell growth and have a cytotoxic effect at higher concentrations altering cell growth and viability. It was demonstrated that 1 μM FB1 totally inhibited de nova sphingolipid biosynthesis in the cultured rat hepatocyte cells (Merrill et al., 1995; 1996). Sphingolipid bases promote dephosphorylation of retinoblastoma protein (pRb), a tumor suppressor that arrests the cell cycle in the hypophosphorylated form. Sphingoid bases have also been reported to promote apoptosis in the cultured keratinocytes and HET-1A cells, an immortalized human esophageal cell line (Tolleson et al., 1996). The exogenous application of sphingoid bases to the growth-arrested Swiss 3T3 cells induced DNA synthesis as a result of their conversion to 1-phosphate (Wolf, 1994).

The intervention of FB1 leading to disruption of the conversion of Sa to So as a result of the 4,5 trans double bond formation was shown by using radioactively labeled serine into the backbone of sphingoid base of ceramides and complex sphingolipids. Fumonisins also block reacylation of sphingoid bases (especially So) which are discharged by hydrolysis of more complex sphingolipids (Merrill et al., 2002). FB1 leads to the accumulate of Sa and increases the formation of Sa1P and degrades the sphingoid base backbone to ethanolamine l-phosphate and fatty aldehydes. This ethanolamine phosphate synthesis route has drawn attention on the contrary to the better-known decarboxylation of phosphatidylserine. The toxicity was elevated partially by adding β-chloroalanine to block serine palmitoyltransferase and reduce sphingoid base accumulation (Yoo et al., 1996).

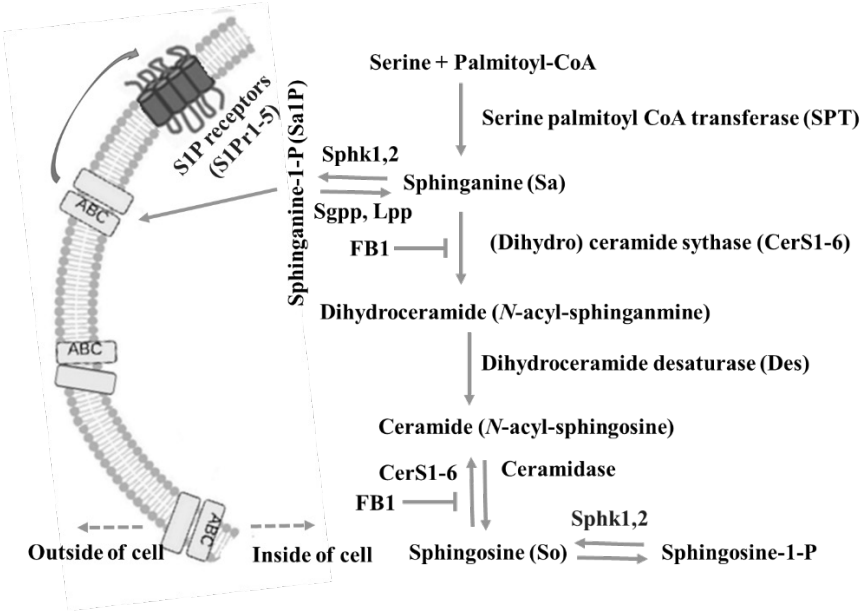

Figure 2. A short representation of the sphingolipid metabolic pathway indicates the probable toxicity mechanisms as a result of disruption by FB1. Sphk1, 2: sphingosine kinases 1 and 2, FB1: Fumonisin B1, ABC: the ABC transporter family work together with cell surface G protein-coupled S1P receptors (S1Pr1–5), Sgpp: sphingosine phosphate phosphatases, Lpp lipid phosphate phosphatases (Merrill et al., 1996; Gardner et al., 2016).

1.3. Toxicity of fumonisins

The versatile symptoms triggered by FBs are reported which are mainly comprising brain lesions, pulmonary edema, neural tube defects in newborns, leukoencephalomalacia, failure of several organs, decrease in reproductive performance, immunotoxicity, mutagenicity, and cancer in several livestock and animals (Marasas et al., 1988b;

Colvin & Harrison, 1992; Scott, 2012; Ahangarkani et al., 2014). But, a particular concern about fumonisin mycotoxins draws attention due to their potential to promote cancer development (Summerell & Leslie 2011). Although FBs are not mutagenic agents, the growth induction during the development of cancer is accompanied by an increase subsequent to the disruption of lipid metabolism by these mycotoxins. As a result of the disrupted sphingolipid metabolism leads to cancer because FB1 intervention decreases the complex sphingolipids together with the accumulation of the sphingoid bases and the loss of a growth-inhibitory sphingolipid complex, such as a ganglioside that downregulates several growth factor receptors. Gangliosides were also demonstrated to function in autophagy by interacting with autophagy-associated molecules. This interaction results in morphogenic remodeling such as altering membrane curvature and fluidity, followed by the formation of mature autolysosome (Matarrese et al., 2014). There are no consistent data of sphingolipid intervention in endocytosis of receptor-ligand complexes or in phagocytosis of particles like microbes or opsonized red blood cells. However, FB1 has shown enhancing phagocytosis of opsonized red blood cells by blocking certain receptor-ligand complex (Tafesse et al., 2015). Furthermore, the disrupted sphingolipid metabolism by FB1 alters cell-cell, cell growth and viability, the activity of protein kinases and the behavior of cell-surface proteins, the metabolism of other lipids. These versatile effect of fumonisins make them the potential toxic and carcinogenic agent for animals and humans (Merrill et al., 1996).

FB1 has been shown as causing organ failure as a result of versatile adverse effects, especially on the kidney, liver and brain in tested animals. These mycotoxins promote regenerative cell proliferation in these organs causing cancer in animals, however, there is no data in the case of humans. There are only a few cases on the effects of fumonisins in humans: one revealed no significant association between the risk of hepatocellular cancer and fumonisin exposure (Persson et al., 2012), while another one revealed that co-exposure of FB1 together with another mycotoxin AFB1 was related with induced carcinoma in the esophageal squamous cell in Huaian area, China (Xue et al., 2019). In other study, FBs was shown to induce liver cancer progression in rat, nephrotoxicity in animals and bleeding in rabbit brains. The toxicity of FBs is also demonstrated in livestock such as chickens and pigs (Ahangarkani et al., 2014). FB1 intervenes myelin synthesis, leading to liver necrosis and leukoencephalomalacia finally causing death in horses. The uptake of FB1 by pigs via contaminated feed causes pulmonary edema (Scott, 2012).

Another concern about fumonisin mycotoxins is the potential to cause immunotoxicity which is seen in mice and pigs at low oral doses. It was reported that intragastric administration of FB1 to mice for two weeks reduced spleen weight and caused thymocyte apoptosis. FB1 affects cytokine expression which was demonstrated on mice exhibiting an increased expression of interleukin-4 (IL-4) and interleukin-10 (IL-10) mRNAs in the spleen and a decrease in the expression of tumor necrosis factor (TNF-α) and interferon-γ (IFN-γ) transcripts (Abbes et al., 2016). Another important observation was reported FB1 uptake effect on animals after vaccination due to interfering of FB1 leading to decrease in antibody level (Taranu et al., 2005). In humans, FB1 inhibits the HLA class I antigen expression and low molecular weight

proteasome 2 (LMP2) and transporter associated with antigen presentation (TAP1) and increases the viability of abnormal cells (Yao et al., 2011). FB1 has a toxic effect on the immune which was observed in broiler chickens by examining FB1 resulting in reduced macrophage chemotaxis and phagocytosis (Cheng et al., 2006; Mwanza et al., 2009).

Although the lack of data addressing fumonisins as a direct mutagenic agent or metabolized into DNA reactive compounds, there are some concerns about the potential of indirect mutagenicity (DNA damage) of them (Chen et al., 2021). Experimental evidence showed that it was due to the oxidative stress induced by FB1 directing to DNA damage that causes cell carcinogenesis. In p53-null mouse embryo fibroblasts and rat C6 glioma cells has been shown that FB1 increases the level of 8-hydroxy2 0-deoxyguanosine (8-OH-DG) which is a biomarker of oxidative DNA damage, coincided with DNA hypomethylation (Mobio et al., 2003). Methylation of tumor-related genes which are p16, VHL, E-cadherin, and c-myc caused by FB1 has been shown on cell lines from rats (Demirel et al., 2015). In HepG2 cells, FB1 suppressed the activity of checkpoint kinase 1 (CHK1) to generate DNA damage by regulating phosphatase and tensin homolog (PTEN), protein kinase B (Akt) and phosphoinositide 3-kinases (PI3K) through the PI3K/Akt signaling pathway, which regulated cell survival (Arumugam et al., 2020; Yu et al., 2021).

The effects of fumonisins on reproductive performance have been demonstrated in pigs and rabbits. The effects of FB1 on the reproductive system mainly include reproductive failure and fetal hypoplasia in some animals (Abdel-Wahhab et al., 2004). FB1 reduces gonadotropin levels, inhibits granulocyte gain, and impairs normal follicle growth and oocyte survival (Somoskői et al., 2018).

Fumonisin mycotoxins can induce leukoencephalomalacia (softening of brain tissue) in horses. This leads to neurotoxic symptoms and, in some cases, abnormal optic nerve function. Fumonisins can pass through the blood-brain barrier which cause degeneration and necrosis of nerve cells as a result of neurotoxicity (Kovacic et al., 2009). Fumonisins prevent the proper function of blood vessels which leads to cerebral edema in horses and pulmonary edema in pigs. In another case reported that the necropsy of beef cattle having a sudden onset of blindness after grazing on Fusarium contaminated maize revealed optic nerve degeneration and acute myelin edema (Sandmeyer et al., 2015).

1.4. Detection methods of fumonisin mycotoxins

Fumonisins are found in foods and feeds at very low concentrations. Therefore, the detection methods require sensitive and reliable protocols. Fumonisins are water-soluble metabolites thanks to having four carboxyl groups and one amino group. On the contrary, FB1 is highly stable in an aqueous solution and acetonitrile. While these mycotoxins commonly occur in free forms, they can make complexes with proteins and carbohydrates. Maize and maize-used products were found to have the highest occurrence and amount of FB1 than any other cereal or cereal-based product (FAO and WHO, 2017). FB1 can also transfer into the products of animals like meat and meat products, milk, dairy products, which are rarely detectable and negligible.

Fumonisins can be detected by instrumental and bioanalytical methods which can be chosen according to requirements. Instrumental detection methods are commonly based on chromatographic techniques like Thin layer chromatography (TLC), High-performance liquid chromatography (HPLC) and Gas chromatography (GS). Among those, TLC is the oldest commonly used mycotoxin detection one and offers qualitative or semi-quantitative data. HPLC can be configured out with different types of detectors like ultraviolet (UV), diode array (DAD), fluorescence (FLD), or mass spectrometry (MS). GS can be configured out with the different type of detectors like electron capture detection (ECD), flame ionization detection (FID), or mass spectrometry (MS). UV and FID are used mostly for confirmation of immunochemical analysis. However, HPLC-FLD together with an efficient extraction and cleanup protocol is the most often used for the detection of mycotoxins quantitatively. These instruments execute the detection of the mycotoxins at high precision and accuracy together with supplying both quantitative and qualitative analyses. On the other hand, these detection methods have some challenges like the requirement of trained staff and long time for sample preparation and being expensive.

MS method is more advantageous for mycotoxin analysis compared to other LC methods by supplying a higher selectivity and sensitivity. Tandem MS/MS and High-resolution MS (HRMS) are useful for the characterization of unknown compounds to learn about their molecular identity and chemical structure. There are several MS analyzers and interfaces is used for mycotoxin analysis like electrospray ionization (ESI), atmospheric pressure chemical ionization (APCI), and atmospheric pressure photo-ionization (APPI). The other mass analyzers are Fourier transform-ion cyclotron resonance (FT-ICR), time-of-flight (TOF), quadrupole and ion-trap, which are also used to detect mycotoxins. Among all chromatographic techniques, MS analyzers, ESI, triple quadrupole, and TOF are the most extensively used for the detection of mycotoxins.

Immunoassay methods offer simple and fast detection of mycotoxins which makes them very useful for routine analyses. These methods are based on antibody-antigen interactions (Zherdev, 2014). Several immunological methods have been improved such as time-resolved immunochromatographic assays, enzyme-linked immunosorbent assays (ELISA), chemiluminescence immunoassays, enzyme-linked aptamer assays, fluorescence resonance energy transfer immunoassays, fluorescence immunoassays, and metal-enhanced fluorescence assays (Chauhan et al., 2016). In an immunoassays-based detection method, the most important parameter is aptamer which can attach to versatile proteins, peptides, amino acids, and organic or inorganic molecules, with high specificity and affinity (Torres-Chavolla & Alocilja, 2009). For the detection of FB1 in maize-used foods, a dipstick assay was developed which has a detection limit in a range of 40–60 ng/g (Schneider et al., 1995).

In addition to chromatographic and immunoassay-based methods introduced above, optical methods such as the incorporate infrared (IR) analyzers coupled with principal component analysis (PCA) were developed for mycotoxins detection. This method offers fast and non-destructive protocols for the quantification and screening of mycotoxins (Pettersson et al., 2003). Another most often used optic instrumental technique for mycotoxin detection is Capillary electrophoresis (CE). CE separates

compound according to their electrochemical properties and identifies them by UV or fluorescence absorbance. CE can be also configured as a laser-based fluorescence detector. The sensitivity of CE for FB1 detection in maize, coffee, and sorghum has increased by parallel to the application of a chromatographic technique (Corneli et al., 1998). In recent years, biosensors have become most attractive for the quantification of mycotoxins because of being reliable, rapid, and low-cost tools (Logrieco et al., 2005). A biosensor is an instrument that measures biological or chemical reactions by generating signals proportional to the concentration of an analyte in the reaction by incorporating a specific biological element (e.g., antibody) resulting in biorecognition. For rapid screening of FB1, competitive surface plasmon biosensors were developed. Jodra et al. (2015) was improved an electrochemical magnetoimmunosensor for the detection of FB1 and FB2. The sensor was made of disposable carbon screen-printed electrodes and magnetic beads. The other tools to detect fumonisin exposure in humans are biomarkers. For this aim, Urinary FB1 (UFB1) is the most commonly used biomarker; it is used to determine the efficiency of dietary interventions for reducing fumonisin exposure in humans.

Fluorescence polarization (FP) has been adapted to mycotoxin analysis. It is based on the measurement of the interaction between a specific antibody and fluorescently labeled antigen (Maragos et al., 2001). Although the FP technique offers rapid determination of fumonisins, it has some drawbacks because of less accuracy and sensitivity compared to HPLC. This happens due to the cross-reactivity of the antibody with other fungal metabolites and also food components. An electronic nose (EN) is a variant of GC that mimics the human olfactory sensory system and supplies non-destructive, rapid, and low-cost analysis of mycotoxins in food samples (Keshri & Magan, 2000). EN is applied for the detection of toxigenic fungi rather than detecting the mycotoxin itself.

1.5. Preventing and controlling strategies of fumonisins

Fumonisins are produced by Fusarium fungi after infection of cereals, primarily maize in the field environment. Fumonisin production rarely occurs post-harvest. The primary application to decrease the incidence of fumonisin production starts with the implementation of good agricultural practice in the field involving rotating crops, implementing good soil management, minimizing factors that increase plant stress, and usage of suitable plant varieties or hybrids according to soil type and climate. In addition to these, numerous post- and preharvest methods have been proposed to prevent and control fumonisin mycotoxins contamination of grains and related commodities.

Recently, the development of transgenic crops is foreseen promising method for the prevention and control of fumonisins. For example, *Bacillus thuringiensis* (Bt) maize has been shown significantly lower levels of fumonisin. It is because of the reduction of insect pest damage on maize subsequently causing less fungal infection through damaged plant tissues. There is also some effort to develop transgenic crops that are eligible to detoxify fumonisin mycotoxins. For example, plant pathologists have been able to employ RNA interference (RNAi) mechanism to prevent and control fumonisins (Johnson et al., 2018). RNAi is the process that results in a short

21–25 nucleotide interfering RNA (siRNA) or micro RNA (miRNA) by cleavage of a double-stranded RNA (dsRNA) by the endonuclease enzyme called Dicer. These newly synthesized small RNAs (sRNAs) are loaded into the RNA-induced silencing complex (RISC) which leads to sRNA to its complementary mRNA target. This cooperation is resulted in the degradation of the targeted mRNA causing gene silencing. The production of mycotoxins in Fusarium were inhibited by RNAi by overexpressing a transgenic dsRNA that is complementary to the target mRNA of fungus (McDonald et al., 2005). This biotechnological method is called host-induced gene silencing (HIGS) and offers a wide range of applications thanks to its being conserved regulatory mechanism between fungal pathogens and plants. In HIGS, a transgenic plant host is engineered to be overexpressing a dsRNA complementary to a fungal gene which is essential for pathogenesis or growth. RNAi machinery of the transgenic plant processes the dsRNA into siRNA, which is then uptaken by the invading fungus (Tinoco et al., 2010). Although the occurrence of RNAi molecules trafficking between cells and systemically throughout the plant are known, how the siRNAs are uptaken into the fungus is not understood yet (Knip et al., 2014). RNAi can be also directly applied to pathogenic fungi by spraying which is called spray-induced gene silencing (SIGS).

Several transgenic plant hosts expressing fungal dsRNAs were engineered successfully to reduce fungal infections (Koch et al., 2013; Govindarajulu et al., 2015; Chen et al., 2015). One of the first examples of HIGS in plants is that the transgenic tobacco plant expressed a dsRNA of E. coli β-glucuronidase produced siRNA which was absorbed by the transgenic *F. verticillioides* expressing *GUS* gene. This work exhibit an example of communication between organisms by the passage of RNA between the plant and its pathogen (Tinoco et al., 2010). Johnson et al. (2018) managed to reduce fumonisins content by downregulating FUM1 (polyketide synthase) and FUM8 (α-oxoamine synthase) which are the first two enzymes of the fumonisin biosynthetic pathway. These findings point out FUM1 or FUM8 genes for implementation of maize plants to engineer host-induced gene silencing of fumonisin production.

Antagonistic microorganisms such as rhizobacteria have also been used as a biocontrol agent for inhibition of *F. verticillioides* growth thank their antifungal production (Cavaglieri et al., 2004). Recently, this application gains a lot of attention thanks to its potential as being an ecologically friendly approach to minimizing pesticides in the fields (Formenti et al., 2012; Samsudin et al., 2016).

Other methods in the prevention and detoxification of these mycotoxins are included the usage of essential oils extracted from plants (Xing et al., 2014). The usages of specific microorganisms such as lactic and propionic acid bacteria are also being investigated to reduce fumonisins during fermentation in maize and related product (Nyamete et al., 2016).

There are some post-harvest attempts to prevent the FB1, FB2 and FB3 contamination in cereals. These methods are based on an adaption of several processing methods mainly including cleaning, milling, sorting, thermal processing (including extrusion), alkaline treatment (nixtamalization), and fermentation. For sorting and cleaning, the initial contamination level is important to rid of fumonisins. The wet milling process can facilitate the reduction of fumonisins due to the solubility of the

toxins in the water. For dry milled processes, the employed milling strategy becomes important for toxin distribution. The traditional and commercial alkaline treatment of maize known as nixtamalization is a proven method for reducing fumonisin contamination and reducing or eliminating the toxic effects of fumonisin in animal models. Feed additives which accomplish the same result as nixtamalization are also effective at reducing fumonisin toxicity

FAO and WHO (2017) develop risk assessment strategies to define the safety level of fumonisins' exposure by evaluating the scientific studies. According to risk assessments, maximum levels for the contamination of fumonisins depend on the types of foods. The prevention and reduction of FB1 and FB2 in food and feed, code of practice for cereals (CXC 51-2003) has established which describes preventive measures. According to the codex, the maximum levels for FB1 and FB2 in raw maize grain and maize flour and meal are 4000 and 2000 µg/kg, respectively.

2. Conclusion

In conclusion, fumonisin mycotoxins were illuminated in perspective of their metabolism, toxicity, detection and prevention. In conclusion, fumonisin mycotoxins are secondary metabolites produced by mainly *Fusarium verticillioides*, which is the most common pathogen of maize plants, and also widespread and unpreventable. There are growing concerns about these mycotoxins due to their adverse effects on plants and animals and humans as a result of consuming the contaminated food and feed. The fumonisins are produced generally after the fungi reach their maturity. The diversity of fumonisin structures induces various toxic effects but FB1 is the most toxic one. Toxicity occurs in animals grazing on the fungus contaminated plants because of the accumulation of sphingoid bases such as Sa and SIP due to inhibition of ceramide synthase which causes the prevention of the biosynthesis of complex sphingolipids. As a result of disrupted sphingolipid metabolism by fumonisins causes alteration of cell-cell interactions, the activity of protein kinases, the metabolism of other lipids, the behavior of cell-surface proteins, and cell growth and viability leading to several adverse effects such as carcinogenicity. The understanding of their biosynthetic metabolic pathway is crucial to developing the prevention strategies in terms of biotechnological implementations. By this end, 17 genes designated FUMs were identified functioning on this pathway. Several instrumental chromatographic and immunoassays-based techniques are employed to detect them and chosen methods can be different according to aims and material types. Furthermore, the use of siRNAs (RNAi) offers a promising implementation to reduce fumonisins by targeting pathogenic or host immunity genes.

References

Abbas, H. K., Shier, W. T., Seo, J. A., Lee, Y. W., & Musser, S. M. (1998). Phytotoxicity and cytotoxicity of the fumonisin C and P series of mycotoxins from *Fusarium spp.* fungi. *Toxicon*, *36*(12), 2033-2037.

Abbès, S., Ben Salah-Abbes, J., Jebali, R., Younes, R. B., & Oueslati, R. (2016). Interaction of aflatoxin B1 and fumonisin B1 in mice causes immunotoxicity

and oxidative stress: Possible protective role using lactic acid bacteria. *Journal of immunotoxicology*, *13*(1), 46-54.

Abdel-Wahhab, M. A., Hassan, A. M., Amer, H. A., & Naguib, K. M. (2004). Prevention of fumonisin-induced maternal and developmental toxicity in rats by certain plant extracts. *Journal of Applied Toxicology: An International Journal*, *24*(6), 469-474.

Ahangarkani, F., Rouhi, S., & Gholamour Azizi, I. (2014). A review on incidence and toxicity of fumonisins. Toxin Reviews, 33(3), 95-100.

Alshannaq, A., & Yu, J. H. (2017). Occurrence, toxicity, and analysis of major mycotoxins in food. *International journal of environmental research and public health*, 14(6), 632.

Arumugam, T., Ghazi, T., & Chuturgoon, A. (2020). Fumonisin B1 epigenetically regulates PTEN expression and modulates DNA damage checkpoint regulation in HepG2 liver cells. *Toxins*, 12(10), 625.

Bartók, T., Tölgyesi, L., Szekeres, A., Varga, M., Bartha, R., Szécsi, Á., & Mesterházy, Á. (2010). Detection and characterization of twenty-eight isomers of fumonisin B1 (FB1) mycotoxin in a solid rice culture infected with *Fusarium verticillioides* by reversed-phase high-performance liquid chromatography/electrospray ionization time-of-flight and ion trap mass spectrometry. *Rapid Communications in Mass Spectrometry*, 24(1), 35-42.

Bezuidenhout, S. C., Gelderblom, W. C., Gorst-Allman, C. P., Horak, R. M., Marasas, W. F., Spiteller, G., & Vleggaar, R. (1988). Structure elucidation of the fumonisins, mycotoxins from *Fusarium moniliforme*. Journal of the Chemical Society, *Chemical Communications*, (11), 743-745.

Burgess, L., General ecology of the fusaria. In: Nelson P.E., Toussoun T.A., Cook R.J., editors. Fusarium: Diseases, Biology, and Taxonomy. Pennsylvania State University Press; University Park, PA, USA: 1981. pp. 225–235.

Calvo, A. M., Wilson, R. A., Bok, J. W., & Keller, N. P. (2002). Relationship between secondary metabolism and fungal development. Microbiology and molecular biology reviews: MMBR, 66(3), 447–459. https://doi.org/10.1128/MMBR.66.3.447-459.2002

Cavaglieri, L., Passone, A., & Etcheverry, M. (2004). Screening procedures for selecting rhizobacteria with biocontrol effects upon *Fusarium verticillioides* growth and fumonisin B1 production. *Research in Microbiology*, 155(9), 747-754.

Chauhan, R., Singh, J., Sachdev, T., Basu, T., & Malhotra, B. D. (2016). Recent advances in mycotoxins detection. *Biosensors and Bioelectronics*, 81, 532-545.

Cheng, Y. H., Ding, S. T., & Chang, M. H. (2006). Effect of fumonisins on macrophage immune functions and gene expression of cytokines in broilers. *Archives of animal nutrition*, 60(4), 267-276.

Chen, J., Wen, J., Tang, Y., Shi, J., Mu, G., Yan, R., & Long, M. (2021). Research Progress on Fumonisin B1 Contamination and Toxicity: A Review. *Molecules*, 26(17), 5238.

Chen, Y., Gao, Q., Huang, M., Liu, Y., Liu, Z., Liu, X., & Ma, Z. (2015). Characterization of RNA silencing components in the plant pathogenic fungus *Fusarium graminearum*. *Scientific reports*, 5(1), 1-13.

Colvin, B. M., & Harrison, L. R. (1992). Fumonisin-induced pulmonary edema and hydrothorax in swine. *Mycopathologia*, 117(1-2), 79-82.

Corneli, S., & Maragos, C. M. (1998). Capillary electrophoresis with laser-induced fluorescence: Method for the mycotoxin ochratoxin A. *Journal of Agricultural and Food Chemistry*, 46(8), 3162-3165.

CXS 193-2003, General standard for contamınants and toxins in food and feed.

Demirel, G., Alpertunga, B., & Ozden, S. (2015). Role of fumonisin B1 on DNA methylation changes in rat kidney and liver cells. *Pharmaceutical biology*, 53(9), 1302-1310.

Desjardins, A. E., Munkvold, G. P., Plattner, R. D., & Proctor, R. H. (2002). FUM1—a gene required for fumonisin biosynthesis but not for maize ear rot and ear infection by *Gibberella moniliformis* in field tests. *Molecular Plant-Microbe Interactions*, 15(11), 1157-1164.

FAO, WHO, Evaluation of certain contaminants in food (Eighty-third report of the Joint FAO/WHO Expert Committee on Food Additives). WHO Technical Report Series, No.1002, 2017.

Frisvad, J. C., Smedsgaard, J., Samson, R. A., Larsen, T. O., & Thrane, U. (2007). Fumonisin B2 production by Aspergillus niger. Journal of agricultural and food chemistry, 55(23), 9727–9732.

Formenti, S., Magan, N., Pietri, A., & Battilani, P. (2012). In vitro impact on growth, fumonisins and aflatoxins production by Fusarium verticillioides and Aspergillus flavus using anti-fungal compounds and a biological control agent. *Phytopathologia Mediterranea*, 247-256.

Gardner, N. M., Riley, R. T., Showker, J. L., Voss, K. A., Sachs, A. J., Maddox, J. R., & Gelineau-van Waes, J. B. (2016). Elevated nuclear sphingoid base-1-phosphates and decreased histone deacetylase activity after fumonisin B1 treatment in mouse embryonic fibroblasts. *Toxicology and applied pharmacology*, 298, 56-65.

Gelderblom, W. C., Thiel, P. G., & van der Merwe, K. J. (1988). The chemical and enzymatic interaction of glutathione with the fungal metabolite, fusarin C. *Mutation Research/Fundamental and Molecular Mechanisms of Mutagenesis*, 199(1), 207-214.

Glenn, A. E., Zitomer, N. C., Zimeri, A. M., Williams, L. D., Riley, R. T., & Proctor, R. H. (2008). Transformation-mediated complementation of a FUM gene cluster deletion in Fusarium verticillioides restores both fumonisin production and pathogenicity on maize seedlings. *Molecular Plant-Microbe Interactions*, 21(1), 87-97.

Govindarajulu, M., Epstein, L., Wroblewski, T., & Michelmore, R. W. (2015). Host-induced gene silencing inhibits the biotrophic pathogen causing downy mildew of lettuce. *Plant biotechnology journal*, 13(7), 875-883.

Hartinger, D., & Moll, W. (2011). Fumonisin elimination and prospects for detoxification by enzymatic transformation. *World mycotoxin journal*, 4(3), 271-283.

Huffman, J., Gerber, R., & Du, L. (2010). Recent advancements in the biosynthetic mechanisms for polyketide-derived mycotoxins. Biopolymers, 93(9), 764–776.

Jodra, A., López, M. Á., & Escarpa, A. (2015). Disposable and reliable electrochemical magnetoimmunosensor for Fumonisins simplified determination in maize-based foodstuffs. *Biosensors and Bioelectronics*, 64, 633-638.

Johnson, E. T., Proctor, R. H., Dunlap, C. A., & Busman, M. (2018). Reducing production of fumonisin mycotoxins in *Fusarium verticillioides* by RNA interference. *Mycotoxin research*, 34(1), 29-37.

Kamle, M., Mahato, D. K., Devi, S., Lee, K. E., Kang, S. G., & Kumar, P. (2019). Fumonisins: Impact on Agriculture, Food, and Human Health and their Management Strategies. Toxins, 11(6), 328. https://doi.org/10.3390/toxins11060328

Keshri, G., & Magan, N. (2000). Detection and differentiation between mycotoxigenic and non-mycotoxigenic strains of two *Fusarium spp*. using volatile production profiles and hydrolytic enzymes. *Journal of Applied Microbiology*, 89(5), 825-833.

Knip, M., Constantin, M. E., & Thordal-Christensen, H. (2014). Trans-kingdom cross-talk: small RNAs on the move. *PLoS genetics*, 10(9), e1004602.

Koch, A., Kumar, N., Weber, L., Keller, H., Imani, J., & Kogel, K. H. (2013). Host-induced gene silencing of cytochrome P450 lanosterol C14α-demethylase–encoding genes confers strong resistance to Fusarium species. *Proceedings of the National Academy of Sciences*, 110(48), 19324-19329.

Kovačić, S., Pepeljnjak, S., Pertinec, Z., & Šegvić Klarić, M. (2009). Fumonisin B1 neurotoxicity in young carp (*Cyprinus carpio* L.). *Arhiv za higijenu rada i toksikologiju*, 60(4), 419-425.

Li, T., Gong, L., Jiang, G., Wang, Y., Gupta, V. K., Qu, H., Duan, X., Wang, J., & Jiang, Y. (2017). Carbon Sources Influence Fumonisin Production in Fusarium proliferatum. *Proteomics*, *17*(19), 10.1002/pmic.201700070.

Logrieco, A., Arrigan, D. W. M., Brengel-Pesce, K., Siciliano, P., & Tothill, I. (2005). DNA arrays, electronic noses and tongues, biosensors and receptors for rapid detection of toxigenic fungi and mycotoxins: A review. *Food additives and contaminants*, 22(4), 335-344.

Logrieco, A., Ferracane, R., Visconti, A., & Ritieni, A. (2010). Natural occurrence of fumonisin B2 in red wine from Italy. *Food Additives and Contaminants*, 27(8), 1136-1141.

Maragos, C. M., Jolley, M. E., Plattner, R. D., & Nasir, M. S. (2001). Fluorescence polarization as a means for determination of fumonisins in maize. *Journal of agricultural and food chemistry*, 49(2), 596-602.

Marasas, WFO, Jaskeiwicz, K., Venter, FS & van Schalkwyk, D. J. (1988a). *Fusarium moniliforme* contamination of maize in oesophageal cancer areas in Transkei. *South African Medical Journal*, 74(3), 110-114.

Marasas, W. F., Kellerman, T. S., Gelderblom, W. C., Coetzer, J. A., Thiel, P. G., & van der Lugt, J. J. (1988b). Leukoencephalomalacia in a horse induced by fumonisin B1 isolated from Fusarium moniliforme. *The Onderstepoort journal of veterinary research*, *55*(4), 197–203.

Marin, S., Ramos, A. J., Vazquez, C., & Sanchis, V. (2007). Contamination of pine nuts by fumonisin produced by strains of Fusarium proliferatum isolated from Pinus pinea. *Letters in applied microbiology*, 44(1), 68-72.

Martins, M. L., Martins, H. M., & Bernardo, F. (2001). Fumonisins B1 and B2 in black tea and medicinal plants. *Journal of Food protection*, 64(8), 1268-1270.

Matarrese, P., Garofalo, T., Manganelli, V., Gambardella, L., Marconi, M., Grasso, M., & Sorice, M. (2014). Evidence for the involvement of GD3 ganglioside in autophagosome formation and maturation. *Autophagy,* 10(5), 750-765.

McDonald, T., Brown, D., Keller, N. P., & Hammond, T. M. (2005). RNA silencing of mycotoxin production in Aspergillus and Fusarium species. *Molecular plant-microbe interactions*, 18(6), 539-545.

Merrill, A. H., Lingrell, S., Wang, E., Nikolova-Karakashian, M., Vales, T. R., & Vance, D. E. (1995). Sphingolipid biosynthesis de novo by rat hepatocytes in culture. Ceramide and sphingomyelin are associated with, but not required for, very low density lipoprotein secretion. *J Biol Chem*, 270, 13834-13841.

Merrill Jr, A. H., Liotta, D. C., & Riley, R. T. (1996). Fumonisins: fungal toxins that shed light on sphingolipid function. *Trends in cell biology*, 6(6), 218-223.

Merrill Jr, A. H., & Sandhoff, K. (2002). Sphingolipids: Metabolism and cell signaling. *New comprehensive biochemistry*, 36, 373-407.

Mobio, T. A., Tavan, E., Baudrimont, I., Anane, R., Carratú, M. R., Sanni, A., & Creppy, E. E. (2003). Comparative study of the toxic effects of fumonisin B1 in rat C6 glioma cells and p53-null mouse embryo fibroblasts. *Toxicology*, 183(1-3), 65-75.

Mogensen, J. M., Frisvad, J. C., Thrane, U., & Nielsen, K. F. (2010). Production of Fumonisin B2 and B4 by Aspergillus niger on grapes and raisins. Journal of agricultural and food chemistry, 58(2), 954–958.

Munkvold, G. P. (2003). Epidemiology of Fusarium diseases and their mycotoxins in maize ears. *European Journal of plant pathology*, 109(7), 705-713.

Musser, S. M., & Plattner, R. D. (1997). Fumonisin composition in cultures of *Fusarium moniliforme*, Fusarium proliferatum, and *Fusarium nygami*. *Journal of Agricultural and Food Chemistry*, 45(4), 1169-1173.

Mwanza, M., Kametler, L., Bonai, A., Rajli, V., Kovacs, M., & Dutton, M. F. (2009). The cytotoxic effect of fumonisin B 1 and ochratoxin A on human and pig lymphocytes using the Methyl Thiazol Tetrazolium (MTT) assay. *Mycotoxin research*, 25(4), 233.

Norred, W. P., Bacon, C. W., Riley, R. T., Voss, K. A., & Meredith, F. I. (1999). Screening of fungal species for fumonisin production andfumonisin-like disruption of sphingolipid biosynthesis. *Mycopathologia*, 146(2), 91-98.

Nyamete, F. A., Mourice, B., & Mugula, J. K. (2016). Fumonisin B1 reduction in lactic acid bacteria fermentation of maize porridges. *Tanzania Journal of Agricultural Sciences*, 15(1).

Parsons, M. W., & Munkvold, G. P. (2010). Associations of planting date, drought stress, and insects with Fusarium ear rot and fumonisin B1 contamination in California maize. Food additives & contaminants. Part A, Chemistry, analysis, control, exposure & risk assessment, 27(5), 591–607.

Persson, E. C., Sewram, V., Evans, A. A., London, W. T., Volkwyn, Y., Shen, Y. J., & Abnet, C. C. (2012). Fumonisin B1 and risk of hepatocellular carcinoma in two Chinese cohorts. *Food and chemical toxicology*, 50(3-4), 679-683.

Pettersson, H., & Åberg, L. (2003). Near infrared spectroscopy for determination of mycotoxins in cereals. *Food Control*, 14(4), 229-232.

Proctor, R. H., Busman, M., Seo, J. A., Lee, Y. W., & Plattner, R. D. (2008). A fumonisin biosynthetic gene cluster in Fusarium oxysporum strain O-1890 and the genetic basis for B versus C fumonisin production. *Fungal genetics and biology: FG & B*, *45*(6), 1016–1026.

Samsudin, N. I. P., & Magan, N. (2016). Efficacy of potential biocontrol agents for control of Fusarium verticillioides and fumonisin B1 under different environmental conditions. *World Mycotoxin Journal*, 9(2), 205-213.

Sandmeyer, L. S., Vujanovic, V., Petrie, L., Campbell, J. R., Bauer, B. S., Allen, A. L., & Grahn, B. H. (2015). Optic neuropathy in a herd of beef cattle in Alberta associated with consumption of moldy corn. *The Canadian Veterinary Journal*, 56(3), 249.

Schneider, E., Usleber, E., & Maertlbauer, E. (1995). Rapid detection of fumonisin B1 in corn-based food by competitive direct dipstick enzyme immunoassay/enzyme-linked immunofiltration assay with integrated negative control reaction. *Journal of Agricultural and Food Chemistry*, 43(9), 2548-2552.

Scott, P. M. (2012). Recent research on fumonisins: A review. *Food additives & contaminants. Part A, Chemistry, Analysis, Control, Exposure & Risk Assessment.,* 29, 242–248.

Sewram, V., Mshicileli, N., Shephard, G. S., Vismer, H. F., Rheeder, J. P., Lee, Y. W., & Marasas, W. F. (2005). Production of fumonisin B and C analogues by several Fusarium species. *Journal of Agricultural and Food Chemistry*, 53(12), 4861-4866.

Somoskői, B., Kovács, M., & Cseh, S. (2018). Effects of T-2 and Fumonisin B1 combined treatment on in vitro mouse embryo development and blastocyst quality. *Toxicology and industrial health*, 34(5), 353-360.

Soriano, J. M., Gonzalez, L., & Catala, A. I. (2005). Mechanism of action of sphingolipids and their metabolites in the toxicity of fumonisin B1. *Progress in lipid research*, 44(6), 345-356.

Summerell, B.A., & Leslie, J.F. (2011). Fifty years of Fusarium: how could nine species have ever been enough?.*Fungal Diversity*, 50, 135.

Tafesse, F. G., Rashidfarrokhi, A., Schmidt, F. I., Freinkman, E., Dougan, S., Dougan, M., & Ploegh, H. L. (2015). Disruption of sphingolipid biosynthesis blocks phagocytosis of *Candida albicans*. *PLoS pathogens*, 11(10), e1005188.

Taranu, I., Marin, D. E., Bouhet, S., Pascale, F., Bailly, J. D., Miller, J. D., & Oswald, I. P. (2005). Mycotoxin fumonisin B1 alters the cytokine profile and decreases the vaccinal antibody titer in pigs. *Toxicological Sciences*, 84(2), 301-307.

Tinoco, M. L. P., Dias, B. B., Dall'Astta, R. C., Pamphile, J. A., & Aragão, F. J. (2010). In vivo trans-specific gene silencing in fungal cells by in planta expression of a double-stranded RNA. *BMC biology*, 8(1), 1-11.

Tolleson, W. H., Melchior Jr, W. B., Morris, S. M., McGarrity, L. J., Domon, O. E., Muskhelishvili, L., & Howard, P. C. (1996). Apoptotic and anti-proliferative effects of fumonisin B1 in human keratinocytes, fibroblasts, esophageal epithelial cells and hepatoma cells. *Carcinogenesis*, 17(2), 239-249.

Torres-Chavolla, E., & Alocilja, E. C. (2009). Aptasensors for detection of microbial and viral pathogens. *Biosensors and bioelectronics*, 24(11), 3175-3182.

Visentin, I., Montis, V., Döll, K., Alabouvette, C., Tamietti, G., Karlovsky, P., & Cardinale, F. (2012). Transcription of genes in the biosynthetic pathway for fumonisin mycotoxins is epigenetically and differentially regulated in the fungal maize pathogen *Fusarium verticillioides*. *Eukaryotic cell*, *11*(3), 252–259.

Voss, K. A., Smith, G. W., & Haschek, W. M. (2007). Fumonisins: Toxicokinetics, mechanism of action and toxicity. *Animal feed science and technology*, 137(3-4), 299-325.

Wang, E., Norred, W. P., Bacon, C. W., Riley, R. T., & Merrill Jr, A. H. (1991). Inhibition of sphingolipid biosynthesis by fumonisins. Implications for diseases associated with *Fusarium moniliforme*. *Journal of Biological Chemistry*, 266(22), 14486-14490.

Williams, L. D., Glenn, A. E., Zimeri, A. M., Bacon, C. W., Smith, M. A., & Riley, R. T. (2007). Fumonisin disruption of ceramide biosynthesis in maize roots and the effects on plant development and *Fusarium verticillioides*-induced seedling disease. *Journal of agricultural and food chemistry*, 55(8), 2937-2946.

Wolf, G. (1994). Mechanism of the mitogenic and carcinogenic action of fumonisin B1, a mycotoxin. *Nutrition reviews*, 52(7), 246-247.

Xing, F., Hua, H., Selvaraj, J. N., Yuan, Y., Zhao, Y., Zhou, L., & Liu, Y. (2014). Degradation of fumonisin B1 by cinnamon essential oil. *Food Control*, 38, 37-40.

Xue, K. S., Tang, L., Sun, G., Wang, S., Hu, X., & Wang, J. S. (2019). Mycotoxin exposure is associated with increased risk of esophageal squamous cell carcinoma in Huaian area, *China. Bmc Cancer*, 19(1), 1-10.

Yao, Z. G., Zhang, X. H., Hua, F., Wang, J., Xing, X., Wang, J. L., & Xing, L. X. (2011). Effects of fumonisin B1 on HLA class I antigen presentation and processing pathway in GES-1 cells in vitro. *Human & experimental toxicology*, 30(5), 379-390.

Yoo, H. S., Norred, W. P., Showker, J., & Riley, R. T. (1996). Elevated sphingoid bases and complex sphingolipid depletion as contributing factors in fumonisin-induced cytotoxicity. *Toxicology and applied pharmacology*, 138(2), 211-218.

Yu, S., Jia, B., Liu, N., Yu, D., Zhang, S., & Wu, A. (2021). Fumonisin B1 triggers carcinogenesis via HDAC/PI3K/Akt signalling pathway in human esophageal epithelial cells. *Science of The Total Environment*, 787, 147405.

Zeng, H. Y., Li, C. Y., & Yao, N. (2020). Fumonisin B1: A tool for exploring the multiple functions of sphingolipids in plants. *Frontiers in plant science*, 11.

Zherdev, V. (2014). Immunochromatographic methods in food analysis. *TrAC Trends in Analytical Chemistry*, 55, 13–19.

Zimmer, I., Usleber, E., Klaffke, H., Weber, R., Majerus, P., Otteneder, H., & Märtlbauer, E. (2008). Fumonisin intake of the German consumer. *Mycotoxin Research*, 24(1), 40-52.

Zitomer, N. C., Mitchell, T., Voss, K. A., Bondy, G. S., Pruett, S. T., Garnier-Amblard, E. C., & Riley, R. T. (2009). Ceramide synthase inhibition by fumonisin B1 causes accumulation of 1-deoxysphinganine: a novel category of bioactive 1-deoxysphingoid bases and 1-deoxydihydroceramides biosynthesized by mammalian cell lines and animals. *Journal of biological chemistry*, 284(8), 4786-4795.

CHAPTER 2

FIRST RECORD OF THE TWO SNAKES MICROBIOTA FROM ÇANAKKALE (TURKEY)

Nurcihan Hacıoğlu Doğru[1] & Çiğdem Gül[2] & Murat Tosunoğlu[3]

[1](Prof. Dr.) Çanakkale Onsekiz Mart Üniversitesi, e- mail: nhacioglu@comu.edu.tr

Orcid:0000-0002-5812-9398

[2](Prof. Dr.) Çanakkale Onsekiz Mart Üniversitesi, e-mail: gulcigdem@comu.edu.tr

Orcid: 0000-0003-4736-2677

[3](Prof. Dr.) Çanakkale Onsekiz Mart Üniversitesi, e-mail:mtosun@comu.edu.tr

Orcid:0000-0002-9764-2477

1. Introduction

Conservation of natural life and ecological balance includes protection of wild animals, which are important members of our ecosystem, as well as human health. Many harmful chemicals and anthropogenic wastes that have emerged in parallel with the development of agriculture and industry in recent years cause many negative effects on nature and therefore wildlife. These negative effects can be traced through the microbiota of the animal species and their various resistance factors. All animals harbor complex relationships with their microbial flora living in their gastrointestinal tract. This intestinal microbiota can also influence the ecology and evolutionary processes of their hosts by affecting their behavioral, immune system, nutritional and reproductive isolations. Large-scale microbial diversity inventory studies have been performed mostly in mammals, birds, fish and lower-scale amphibians, but there are limited number of studies in reptiles. Reptiles are represented by about 10,000 species; revealing that the intestinal microbial ecology of these groups is essential to begin to understand the generalized patterns among vertebrate groups (Kohl *et al*., 2017). Snakes are more than 2900 species in the world and various snake species have gained as much popularity as pets in the past few years (Mitchell, 2009). However, although this growing popularity is positive for veterinarians and herpetoculturalists who are concerned with the sale and management of these animals in pet shops, it has increased concerns among public health officials due to the zoonotic potential (eg, *Salmonella*) associated with these animals.

Eryx jaculus (Javelin Sand Boa) belongs to Boidae family is distributed in Southern Balkans, Aegean islands, Transcaucasia, Eastern Caucasus, North of Africa

and Middle East (Sindaco *et al*., 2013). Except for the Black Sea coastal region, it is seen all over the Turkey and prefers arid, sandy and low vegetation habitats and this species is listed as Least Concern (Baran *et al*., 2012). *Montivipera xanthina* (Ottoman Viper) belongs to Viperidae family and is a venomous snake species. This species is distributed in Turkey and Greece. Although it is mostly found in stony rocky areas, it can come to settlements and agricultural areas for feeding purposes (Tosunoğlu *et al.,* 2017). *M. xanthina* is listed in the Least Concern category due to its wide distribution and large population (Mebert *et al*., 2020).

Snakes can be potential reservoirs of infection for other organisms, especially humans and wildlife animals, due to asymptomatically the pathogenic microorganisms they contain. Determination of microbial flora isolated from these animals and antibiotic heavy metal resistance and enzyme production capacities of their flora are important in terms of understanding the extent of anthropogenic and industrial pollution and the effects of potential pathogens to which these animals are exposed (Corrento *et al*., 2004). Most studies in this area have focused particularly on zoonotic infections in commercially available snake species (Schröter *et al*., 2004). However, there is no data related to bacterial flora of freeliving snake -*E. jaculus* and *M. xanthina*- species. This is the first comprehensive report on the microbiological parameters of *E. jaculus* and *M. xanthina* snake species from Çanakkale (Turkey).

The aim of this study is to identify and characterize of Gram negative culturable bacteria of two wildlife snake and to put forth the antibiotic and heavy metal susceptibility and enzymatic activity of the isolates, thus obtained data serve epidemiological studies and conservation programs in *E. jaculus* and *M. xanthina* species.

2. Materials and Methods

2.1. Snake samples

Each individual belonging to *E. jaculus* (n=1) and *M. xanthina* (n=1) snake species caught in the field studies carried out in Çanakkale Center in 2015-2016 within the scope of "Biodiversity Inventory and Monitoring Project of Çanakkale Province" of the Ministry of Agriculture and Forestry. Cloaca, skin, oral swabs and feces samples of two healthy snakes were taken in the field and then the snakes were released back to the field. Samples were stored at 4 ^{o}C until they were brought to the laboratory for microbial analyzing.

2.2. Bacterial identification assay

Cloacal, skin, oral swabs and feces samples of snakes incubated in buffered peptone water for 24 hr 35-37 ^{o}C and then the spread on different culture media like MacConkey agar (MAC), Thiosulfate citrate bile salts sucrose agar (TCBS), Glutamate starch phenol red agar (GSP), Chromogenic *E. coli* agar (CE) at 25– 30 °C for 24–48 h. Identification of isolates were done according to Murray *et al*., (2011). Microgen Gram negative panel (MID-64) was used for verification tests of isolates.

2.3. Antibiotic susceptibility test

Standard antibiotics of Trimethoprim (TR10 µg/mL), Tobramycin (TB10 µg/mL), Kanamycin (K30 µg/mL), Amoxycillin (AM10 µg/mL), Oxytetracycline (O30 µg/mL), Cephalothin (CH30 µg/mL), Cefmetazole (CMZ30 µg/mL), Gentamicin (G10 µg/mL), Furazolidone (FR50 µg/mL), Erythromycin (E15 µg/mL), Cefoxitin (CN30 µg/mL), Ampicillin (A10 µg/mL), Cefotaxime (CE30 µg/mL) and Chloramphenicol (C30 µg/mL) were used for determined antibiotic susceptibility of isolated bacteria by Kirby–Bauer Disc Diffusion method (Bauer *et al*., 1966; CLSI, 2009). The multiple antibiotic resistances (MAR) index of isolates was calculated as described by Krumperman, (1983).

2.4. Heavy metal resistance analysis

Analytical grades of metal salts ($CdCl_2.2H_2O$, $CuSO_4.5H_2O$, $CrCl_3$, $Pb(NO_3)$ and $MnCl_2.2H_2O$) were used for determinations of the minimal inhibitory concentration (MIC) of each isolates against heavy metals of Cd^{+2}, Cu^{+2}, Cr^{+3}, Pb^{+2}, Mn^{+2} (100 to 3.200 µg/mL). The isolates were considered resistant if the MIC values exceeded that of the *Escherichia coli* K-12 strain, which was used as the control (Hacıoğlu and Tosunoğlu, 2014).

2.5. Determination of enzymatic activities

Standardized enzymatic activity tests (DNAse, hemolysis, protease, lipase and amylase) were used to evaluate the virulence properties of isolated bacteria (Sokol *et al*., 1979; Collins *et al*., 2003).

3. Results

47 Gram negative isolates from two snake species were identified. 24 bacteria were isolated from *E. jaculus* (cloacal: 6, skin: 5; oral: 6, feces: 7) and 23 bacteria were isolated from *M. xanthina* (cloac: 6, skin: 1; oral: 6, feces: 10). The most frequent isolates were *Aeromonas hydrophila* and *Klebsiella oxytoca* (16.66%) for *E. jaculus* and *Pseudomonas aeruginosa* (34.78%) and *Pantoea agglomerans* (21.73%) for *M. xanthina* (Table 1).

Table 1. Microbiota of ***E. jaculus*** and ***M. xanthina*** snake species

Isolate No	Bacterial species	Source	Isolate No	Bacterial species	Source
EJ1	*A. lwoffii*	Feces	**MX1**	*A.hydrophila*	Feces
EJ2	*S. rubidaea*	Feces	**MX2**	*A. hydrophila*	Feces
EJ3	*E. coli*	Feces	**MX3**	*E. coli*	Feces
EJ4	*E. coli*	Feces	**MX4**	*K. oxytoca*	Feces
EJ5	*E. coli*	Feces	**MX5**	*P. agglomerans*	Feces

EJ6	*K. oxytoca*	Feces	**MX6**	*P. agglomerans*	Feces
EJ7	*K. oxytoca*	Feces	**MX7**	*P. agglomerans*	Feces
EJ8	*A. hydrophila*	Skin	**MX8**	*P. agglomerans*	Feces
EJ9	*A. lwoffii*	Skin	**MX9**	*P. agglomerans*	Feces
EJ10	*A.hydrophila*	Oral	**MX10**	*A. hydrophila*	Feces
EJ11	*P. aeruginosa*	Oral	**MX11**	*P. aeruginosa*	Oral
EJ12	*B. pseudomallei*	Cloac	**MX12**	*P. aeruginosa*	Cloac
EJ13	*A. hydrophila*	Cloac	**MX13**	*A. hydrophila*	Cloac
EJ14	*Actinobacilllus sp.*	Skin	**MX14**	*K. oxytoca*	Oral
EJ15	*K. oxytoca*	Skin	**MX15**	*K. oxytoca*	Cloac
EJ16	*S. rubidaea*	Skin	**MX16**	*P. aeruginosa*	Oral
EJ17	*C. sakazakii*	Oral	**MX17**	*P. aeruginosa*	Cloac
EJ18	*P. mirabilis*	Cloac	**MX18**	*P. aeruginosa*	Oral
EJ19	*A. hydrophila*	Cloac	**MX19**	*A.hydrophila*	Cloac
EJ20	*E. aerogenes*	Oral	**MX20**	*P. aeruginosa*	Oral
EJ21	*C. sakazakii*	Cloac	**MX21**	*P. aeruginosa*	Oral
EJ22	*S. putrefaciens*	Oral	**MX22**	*P. aeruginosa*	Cloac
EJ23	*E. aerogenes*	Oral	**MX23**	*S. arizonae*	Skin
EJ24	*K. oxytoca*	Cloac			

EJ: *E. jaculus*; MX: *M. xanthina*

The antibiotic susceptibility test showed that the most effective antibiotics G120 and C30 for the bacterial isolates of *E. jaculus* and *M. xanthina*, respectively. However, *E. jaculus* and *M. xanthina* bacterial isolates showed the highest resistance against CMZ30 and CN30 antibiotics, respectively (Figure 1). The MAR Index of isolates was found *P. aeruginosa* (*M. xanthina*) (0.64) > *S. putrefaciens* (*E. jaculus*) (0.57) > *B. pseudomallei* (*E. jaculus*) (0.5) = *P. mirabilis* (*E. jaculus*) (0.5) (Figure 2).

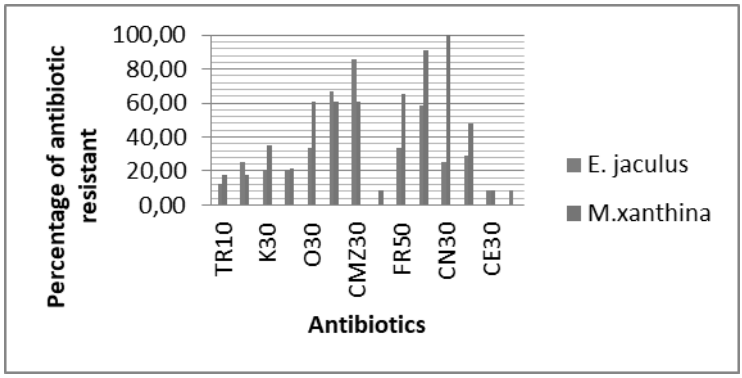

Figure 1. Antibiotic susceptibility profile of isolates

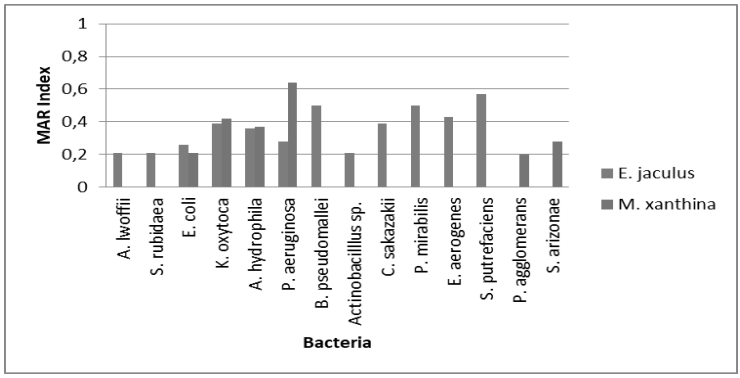

Figure 2. MAR index of isolates from *E. jaculus* and *M. xanthina*

The heavy metal resistance profiles of isolates are shown in Table 2 from *E. jaculus* and *M. xanthina*, respectively; Cd (91.66%) > Pb (87.5%) > Mn (83.33%) > Cu= Cr (66.66%); Cr (100%) > Mn (82.6%) > Pb (78.26%) > Cd (60.86%) > Cu (66.66%).

Table 2. Heavy metal resistance profile of isolates

Heavy metal	*E. jaculus* / *M. xanthina*	Metal concentrations (µg/mL) with number of tolerant isolates					Resistant isolates	
	N=24/23	400	800	1600	3200	>3200	n	%
Cadmium			*					
				13/5	9/9	0/0	22/14	91.66/60.86
Copper		*						
			13/8	2/2	1/1	0/0	16/11	66.66/47.82
Chromium			*					
				10/11	5/11	1/1	16/23	66.66/100
Lead			*					
				18/17	2/1	1/0	21/18	87.5/78.26
Manganese				*				
					15/17	3/2	20/19	83.33/82.60

* MIC values of the *E. coli* K-12

The enzymatic activity findings of isolates obtained from *E. jaculus* and *M. xanthina* snake species against 5 different enzymes used in the study are given in Table 3. DNase, amylase, lipase, haemolysin and protease activity of *E. jaculus* and *M. xanthina* isolates were 25%, 66.66%, 45.83%, 20.83%, 95.83% and 69.56%, 73.91%, 86.95%, 47.82%, 56.52%, respectively. In addition, it was determined that EJ9, EJ16, EJ23 and MX23 isolates carry only amylase enzyme.

Table 3. Extracellular enzyme profile of isolates from snakes

Isolates	Enzyme					Isolates	Enzyme				
	DNase	Haemolysin	Protease	Lipase	Amylase		DNase	Haemolysin	Protease	Lipase	Amylase
EJ1	-	-	+	-	+	**MX1**	+	+	+	-	+
EJ2	-	-	+	-	+	**MX2**	+	+	+	-	+
EJ3	-	+	+	-	+	**MX3**	+	+	+	-	+
EJ4	-	+	-	-	+	**MX4**	+	+	+	-	+
EJ5	-	+	-	+	+	**MX5**	+	-	+	-	+
EJ6	-	+	-	+	+	**MX6**	-	-	+	-	+
EJ7	-	+	-	-	+	**MX7**	-	-	+	-	+
EJ8	-	+	-	-	+	**MX8**	-	-	+	-	-
EJ9	-	-	-	-	+	**MX9**	+	-	+	-	+
EJ10	-	+	-	-	+	**MX10**	+	+	+	+	+
EJ11	-	+	-	-	+	**MX11**	+	+	+	+	-
EJ12	+	-	+	-	+	**MX12**	+	+	+	+	-
EJ13	+	+	+	-	+	**MX13**	+	+	+	+	-
EJ14	-	+	+	-	+	**MX14**	-	+	-	+	-
EJ15	-	+	-	-	+	**MX15**	-	+	-	+	+
EJ16	-	-	-	-	+	**MX16**	+	+	+	+	-
EJ17	-	+	-	-	+	**MX17**	+	+	+	+	-
EJ18	+	+	+	+	+	**MX18**	+	+	+	+	-

EJ19	+	+	+	-	+	**MX19**	+	+	+	+	-
EJ20	-	-	-	+	+	**MX20**	-	+	+	-	+
EJ21	+	+	+	-	+	**MX21**	+	+	+	+	-
EJ22	-	-	+	+	-	**MX22**	+	+	+	-	+
EJ23	-	-	-	-	+	**MX23**	-	-	-	-	+
EJ24	+	+	+	-	+						

EJ: *E. jaculus*; MX: *M. xanthina*

4. Discussion

Canakkale (Turkey), which is an important element of the ecological balance of amphibians, reptiles, etc. animals are very rich in terms of geography. This preliminary study, carried out in two different snake species, is very important in terms of examining the possible threats of the both species in the region. Researching of this topic is so important in terms of public health because of the intense human contact with these two snake species, which can be easily found in nature. There are many researches with different snake species that includes numerous microbial floras, pathogen epidemiology and antibiotic resistance profiles all over the world (Correnti *et al*., 2004; Schröter *et al*., 2004; Kobolkuti *et al*., 2009; Kobolkuti *et al*., 2013; Hacıoğlu and Tosunoglu, 2014; Iqbal *et al*., 2014; Schmidt *et al*., 2014; Hacıoğlu *et al*., 2015; Pawlak *et al*., 2020) and our study confirms their findings that snake species carry Gram negative bacteria.

Many snake species oral and cloaks mixed with especially Gram(-) bacteria. These species are opportunistic pathogens and detection of these species is accepted as an indicator of important clinical conditions (Rosenthal and Mader, 1996; Iqbal *et al*., 2014). In our research, member of Moraxellaceae (n=2), Enterobacteriaceae (n=14), Aeromonadaceae (n=4), Pseudomonadaceae (n=1), Burkholderiaceae (n=1), Neisseriaceae (n=1), Shewanellaceae (n=1) from *E. jaculus* and Enterobacteriaceae (n=10), Aeromonadaceae (n=5), Pseudomonadaceae (n=8) were isolated from *M. xanthina*. The isolated bacterial species diversity is similar to the data in the literature (Aviles *et al*., 2008; Iqbal *et al*., 2014; Schmidt *et al*., 2014; Artavia-Leon *et al*., 2017; Pawlak *et al*., 2020). Although there are some differences between the two species in terms of their natural flora, it can be said that all the isolates are opportunistic pathogens (Artavia-Leon *et al*., 2017; Liu *et al*., 2017). Shek *et al*. (2009) stated that these discrepancies may be caused by habitat diversity, different predation strategies and type of prey. The Gram negative bacteria which were found in *E. jaculus* and *M. xanthina* appear to be the natural microbiota of these snakes. Human who are the natural hosts of these isolated pathogens should be especially careful at contact with these animals. As stated in previous studies about different snake species that immunocompromised people, young children (under 5 years old), the elderly, and pregnant women are at risk of infection and can be augmented by pets as additional vectors that come into contact with free-living snakes (Schmidt *et al*., 2014; Pawlak *et al*., 2020). The most common bacterial species is *A. hydrophila* and is found in the skin, oral and cloacal microbiota of *E. jaculus*; it was previously obtained from the oral cavity, skin and internal organs of snakes such as anacondas, cobras and vipers (Shek *et al.,* 2009; Schmidt *et al*., 2014; Hacıoğlu-Doğru *et al*., 2018). In snakes, *P. aeruginosa* which is also the most common isolate of *M. xanthina*, is considered a normal component of the microflora of oral and intestinal tract as well as an opportunistic pathogen causing diseases in susceptible animals *(*Colinon *et al*., 2010; Foti *et al*., 2013; Iqbal *et al*., 2014). These isolated pathogen bacteria may be also a significant threat in people who share the same habitat or are in close contact with these snake species.

Antibiotic resistance is a growing threat to public health around the world. Undoubtedly, not writing proper prescriptions is one of the biggest reasons and

this is a big problem, but also in agriculture and livestock this resistance deserves more focused study. Moreover, the increasing number of antimicrobial agents in veterinary medicine creates animal's potential habitat of resistant bacteria (Hacıoğlu and Tosunoglu, 2014). In the present research, the high resistance rates of isolates to different antibiotics and high MAR indexes are proof that the habitats of both *E. jaculus* and *M. xanthina* species are contaminated with antibiotic residues. Our findings on high multi resistance incidences, similar to other investigations about different snake species except *E. jaculus* and *M. xanthina* (Colinon *et al*., 2010; Foti *et al*., 2013; Hacıoğlu and Tosunoglu, 2014; Hacıoğlu *et al*., 2015; Artavia-Leon *et al*., 2017; Hacıoğlu-Doğru *et al*., 2018). This is also the first report about frequency of antibiotic resistant of isolated bacteria from these two snake species. Additionally, the tested G120, CE30 and C30 antibiotics worked well against the isolates.

Heavy metal resistance may have been observed in this study as a result of heavy metals contamination of snake species habitats. Cu, Cr and Mn etc. metals have an important place in the biological systems, but it is also known that uninterrupted exposure to high doses causes toxic effects (Nies, 1999). Heavy metals entering the environment in various ways can cause significant changes in the structure and function of microbial communities. Over the past decade, a number of studies have reported that antibiotic-resistant bacteria can emerge in the environment through common or cross-resistance or co-regulation of resistance pathways to metals (McArthur and Tuckfield, 2000; Akinbowlale *et al*., 2007). As the increase in heavy metal and antibiotic resistance to pathogens continues, the ongoing global war against infectious diseases will become more difficult. No studies on heavy metal susceptibility of bacterial isolates obtained from both snake species were found in the literature. However, high resistance to the same heavy metals was found similar to the studies with other reptile species in the region (Hacıoğlu and Tosunoglu, 2014; Hacıoğlu *et al*., 2015; Hacıoğlu-Doğru *et al*., 2018).

Bacterial pathogenicity is highly positively correlated with some virulence factors such as extracellular enzyme production (Soler *et al.,* 2002; Hacıoğlu-Doğru *et al.,* 2018), so some enzymatic activities of the isolates have been. In our study, the high enzymatic activities of the isolates indicate that both snake species naturally spreading in Çanakkale and people in contact with them may be exposed to bacterial flora with high virulence.

5. Conclusion

Our research is the first study to reveal the bacterial flora (also the antibiotic-heavy metal susceptibility and extracellular enzyme profile) of venomous and non-venomous snake species from Çanakkale (Turkey). Our results revealed that the majority of the 14 bacterial species could bring health complications especially after a snake bite. While these data determine the importance of epidemiological surveillance and microbiological monitoring, they once again reveal the need to implement environmental protection programs for free-living snakes.

Acknowledgements: This study was financially supported by the Çanakkale Onsekiz Mart University Scientific Research Projects Coordination Unit, Turkey (FHD-2019-2802).

References

Akinbowlale, O.L., Peng, H. & Barton, M. D. (2007). Diversity of tetracycline resistance genes in bacteria from aquaculture sources in Australia. *Journal of Applied Microbiology, 30*(2), 177-182.

Artavia-León, A., Romero-Guerrero, A. Sancho-Blanco, C., Rojas, N. & Umaña-Castro, R. (2017). Diversity of aerobic bacteria isolated from oral and cloacal cavities from free-living snake species in Costa Rica Rainforest. *International Scholarly Reserach Notices,* 1-9.

Avilés, D. E., Salomón-Soto, V. M. & Morales-Martínez, S. (2008). Hematology, blood chemistry, and bacteriology of the free-ranging Mexican beaded lizard (*Heloderma horridum*). *Journal of Zoo Wildlife Medicine*, *39*(1), 21-27.

Baran, İ., Ilgaz, Ç., Avcı, A., Kumlutaş, Y. & Olgun, Y. (2012). Türkiye amfibi ve sürüngenleri. *Tübitak Popüler Bilim Kitapları*, (pg. 204).

Bauer, A. W., Kirby, W. M., Sherris, J. C. & Turck, M. (1966). Antibiotic susceptibility testing by a standardized single disk method. *American Journal of Clinical Pathology*, *45*(4), 493-6.

Clinical and Laboratory Standard Institute (CLSI). (2009). Performance standards for antimicrobial disk susceptibility tests. NCCLS Document M2-A7. *National Committee for Clinical Laboratory Standards*, *27*(1), Wayne.

Colinon, C., Jocktane, D. & Brothier, E. (2010). Genetic analyses of *Pseudomonas aeruginosa* isolated from healthy captive snakes: evidence of high inter and intricate dissemination and occurrence of antibiotic resistance genes. *Environmental Microbiology*, *12,* 716-729.

Collins, Y. F., McSweeney, P. L. H. & Wilkinson, P. L. H. (2003). Lipolysis and free fatty acid catabolism in cheese: a review of current knowledge. *Lnt Dairy Journal*, *13*, 841–866.

Corrento, M., Madio, A., Friedrich, K.G., Greco, G., Desario, C., Tagliabue, S., D'Incau, M., Campolo, M. & Buonavoglia, C. (2004). Isolation of *Salmonella* Strains from reptile faeces and comparison of different culture media. *Journal of Applied Microbiology, 96*, 709-715.

Foti, M., Giacopello, C., Fisichella, V., & Latella, G. (2013). Multidrug- resistant *Pseudomonas aeruginosa* isolates from captive reptiles. *Topics in Medicine and Surgery*, *22*, 270-274.

Hacıoğlu, N. & Tosunoglu, M. (2014). Determination of antimicrobial and heavy metal resistance profiles of some bacteria isolated from aquatic amphibian and reptile species. *Environmental Monitoring and Assessment*, *186*, 407-413.

Hacıoğlu, N., Gül, Ç. & Tosunoğlu, M. (2015). Bacteriological screening and antibiotic – heavy metal resistance profile of the bacteria isolated from some amphibian and reptile species of the Biga stream in Turkey. *World Academy of Science, Engineering and Technology International Journal of Biological, Biomolecular, Agricultural, Food and Biotechnological Engineering*, *9*(4), 369-373.

Hacıoğlu-Doğru, N., Gül, Ç. & Tosunoğlu, M. (2018). Some Virulence Factors of Gram negative Bacteria Isolated from Some Amphibian and Reptilian

Species of the Biga Stream in Turkey. *American Journal of Innovative Research and Applied Sciences*, *6,* 29-34.

Iqbal, J., Sagheer, M., Tabassum, N., Siddiqui, R. & Khan, N. A. (2014). Culturable aerobic and facultative anaerobic intestinal bacterial flora of Black Cobra (*Naja Naja Karachiensis*) in Southern Pakistan. *ISRN Veterinary Science,* http//:dx.doi.org/10.1155/2014/878479.

Kobolkuti, L., Spinu, M., Cadar, G., Czirjak, G. & Kiss, G. (2009). Classical and molecular monitoring of the prevalence of *Salmonella* spp. carriage in free-living and captive snakes in Romania. *Lucrari Stiinifice Medicina Veterinara*, *XLII*, 294-297.

Kobolkuti, L.B., Czirjak, G. A., Tenk, M., Szakacs, A., Kelemen, A. & Spinu, A. (2013). *Edwardsiella tarda* associated subcuteneous abscesses in A captive Grass Snake (*Natrix natrix*, Squamata:Colubridae). *Kafkas Universitesi Veteriner Fakultesi Dergisi*, *19*(6), 1061-1063.

Kohl, K. D., Brun, A., Magallanes, M., Brinkerhoff, J., Laspiur, A., Acosta, J. C., Caviedes-Vidal, E. & Bordenstein, S. R. (2017). Gut microbial ecology of lizards: insights into diversity in the wild, effects of captivity, variation across gut regions and transmission, *Molecular Ecology*, *26*, 1175–1189.

Krumpermann, P. H. (1983). Multiple antibiotic resistances indexing of *E. coli* to identify high-risk sources of fecal contamination of foods. *Applied and Environmental Microbiology*, *46*(1), 165–170.

Liu, P., Weng, L., Tseng, S., Huang, C., Cheng, C., Mao, Y., & Tung, K. (2017). Colistin Resistance of *Pseudomonas aeruginosa* isolated from Snakes in Taiwa. *Canadian Journal of Infectious Diseases and Medical Microbiology*, 1-5.

McArthur, J. V. & Tuckfield, R. C. (2000). Spatial patterns in antibiotic resistance among stream bacteria: effects of industrial pollution. *Applied and Environmental Microbiology*, *66*(9), 3722–3726.

Mebert, K., Göçmen, B., İğci, N., Kariş, M., Oğuz, M. A., Yıldız, M. Z., Teynié, A., Stümpel, N. & Ursenbacher, S. (2020). Mountain Vipers in Central-Eastern Turkey: Huge Range Extensions for Four Taxa Reshape Decades of Misleading Perspectives. *Herpetological Conservation and Biology, 15*(1), 169–187.

Mitchell, M. A. (2009). *Snakes. In Manual of Exotic Pet Practice* ed. Mitchell, M.A. and Tully, T.N. (pg. 136–163). St. Louis: Saunders Elsevier.

Murray, P.R., Baron, E. J., Pfaller, M. A., Tenover, F. C. & Yolken, R.H. (2011). *Manual of clinical microbiology* (10th ed.). Washington, D.C.: American Society for Microbiology.

Nies, D. H. (1999). Microbial heavy metal resistance. *Applied Microbiology and Biotechnology*, *51*, 730–750.

Pawlak, A., K. Morka, S. Bury, Z. Antoniewicz, Z., Wzorek, A., Cieniuch, G., Korzeniowska-Kowal, A., Cichoń, M., & Bugla-Płoskońska, G. (2020). Cloacal Gram-Negative Microbiota in Free-Living Grass Snake *Natrix natrix* from Poland. *Current Microbiology*, *77*, 2166-2171.

Rosenthal, K. L. & Mader, D. R. (1996). Microbiology. In: Mader, D.R. editor. *Reptile Medicine and Surgery, Philadelphia,* (pg. 117-125). W.B. Saunders.

Schmidt, V., Mock, R., Burgkhardt, E., Junghanns, A., Ortlieb, F., Szabo, I., Marschang, R., Blindow, I. & Krautwald-Junghanns, M. E. (2014). Cloacal aerobic bacterial flora and absence of viruses in free-living Slow Worms (*Anguis fragilis*), Grass Snakes (*Natrix natrix*) and European Adders (*Vipera berus*) from Germany. *Ecohealth*, DOI: 10.1007/s10393-014- 0947-6.

Schröter, M., Roggentin, P., Hofmann, J., Speicher, A., Laufs, R., & Mack, D. (2004). Pet snakes as a reservoir for *Salmonella enterica* subsp. d*iarizonae* (Serogroup IIIb): a prospective study. *Applied Environmental Microbiology*, 70, 613–615.

Shek, K., Tsui, K., Lam, K., Crow, P., Ng, K., Ades, G., Yip, K., Grioni, A., Tan, K. & Lung, D. C. (2009). Oral bacterial flora of the Chinese cobra (*Naja atra*) and bamboo pit viper (*Trimeresurus albolabris*) in Hong Kong SAR, China. *Hong Kong Medical Journal*, *15*(3), 183–190.

Sindaco, R., Venchi, A. & Grieco, C. (2013). The Reptiles of the Western Palearctic. *2. Annotated checklist and distributional atlas of the snakes of Europe, North Africa.* Middle East and Central Asia, with an update to the, 1, Edizioni Belvedere, Latina.

Sokol, P. A., Ohman, D. E. & Iglewski, B. H. (1979). A more sensitive plate assay for detection of protease production by *Pseudomonas aeruginosa*. *Journal of Clinical Microbiology, 9*, 538-540.

Soler, L., Figueras, M. J., Chacón, M. R., Vila, J., Marco, F., Martínez-Murcia, A. & Guarro, J. (2002). Potential virulence and antimicrobial susceptibility of *Aeromonas popoffii* recovered from freshwater and seawater. FEMS Immunology and Medical Microbiology, *32*, 243–247.

Tosunoğlu, M., Gül, Ç. & Uysal, İ. (2017). *Çanakkale Amfibi ve Sürüngenleri*, (pg. 1-71.) Orman ve Su İşleri Bakanlığı.

CHAPTER 3

DETERMINATION OF SOME NUTRIENT CONCENTRATIONS AND ANTIOXIDANT ENZYME ACTIVITIES OF NATURALLY GROWN SPINACH (*Spinacia oleracea* L.) PLANT IN FIELD CONDITIONS

Handan Sarac[1] & Hasan Durukan[2] & Ahmet Demirbas[3]

[1](Asst. Prof.) Sivas Cumhuriyet University, e-mail:handansarac@cumhuriyet.edu.tr

Orcid: 0000-0001-7481-7978

[2](Dr.) Sivas Cumhuriyet University, e-mail:hasandurukan@cumhuriyet.edu.tr

Orcid: 0000-0002-2255-7016

[3](Assoc. Prof.) Sivas Cumhuriyet University, e-mail:ademirbas@cumhuriyet.edu.tr

Orcid: 0000-0003-2523-7322

1. Introduction

Free radicals are unstable, low molecular weight and short-lived reactive molecules with one or more unpaired electrons in their structure that occur due to endogenous or exogenous factors in the living organism (Mercan, 2004; Sezer and Keskin, 2014; Karabulut and Gülay, 2016b; Shrivastava et al., 2019). These molecules, which easily exchange electrons with other molecules, are also called “oxidant molecules” (Cavdar et al., 1997; Kasnak and Palamutoğlu, 2015). Free radicals have two different sources, oxygen and nitrogen (Karabulut and Gülay, 2016b). Among them, the most important for living things are oxygen-derived free radicals (Mercan, 2004). Oxygen is an indispensable element for many living things, and the oxygen taken into the living body can turn into reactive oxygen species (ROS) or reactive nitrogen species (RNS) in low amounts depending on many factors such as environmental pollution, radiation and pesticides during normal aerobic metabolism (Koca and Karadeniz, 2003; Karabulut and Gülay, 2016b). ROS mostly occur in organelles where oxidation reactions take place, such as chloroplasts, mitochondria, peroxisomes, and glyoxysomes (Doğru, 2020). The main oxygen-derived free radicals are singlet oxygen (O_2 ^{1}), superoxide ($O_2^{\cdot -}$), hydroxyl ($OH^{\cdot -}$), hydroperoxyl (HOO^-), peroxyl ($ROO\cdot$) and alkoxyl ($RO\cdot$) radicals (Koca and Karadeniz, 2003; Kaur and Kapoor, 2001). These unstable reactive oxygen species attack cells in order to become stable by taking electrons, and react with the cell’s lipids, proteins, carbohydrates and DNA (Shinde et al., 2012; Sezer and Keskin, 2014). When they occur in large quantities, they cause peroxidation of membrane lipids, causing permeability to deteriorate and intracellicular ion imbalance. They deactivate useful intracellular enzymes and

activate lytic enzymes. They also play an important role in the formation of many diseases by disrupting the structure of molecules such as protein, DNA and RNA (Sezer and Keskin, 2014; Özcan et al., 2015; Sevindik et al., 2020). Studies have shown that oxygen radicals are effective in the emergence of many important diseases such as cancer and cardiovascular diseases (Koca and Karadeniz, 2003; Mercan, 2004; Özcan et al., 2015). In plants, ROS formation occurs naturally, as well as is mostly affected by various environmental stress factors such as drought, salinity, light and temperature (Candan and Tarhan, 2003; Duman et al., 2016). The substances that serve to prevent the formation of ROS, to prevent damage caused by ROS in lipid, protein, carbonhydrate and DNA, and to provide detoxification are called "antioxidants", and their defense systems are called "antioxidant defense systems" (Sezer and Keskin, 2014; Karabulut and Gülay, 2016a). While the living metabolism is healthy, there is a balance (homeostasis) between antioxidants and free radicals under normal conditions (Karabulut and Gülay, 2016a; Shrivastava et al., 2019). When this balance is disrupted and the amount of free radicals increases and the capacity of the antioxidant defense system is exceeded, oxidative stress occurs that causes damage to the cells (Candan and Tarhan, 2003; Karabulut and Gülay, 2016a). Oxidative stress can be defined as the imbalance between the organism's antioxidant defense and the production of free radicals (Mercan, 2004; Sharma, 2014; Özcan et al., 2015).

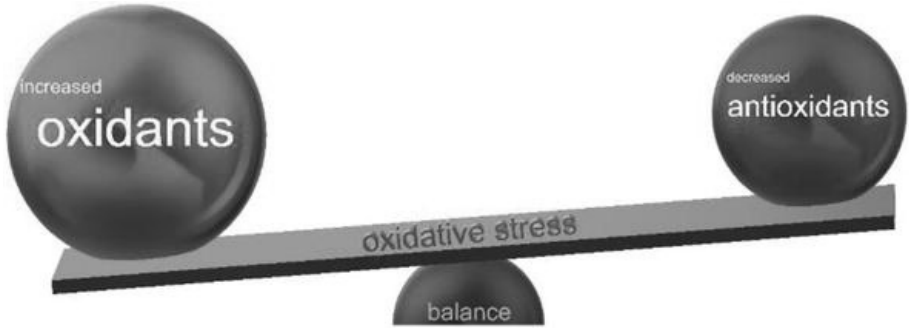

Figure 1. Oxidative stress formation (Boonla, 2018)

Antioxidants are the most important molecules that can eliminate the oxidative stress generated by free radicals and prevent cell damage (Karabulut and Gülay, 2016a; Shrivastava et al., 2019). They also have a protective effect against cancer by reducing the effect of oxidative damage on DNA and preventing abnormal cell division. These positive effects of antioxidants on important diseases such as cancer have become one of the most attractive issues especially in recent years (Sezer and Keskin, 2014). There are many different enzymatic and non-enzymatic molecules that show antioxidant properties (Rios-Gonzalez et al., 2002; Sezer and Keskin, 2014). Plant cells have both defense components against the harmful effects of oxidative stress (Rios-Gonzalez et al., 2002; Candan and Tarhan, 2003; Duman et al., 2016; Doğru, 2020). Some of the non-enzymatic antioxidants are α-tocopherol (vitamin E), ascorbic acid (vitamin C), glutathione (GSH), carotenoids (β-carotene, zeaxanthin), anthocyanins, flavonoids and other phenolic compounds (Valko et al., 2007; İlhan

et al., 2019). Enzymatic ones are enzymes such as superoxide dismutase (SOD), ascorbate peroxidase (APX), glutathione reductase (GR), catalase (CAT), peroxidase (POD) (Valko et al., 2007; Duman et al., 2016; Shrivastava et al., 2019). Antioxidant enzymes can show their effect in two different ways, either by directly destroying reactive oxygen types or by producing a non-enzymatic antioxidant (Candan and Tarhan, 2003). In both cases, they protect the plant from the harmful effects of ROS (Duman et al., 2016). The superoxide group of ROS, which causes cell damage, is converted into hydrogen peroxide (H_2O_2) and oxygen by SOD, a copper-containing enzyme (Mercan, 2004). H_2O_2, which is formed by taking an electron from the molecules around the superoxide ($O_2^{\cdot -}$) radical or by combining peroxide with two protons (H^+), which is formed by taking two electrons from the molecules around molecular oxygen, is a weaker oxidant than the superoxide group and is detoxified and neutralized by the catalase and peroxidase enzymes into water and molecular oxygen (Candan and Tarhan, 2003; Duman et al., 2016).

Vegetables within the scope of agricultural activities have a rich content in vitamins, minerals and antioxidant substances that are important for human health (Şenlikoğlu, 2015). One of these vegetables, Spinach (*Spinacia oleracea* L.), is an annual herbaceous plant belonging to the Chenopodiaceae family (Şenlikoğlu, 2015; Özenç and Şenlikoğlu, 2017). Spinach, which can be consumed cooked or fresh, is a very rich plant in terms of ascorbic acid (Vitamin C) content and water soluble-vitamins, although it is low in calories (Alibas and Okursoy, 2012; Jabeen et al., 2019). It is also known that the spinach plant, which contains 90-92% water, is nutritious in terms of nutrients, as well as rich in Calcium (Ca), Iron (Fe) and Potassium (K) nutrients (Şenlikoğlu, 2015). Moreover, it also contains bioactive molecules with strong antioxidant activation, such as flavanoids. Due to its rich content of vitamins, antioxidants and mineral substances that are important for human health, spinach is among the most popular and widely consumed vegetables worldwide (Jabeen et al., 2019). It is produced by seeds and is a cold-resistant, cool-climate vegetable that develops optimally at 16-18 °C and can be grown successfully in all types of soils that does not hold much water and is not heavy (Şenlikoğlu, 2015; Özenç and Şenlikoğlu, 2017). Due to the fact that it is easy to grow and the demand is high, it is cultivated in many countries of the world and the amount of production is gradually increasing (Deveci and Uzun, 2011).

In this study, it is aimed to determine some macro and micro element concentrations, chlorophyll amounts and some antioxidant enzyme activities of spinach (*Spinacia oleracea* L. cv. Matador) plant.

2. Experimental

2.1. Characteristics of the area where the plant is grown

The study was carried out in field conditions in the research trial area of Sivas Cumhuriyet University, Department of Crop and Animal Production in 2021. The study was carried out on an area of 100 m^2 and no fertilization was applied. The soil of the study area is clayey loam, with slightly alkaline pH, free of salt, low in phosphorus (P), and sufficient in potassium (K) (Table 1).

Table 1. Some physical and chemical properties of experimental soil

Soil Properties	**Depth (0-30cm)**
Texture	CL
pH (1:1 H_2O)	7.71
Lime (%)	11.3
Salt (%)	0.03
Organic matter (%)	1.95
Available P_2O_5 (kg ha^{-1})	45.9
Available K_2O (kg ha^{-1})	1145.0
Available Fe (mg kg^{-1})	5.23
Available Mn (mg kg^{-1})	2.33
Available Zn (mg kg^{-1})	0.45
Available Cu (mg kg^{-1})	0.96

2.2. Macro and micro element analyzes

In the study, planting of spinach (*Spinacia oleracea* L. cv. Matador) plant was done at the end of April, and leaf samples were taken in July. Leaf samples were taken as 5 replications. The leaves brought to the laboratory were first washed with tap water and then pure water for mineral element analysis, and excess water was taken on coarse filter paper. The plants placed in the paper bag were dried in the air circulation drying cabinet at 70 ^{0}C until they reached a constant weight and ground in the plant grinding mill. 0.2 g of the plant samples were weighed and burned in a H_2O_2-HNO_3 acid mixture in a microwave device according to the wet burning method, the final volume was completed to 20 mL with distilled water and filtered through blue band filter paper. In these filters, P was determined colorimetrically at 882 nm in spectrophotometer (Murphy and Riley, 1962), K, zinc (Zn), manganese (Mn), iron (Fe) and copper (Cu) Atomic Absorption Spectrophotometer device (Shimadzu AA-7000) (Kacar and Inal, 2008). N analysis was performed according to the Kjeldahl distillation method (Bremner, 1965). Leaf samples were stored at -80 ^{0}C until chlorophyll and antioxidant enzyme activity analyzes were performed.

2.3. Quantitative analysis of chlorophyll

In the study, the extraction of chlorophyll was carried out according to the Arnon's method (Arnon, 1949). Accordingly, 0.1 g of veinless leaf tissue was put in the porcelain mortar and homogenized by crushing it in 80% acetone. This process was carried out by taking care to keep the porcelain mortar cold on the ice. $MgCO_3$ was also added during crushing. Then, the obtained homogenate was centrifuged at 3000 rpm for 10 minutes. After the centrifugation, the supernatant part was filtered and transferred to a new tube. On the pellet remaining in the other centrifugal tube,

80% acetone was added as much as 4 mL and mixed and centrifuged again. After the centrifugation, it was filtered and combined with the first supernatant and the final volume was completed to 10 mL with 80% acetone. The values obtained by measuring 645 and 663 nm on the spectrophotometer were replaced in the formula below and the amounts of chlorophyll were found as mg/g (Yaban and Kabay, 2019).

Chlorophyll a (mg g^{-1}) = (12.7×A663 nm) – (2.69×A645 nm) × V/W × 10000
Chlorophyll b (mg g^{-1}) = (22.91×A645 nm) – (4.68×A663 nm) × V/W ×10000
Total Chlorophyll (mg g^{-1}) = Chlorophyll a (mg g^{-1}) + Chlorophyll b (mg g^{-1})

(A: Absorbance value measured at the specified wavelength (nm), W: Extracted fresh leaf weight (g), V: Extract volume (mL))

2.4. Antioxidant enzyme analysis

In order to determine the enzyme activity, 0.3 g of wet leaf tissue was taken into the porcelain mortar and liquid nitrogen was added to it and crushed until it turned into powder. It is then homogenized with 50 mM KH_2PO_4 (pH=7) added on it. The obtained homogenate was centrifuged at 15000 rpm for 20 minutes. After centrifugation, the supernatants were used to determine the enzyme activities of catalase (CAT), peroxidase (POD) and ascorbate peroxidase (APX). The results were determined as EU g^{-1} leaf.

2.4.1. Determination of the catalase enzyme activity

The activity of the catalase enzyme was determined by measuring spectrophotometrically at 240 nm according to the method reported by Cakmak and Marschner (1992).

2.4.2. Determination of the peroxidase enzyme activity

The activity of the peroxidase enzyme was determined by measuring spectrophotometrically at 470 nm according to the method reported by Wakamatsu and Takahama (1993).

2.4.3. Determination of the ascorbate peroxidase enzyme activity

The activity of the ascorbate peroxidase enzyme was determined by measuring spectrophotometrically at 290 nm according to the method reported by Cakmak (1994).

3. Results and Discussion

3.1. Macro and micro element concentrations

Some macro and micro element concentrations of naturally grown spinach plant are given in Table 2.

Table 2. Some macro and micro element concentrations

Element	Value
Nitrogen (%)	4.47
Phosphorus (%)	0.14
Potassium (%)	5.02
Calcium (%)	0.49
Magnessium (%)	0.78
Iron (mg kg^{-1})	91.4
Zinc (mg kg^{-1})	35.6
Manganese (mg kg^{-1})	61.1
Copper (mg kg^{-1})	9.9

According to the results of the study, the macro element concentrations of the spinach plant such as nitrogen, phosphorus, potassium, calcium and magnesium were determined as 4.47% N, 0.14% P, 5.02% K, 0.49% Ca and 0.78% Mg, respectively (Table 2). Among the microelement concentrations, iron, zinc, manganese and copper were determined as 91.4 mg kg^{-1}, 35.6 mg kg^{-1}, 61.1 mg $kg^{-1}$and 9.9 mg kg^{-1}, respectively. Similar results were found in other studies as well. Özenç and Şenlikoğlu (2017), in their study where they applied hazelnut husk compost, enriched compost, animal manure and chemical nitrogen (15 kg pure N da^{-1}), reported that compost and animal manure applications significantly increased the nutrient content of the spinach plant. In addition, they reported that the phosphorus, potassium and nitrate nitrogen concentrations of the spinach plant were between 0.12-0.52% P, 4.04-7.95% K and 332-1752 NO_3-N mg kg^{-1}, respectively. Şimşek (2019), in his study to determine the effects of increasing doses of iron on the development of the spinach plant, the iron and some plant nutrient content and the removed amounts, nitrogen, phosphorus, potassium, calcium, magnesium, copper, zinc, manganese, 5.64%-6.09% N, 0.63-0.85% P, 6.94-11.14% K, 0.44-0.61% Ca, 0.80-0.98% Mg, 11.33-13.25 mg Cu kg^{-1}, 56.22-82.64 mg Zn kg^{-1}, 67.85-90.62 mg Mn kg^{-1} between has determined. Gürses and Artık (1984) reported that the nutrients in the leaves of spinach plants taken from different places and at different dates were iron 6.75-11.58 (mg 100 g^{-1}), zinc 0.35-0.94 (mg 100 g^{-1}), potassium 295.5-397.2 (mg 100 g^{-1}), calcium 117.4-127.7 (mg 100 g^{-1}), and phosphorus 34.01-44.14 (mg 100 g^{-1}) they determined that it is between. Topcuoğlu and Yalçın (1996) investigated the effect of nitrogen and phosphorus fertilization on some macro and micronutrient contents of the spinach (*Spinaceae oleraceae* L.) plant. In the study, it was determined that increasing doses of nitrogen and phosphorus fertilizers decreased the Ca, Fe, Cu, Zn and Mn contents of the spinach plant, increasing nitrogen fertilizer applications increased the N and Mg contents of the plant, and increasing the phosphorus fertilizer applications increased the P content.

3.2. Amount of chlorophyll

Quantitatively determined chlorophyll a (mg g^{-1}), chlorophyll b (mg g^{-1}) and total chlorophyll (mg g^{-1}) amounts in the leaf of the spinach plant are given in Figure 2.

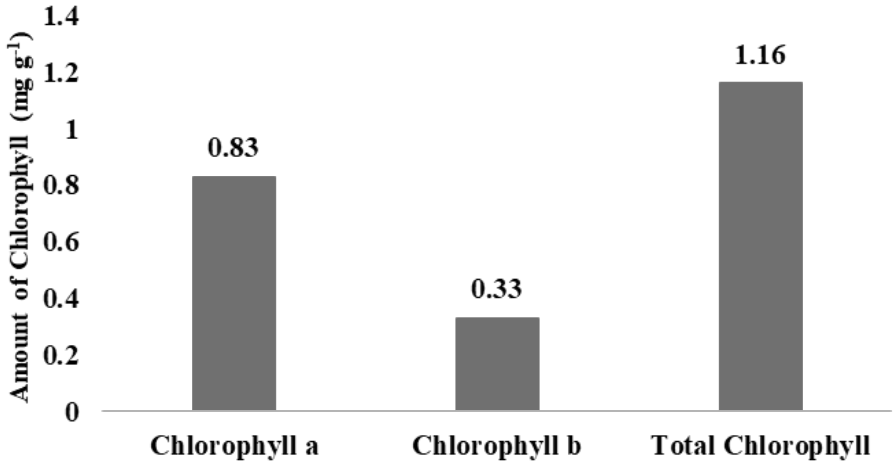

Figure 2. Chlorophyll a, chlorophyll b and total chlorophyll amount (mg g^{-1}) of spinach plant

In this study, chlorophyll a amount of spinach plant was determined as 0.83 mg g^{-1}, chlorophyll b amount was 0.33 mg g^{-1}, and total chlorophyll amount was determined as 1.16 mg g^{-1}. Chlorophyll amount in the leaf varies depending on many factors such as the type of plant, the amount of fertilizer used, the amount of irrigation, and stress factors. Kalkan (2019) investigated the effects of different solid environments on spinach cultivation in hydroponic agriculture and found the highest content of chlorophyll (0.88 mg mL^{-1}) in a mixture of 50% perlite +50% zeolite, the lowest chlorophyll a content was determined in the mixture (0.51 mg mL^{-1}) where perlite, zeolite and pomza were applied equally (1:1:1). In another study, the amounts of chlorophyll in cotyledon, 5 true leaves and harvest period of the leaves of the Matador variety spinach plant grown in the greenhouse, open field and growth chamber were determined. In the study, the highest amount of chlorophyll (1032.95 mg L^{-1}) was determined in the spinach during the harvest period grown in the greenhouse, while the lowest amount of chlorophyll (288.02 mg L^{-1}) was determined during the growth chamber cotyledon period (Deveci and Uzun, 2011).

3.3. Catalase, peroxidase and ascorbate peroxidase enzyme activities

The enzyme activity values of catalase, peroxidase and ascorbat peroxidase determined in the spinach plant are given in Figure 3.

In the study, catalase enzyme activity in spinach plant was found to be 26.62 EU g^{-1} leaf, peroxidase enzyme activity was 0.47 EU g^{-1} leaf and ascorbat peroxidase enzyme activity was 1.65 EU g^{-1} leaf (Figure 3).

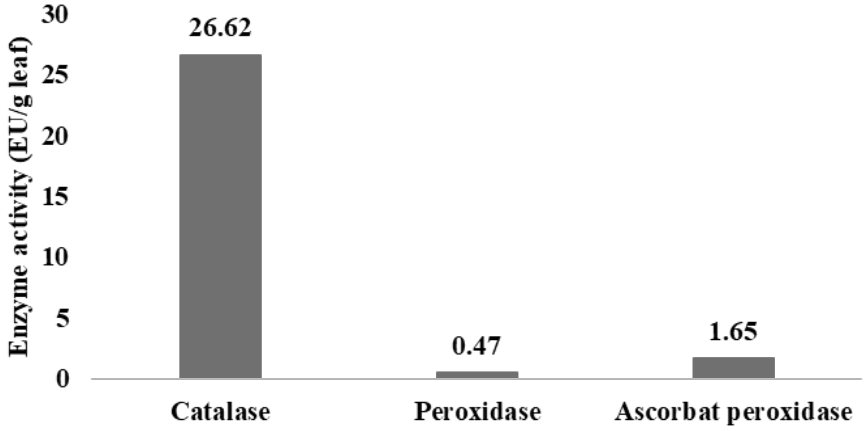

Figure 3. Catalase, peroxidase, ascorbat peroxidase enzyme activities of the spinach plant

4. Conclusion

Considering the relationship between nutrition and health, vegetables are essential nutrients in our daily diets. In this study, some nutrient element concentrations, amount of chlorophyll and some antioxidant enzyme activities of the spinach plant, which has an important place in nutrition, were tried to be determined.

In the study, it was determined that other nutrients, except phosphorus and calcium, were at a sufficient level according to Jones et al., (1991). Jones et al., (1991) determined the nitrogen, phosphorus, potassium, calcium, magnesium, iron, zinc, manganese and copper concentrations of the spinach plant 4-6% N, 0.30-0.60% P, 5-8% K, 0.70-1.20% Ca, 0.60-1.00% Mg, 60-200 mg Fe kg-1, 25-100 mg Zn kg-1, 30-250 mg Mn kg-1 and 5-25 mg Cu kg-1 respectively. On the other hand, the CAT, POD and APX enzyme activities of the spinach plant were determined as 26.62 EU g-1 leaf, 0.47 EU g-1 leaf and 1.65 EU g-1 leaf respectively. The amount of chlorophyll a, chlorophyll b and total chlorophyll in the leaves of the plant were found as 0.83 mg g-1, 0.33 mg g-1 and 1.16 mg g-1, respectively.

Spinach plant, which has a high agricultural production and consumption, has an important place in the nutrition of people both in terms of vitamins and minerals and because of its antioxidant properties. Therefore, it is thought that this study and similar studies to be carried out in the future will contribute to the literature.

References

Alibas, İ., & Okursoy, R. (2012). Karalahana (*Brassica oleracea* L. var. *acephala*), Pazı (*Beta vulgaris* L. var. *cicla*) ve Ispanak (*Spinacia oleracea* L.) yapraklarının bazı teknik özellikleri. *Uludağ Üniversitesi Ziraat Fakültesi Dergisi*, *26*(1), 39-48.

Arnon, D. I. (1949). Copper enzymes in isolated chloroplasts. Polyphenoloxidase in *Beta vulgaris*. *Plant physiology*, *24*(1), 1-15.

Bremner, J. M. (1965). Total nitrogen. *Methods of Soil Analysis: Part 2 Chemical and Microbiological Properties*, *9*, 1149-1178.

Boonla, C. (2018). Oxidative Stress in Urolithiasis. *Reactive Oxygen Species (ROS) in Living Cells*, 129-159.

Cakmak, I. (1994). Activity of ascorbate-dependent H_2O_2-scavenging enzymes and leaf chlorosis are enhanced in magnesium and potassium deficient leaves, but not in phosphorus-deficient leaves. *Journal of Experimental Botany, 45*, 1259- 1266.

Cakmak, I., & Marschner, H. (1992). Magnesium deficiency and high light intensity enhance activities of superoxide dismutase, ascorbate peroxidase, and glutathione reductase in bean leaves. *Plant Physiology, 98*(4), 1222-1227.

Candan, N., & Tarhan, L. (2003). Relationship among chlorophyll-carotenoid content, antioxidant enzyme activities and lipid peroxidation levels by Mg^{2+} deficiency in the *Mentha pulegium* leaves. *Plant Physiology and Biochemistry*, *41*(1), 35-40.

Cavdar, C., Sifil, A., & Camsari, T. (1997). Reactive oxygen particles and antioxidant defence. *Office Journal of the Turkish Nephrology, Association*, *3*(4), 92-5.

Deveci, M., & Uzun, E. (2011). Determination of phenolic compounds and chlorophyll content of spinach (*Spinacia oleracea* L.) at different growth stages. *Asian Journal of Chemistry*, *23*(8), 3739-3743.

Doğru, A. (2020). Bitkilerde Aktif oksijen türleri ve oksidatif stres. *International Journal of Life Sciences and Biotechnology*, *3*(2), 205-226.

Duman, Y. A., Acemi, A., Toygar, H. İ., Yüzügüllü, Y., & Özen, F. (2016). Tuz stresi ve BAP varlığında *Amsonia orientalis*' in antioksidan enzimlerinin incelenmesi. *Celal Bayar Üniversitesi Fen Bilimleri Dergisi*, *12*(3), 543-551.

Gürses, Ö. L., & Artık, N. (1984). Pazı, ebegümeci, semizotu ve ıspanak sebzelerinin bileşimi üzerinde araştırmalar. *Gıda Dergisi, 9*(2), 83-93.

İlhan, E. P., Çakır, Ö. Ü. Ö., Dertli, E., & Şahin, E. (2019). Yabani meyvelerin antioksidan potansiyeli. *Mas International Conference on Mathematics-Engineering-Natural&Medical Sciences-V*, May 2-5, pp. 918-927, Erzurum-Turkey.

Jabeen, M., Akram, N. A., Ashraf, M., & Aziz, A. (2019). Assessment of biochemical changes in spinach (*Spinacea oleracea* L.) subjected to varying water regimes. *Sains Malaysiana*, *48*(3), 533-541.

Jones Jr, J. B., Wolf, B., & Mills, H. A. (1991). *Plant analysis handbook. I. Methods of Plant Analysis and Interpretation.* Micro-Macro Publishing, Inc., USA.

Kacar, B., & Inal, A. (2008). Plant analysis. *Nobel Pres, 1241,* 891.

Kalkan, P. (2019). "Topraksız Tarımda Farklı Katı Ortamların Ispanak Yetiştiriciliği Üzerine Etkileri", *Akdeniz Üniversitesi. Fen Bilimleri Enstitüsü*, Yüksek Lisans Tezi.

Karabulut, H., & Gülay, M. Ş. (2016a). Antioksidanlar. *Veterinary Journal of Mehmet Akif Ersoy University*, *1*(1), 65-76.

Karabulut, H., & Gülay, M. Ş. (2016b). Serbest radikaller. *Mehmet Akif Ersoy University Journal of Health Sciences Institute*, *4*(1), 50-59.

Kasnak, C., & Palamutoğlu, R. (2015). Doğal antioksidanların sınıflandırılması ve insan sağlığına etkileri. *Turkish Journal of Agriculture-Food Science and Technology*, *3*(5), 226-234.

Kaur, C., & Kapoor, H. C. (2001). Antioxidants in fruits and vegetables–the millennium's health. *International journal of food science & technology*, *36*(7), 703-725.

Koca, N., & Karadeniz, F. (2003). Serbest radikal oluşum mekanizmaları ve vücuttaki antioksidan savunma sistemleri. *Gıda Mühendisliği Dergisi*, *16*, 32-37.

Mercan, U. (2004). Toksikolojide serbest radikallerin önemi. *Yüzüncü Yıl Üniversitesi Veteriner Fakültesi Dergisi*, *15*(1), 91-96.

Murphy J., & Riley J. P. (1962). A modified single solution for the determination of phos-phate in natural waters. *Analtica Chemica Acta., 27*, 31-36.

Özcan, O., Erdal, H., Çakırca, G., & Yönden, Z. (2015). Oksidatif stres ve hücre içi lipit, protein ve DNA yapıları üzerine etkileri. *Journal of Clinical and Experimental Investigations, 6*(3), 331-336.

Özenç, D.B., & Şenlikoğlu, G. (2017). Organik ve kimyasal azot kaynağının ıspanak bitkisinin bazı besin içeriği ve nitrat birikimi üzerine etkileri. *Anadolu Tarım Bilim. Derg., 32*(3): 398-406.

Rios-Gonzalez, K., Erdei, L., & Lips, S. H. (2002). The activity of antioxidant enzymes in maize and sunflower seedlings as affected by salinity and different nitrogen sources. *Plant Science*, *162*(6), 923-930.

Sevindik, M., Akgul, H., Selamoglu, Z., & Braidy, N. (2020). Antioxidant and antigenotoxic potential of *Infundibulicybe geotropa* mushroom collected from Northwestern Turkey. *Oxidative Medicine and Cellular Longevity*, *2020*, 1-8.

Sezer, K., & Keskin, M. (2014). Serbest oksijen radikallerinin hastalıkların patogenezisindeki rolü. *FÜ Sağ. Bil. Vet. Dergisi*, *28*(1), 49-56.

Shinde, A., Ganu, J., & Naik, P. (2012). Effect of free radicals & antioxidants on oxidative stress: A review. *Journal of Dental and Allied Sciences*, *1*(2), 63-66.

Sharma, N. (2014). Free radicals, antioxidants and disease. *Biology and Medicine*, *6*(3), 1-6.

Shrivastava, A., Aggarwal, L. M., Mishra, S. P., Khanna, H. D., Shahi, U. P., & Pradhan, S. (2019). Free radicals and antioxidants in normal versus cancerous cells—An overview. *Indian Journal of Biochemistry and Biophysics (IJBB)*, *56*(1), 7-19.

Şenlikoğlu, G. (2015). "Organik Materyal İlavesi ve Azotlu Gübre Uygulamalarının Ispanak Bitkisinin (*Spinacia oleracea* L.) Gelişimi ve Nitrat Akümülasyonuna Etkileri", *Ordu Üniversitesi Fen Bilimleri Enstitüsü*, Yüksek Lisans Tezi.

Şimşek, O. (2019). "Artan Miktarlarda Uygulanan Demir Dozlarının Ispanak Bitkisinin Gelişimi ve Kimi Besin Elementi İçeriğine Etkisi", Bursa Uludağ Üniversitesi *Fen Bilimleri Enstitüsü,* Yüksek Lisans Tezi.

Topcuoğlu, B., & Yalçın, S. R. (1996). Azotlu ve fosforlu gübrelemenin ıspanak bitkisinin (*Spinaceae oleraceae* L.) bazı makro ve mikro besin maddesi içerikleri üzerine etkisi. *Tarım Bilimleri Dergisi, 2*(2), 39-48.

Valko, M., Leibfritz, D., Moncol, J., Cronin, M. T., Mazur, M., & Telser, J. (2007). Free radicals and antioxidants in normal physiological functions and human disease. *The international journal of biochemistry & cell biology*, *39*(1), 44-84.

Wakamatsu, K, & Takahama U. (1993). Changes in peroxidase activity and in peroxidase isozymes in carrot callus. *Physiologia Plantarum, 88*, 167-171.

Yaban, İ., & Kabay, T. (2019). Kuraklık stresinin urfa biberinde iyon klorofil ve enzim içerikleri üzerine etkisi. *Toprak Su Dergisi, 8*(1), 11-17.

CHAPTER 4

OPTICAL PROPERTIES OF PDLC FILMS

Rıdvan KARAPINAR

(Prof. Dr.), Burdur Mehmet Akif Ersoy University, rkarapinar@mehmetakif.edu.tr

Orcid: 0000-0002-4694-6876

1. Introduction

Polymer-dispersed liquid crystals (PDLCs) are novel materials for display applications (Bloisi and Vicari, 2003; Coates, 2000; Crawford et al., 1998; Drzaic, 1995; Kitzerow, 1994; Vaz, 1989). They exhibit interesting electro-optic properties such as wide viewing angle and high brightness. They do not need polarizers which absorb transmitted light and they require no alignment layers. Since the fabrication process of PDLC film is easy, these materials offer some advantages over the well-established twisted nematic devices in the market of liquid crystal display technology. The PDLCs are used in a wide variety of applications, such as switchable privacy windows and light shutters (Fuh et al., 2004; Hakemi et al., 2019; Karapinar, 2017; Simoni, 1992; Zhang et al., 2013). By using different phases of liquid crystals and nano materials, several types of PDLCs have been developed. Polymer-dispersed cholesteric liquid crystals are important classes of liquid crystal-polymer composite materials (Dierking, 2000). Dye-doped PDLC films are also attractive materials for smart window applications (Kim et al., 2015). Polymer-dispersed ferroelectric liquid crystal films are of great interest due to fast switching response (Karapinar and O'Neill, 1998). On the other hand, PDLC films can also be made by using biomaterials (Marin and Karapinar, 2016). Regarding nanomaterials, nanoparticle-doped PDLCs demonstrate better performance relative to conventional PDLC materials (Jamil et al., 2011).

PDLC materials consist of micron-sized droplets of a low-molecular weight nematic liquid crystal dispersed in a polymer matrix (Drzaic and Drzaic, 2006). These materials operate on the principle of electrically controlled light scattering effect. When a PDLC material is sandwiched between glass substrates with transparent conductive electrodes, it can be switched from an opaque state to a transparent state upon application of an electric field. Physical mechanism of this effect depends on anisotropic behaviour of liquid crystal materials. The birefringent nature of the material is due to the orientation of the molecules within the droplet. Since the nematic liquid crystals are anisotropic, they can be described by two principal indices of refraction, namely the ordinary refractive index (n_o) and extraordinary refractive index (n_e). At

zero electric field, the nematic liquid crystal molecules inside droplets show different orientations. Because of the mismatch between effective refractive index of the liquid crystal and the refractive index of the polymer matrix (n_p), the incident light is scattered by the droplets. The scattering phenomenon occurs when the wavelength of the incoming light is comparable with the dimensions of the liquid crystal domains in the dispersion. Under the unpolarized incident light, the cell shows milky appearance because of the light scattering. However, the application of the electric field which is normally directed to the surface of the film causes orientation of the liquid crystal molecules, so that the light only experiences the ordinary refractive index which is close to the value of the index of refraction of the polymer matrix. That is, the index of refraction of the LC droplets (n_o) is nearly the same as that of the polymer (n_p). So, at an oblique angle of incidence, there is no light scattering and the PDLC film becomes transparent since it only experiences one refraction index. Removal of the electric field returns the PDLC system to the opaque state since the elastic torques due to the surface interactions at the droplet walls returns the molecules to their initial state of alignment. Thus, the PDLC film can switch between highly scattering state and the transparent state with the application of the electric field. The schematic diagram of the operation principle of a PDLC film is shown in Figure 1.

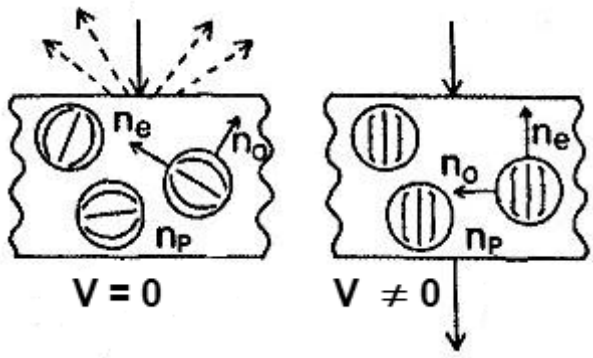

Figure 1. The principle of operation of a PDLC film.

The PDLC materials are fabricated by phase separating the liquid crystal from the polymer, by microencapsulation, emulsion method, and electron-beam cure method (Chen et al., 2009; Drzaic and Muller, 1989; Mucha, 2003; Vaz et al., 1991). Preparation of the PDLC films containing a small amount of liquid crystalline polymer and their applications has also been reported (Park et al., 2000). The properties of the PDLCs are depended on the related used method. The size and morphology of the liquid crystal droplets and preparation conditions are important factors in the production of PDLCs. The phase separation method has some advantages such as the ability of controlling size and uniform droplet formation (Di Bella, et al., 1998). The phase separation can be achieved by different processes, namely phase separation by thermal, by solvent evaporation and by photopolymerization (Bronnikov, et al., 2013;

Challa et al., 1995). In each of these processes a homogenous solution of polymer with a liquid crystal material is formed and followed by phase separation which leads to droplet formation. Thermally induced phase separation (TIPS) occurs when the polymer has a melting temperature below its decomposition temperature. Liquid crystal is mixed with a melted polymer and then the mixture is cooled at a specific rate to obtain phase separation. While the polymer hardens, liquid crystal droplets appear. The droplet size is affected by the cooling rate of the PDLC material. In this method, large concentration of liquid crystal is needed for the preparation of the PDLC sample. Solvent-induced phase separation (SIPS) occurs when the mixture of polymer and liquid crystal is dissolved in the same solvent. The solvent evaporation at a specific rate causes the phase separation. The liquid crystal droplets start to grow as the polymer and liquid crystal come out of the solution and stop their growth when the solvent is completely removed. For the preparation of PDLC samples, the photopolymerization-induced phase separation (PIPS) is so well-known method (Park et al., 2010). In this technique a homogeneous mixture of prepolymer and liquid crystal is cured under the ultraviolet (UV) light and the curing leads to a phase separation process resulting in the formation of nematic microdomains. The solubility of liquid crystals decreases as the polymer weights increases until the droplets formation. These droplets grow until gelation of the polymer constrains change of the droplet morphology. Droplet size and morphology are dependent on the type and relative concentration of liquid crystal and polymer material and also some physical parameters such as viscosity, solubility of the liquid crystal in the polymer. Thus, the morphology of PDLC is affected by both the photopolymerization and phase separation processes. The main factors that influence the size of the liquid crystal droplets are the curing temperature, polymerization rate and concentrations of materials (Magagnini et al., 1999; Raina et al., 2006; Roussel et al., 1998). The polymerization rate is determined by the UV intensity; more UV intensity results in fast curing and short curing time and small droplet size. Curing temperature also affects the mutual solubility of liquid crystals and polymer. A change in curing temperature also affects droplet morphology. Best droplet formation occurs in the temperature range where curing is complete. The relationship between formation kinetics and microdroplet size epoxy based PDLCs has been studied by Smith and Vaz (1998). The PDLC materials with nano-sized droplets have also been characterized (Karapinar et al., 2009; Lucchetta et al. 2002). The nanosized droplets of liquid crystal, ranging from 100-250 nm, can be prepared by rapid polymerization of a highly functionalized monomer (Natarajan et al., 1997). By controlling the polymerization rate and adjusting the concentrations of the liquid crystal and polymer material, it is possible to obtain different types of morphologies.

Electro-optical properties of PDLC films are of interest due to many applications in display devices (Karapinar, 1998; Liu et al., 2002; Olenik et al., 2006; Vorflusev and Kumar, 1998). There is an experimental study about electro-optic characteristics of a polymer-stabilized, in-plane-switching liquid crystal cell as the UV curing temperature. It has been reported that the response time of the cell could be reduced through low-temperature UV curing of a low concentration of polymer material. It has also been found that fast switching might also be achieved at a low operating voltage. Curing of the polymer at lower temperature could reduce the average distance

between polymer bundles even at low polymer concentrations (Woo et al., 2017). Theory of nematic-isotropic phase transitions in restricted geometry is one of research topics (Poniewierski and Sluckin, 2006). Electro-optical modulation by PDLC films has been studied (Vicari, 1997). Light modulation by nano-sized PDLC materials has been reported (Karapinar, 2014). Different types of materials have been used as polymer matrix in PDLC films (Hoppe et al., 2003; Klosowicz, 1994). On the other hand, there are some eutectic liquid crystal polymer blends for PDLC applications (Hakemi and Hakemi, 2019). The different sizes of the liquid crystal droplets lead to different macroscopic optical properties. In this study, thin PDLC films were fabricated by photopolymerization induced phase separation method. The fabrication of these films and their optical characteristics were reported.

2. Experimental Section

The liquid crystal material used in this experiment was a cyanobiphenyl mixture (BL001) which has high nematic-isotropic phase transition point (T_{NI} = 61˚C). BL001 is an eutectic mixture consisting of several cyanobiphenyl and cyanoterphenyl compounds (Figure 2) and it has better solubility in UV cured polymers. Due to mixing of several liquid crystal compounds, BL001 has a broad liquid crystal phase of between -10 and 61°C. Phase transition temperatures were measured by DSC instrument. This material has an ordinary refractive index, $n_o \cong 1.522$.

The prepolymer used was Norland Optical Adhesive 65 (NOA65) which is a UV curable polymer and has a refractive index $n_p \cong 1.524$ at room temperature. All materials were used without any further purification. NOA65 is a clear and colourless photopolymer that is cured when exposed to UV light. Its viscosity 1200 cps at 25 °C. Since it is one-part system, it has many advantages in bonding of optical materials where the bonding surface can be exposed to light. For this material, curing time is remarkably fast, and is dependent upon the intensity of UV light. NOA65 has a maximum absorption within the range of 350-380 nm. The PDLC mixture consists of 50% of BL001 and 50% of NOA65.

The PDLC films were formed by PIPS process. For this aim, the liquid crystal was initially dissolved in a polymer to form a homogenous isotropic solution. This homogenous mixture was filled into two glass plates with conductive ITO electrodes and then irradiated by UV light. The PDLC film becomes completely homogeneous over the whole area, which are commonly generated if the mixture is injected by capillary action. The film thickness was maintained constant by spacers of 23 mm thickness. Schematic structure of the PDLC film is shown in Figure 3. Thus, the PDLC film is made of two layers of transparent conductive films sandwiched with PDLC material. When voltage is applied to the film the liquid crystals in the droplets are aligned along the electric field and the films becomes transparent. When the voltage is turned off, the liquid crystals return to their scattering state and turn the film to translucent state.

The PDLC sample was cured by UV light with an emission maximum at 254 nm using a uniform light source of 24 mW/cm^2. During the exposure, the nematic range temperature of the cell was controlled by a heating plate. The cells were irritated for

10 minutes in order to ensure that the polymer matrix was completely crosslinked. The sample was opaque white upon cooling to room temperature.

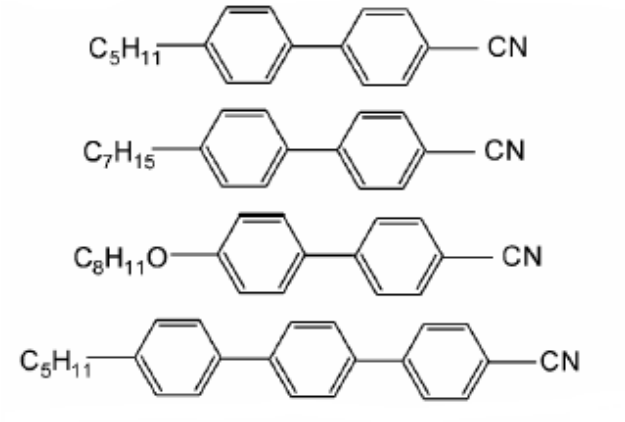

Figure 2. Chemical structure of the liquid crystal mixture.

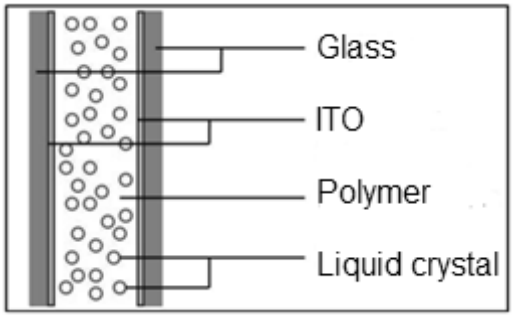

Figure 3. Schematic structure of the PDLC film.

The PDLC samples were observed under the polarizing microscope. Polarized Optical Microscopy (POM) is very useful method in characterizing PDLC films such as mapping droplet configurations. This type of visual technique provides information about the shape and distribution of the liquid crystal droplets.

In order to investigate the droplet size and presence of phase separation, the PDLC films were observed by Scanning Electron Microscope (SEM) at a 500x magnification. This analysis technique enables to investigate the morphology of the PDLC structures. For the observation of SEM micrographs, after removing one of the two glasses, samples were placed under vacuum for some hours. Samples cross sections were obtained fracturing the samples in liquid nitrogen. The liquid crystal was removed from the samples by immersing them in a solvent. Then, the samples were dried in an oven and coated with a thin layer of gold using a sputter coater. Thus, SEM photographs of the polymer microstructures were taken.

To measure the light transmittance of the films, the PDLC cell was held in a cell holder on an electro-optical bench. The light source used was a He-Ne laser (λ = 633 nm). The light passing through the film was focused on to a photodiode. The transmittance of the sample was obtained by measuring the intensity of the probe beam. The photodetector output was recorded on an oscilloscope. Thus, applying AC voltages to the film while monitoring the transmission, the voltage-transmission curves were plotted.

In order to determine the electro-optical response of the film, a square wave with a certain frequency was applied to the PDLC film and the optical response was monitored on the oscilloscope screen. All measurements were carried out at room temperature.

3. Results and Discussion

PDLC films are composite materials in which liquid crystals are randomly distributed in polymer matrix. The PIPS process takes place when a liquid crystal is mixed with a prepolymer that has not yet undergone polymerization to obtain a homogenous solution, and then cured by UV light. As the reaction progress, the liquid crystal molecules come out of mixture and begin to form micron-sized droplets. It is possible to control the curing conditions of the PDLC films.

Birefringence of the liquid crystal gives interesting textures under polarized light. The PDLC samples are birefringent, however the heating of the samples above phase transition point causes to the isotropic state of the liquid crystal droplets. A typical optical image of the PDLC film is shown in Figure 4.

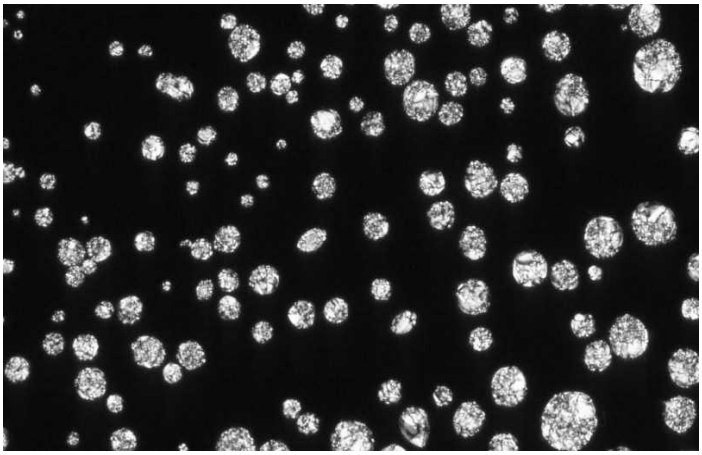

Figure 4. Liquid crystal droplets in the PDLC film.

Temperature dependence and phase behaviour of PDLC film is a research area (Amundson, 1996; Challa et al., 1995). Droplets grow until polymer matrix becomes solid enough that molecules are trapped and can no longer move easily. The main parameters which affect the size of liquid crystal droplets in the PIPS process are the

cure temperature and the proportions of the materials used. The curing temperature affects the reaction speed of the polymerization and solubility of the liquid crystal in the polymer. The liquid crystal concentration also affects clarity of the PDLC film. More clear film was the film containing the lowest concentration of polymer. Clarity of the film can be affected by several factors. These factors are all related to the rate at which UV phase separates during the PDLC formation. The orientation of the molecules inside droplets can be radial or bipolar (Figure 5). The radial configuration occurs when the liquid crystal molecules are anchored with their long axes perpendicular to the droplet wall. Radial droplets indicate the order of the liquid crystal molecules in the polymer matrix because of strong interfacial forces between the liquid crystal molecules and the polymeric matrix. The bipolar configuration is obtained by tangential anchoring the liquid crystal molecules. Optical microscopy images indicate a predominant bipolar structure in different types of PDLC films but with varying size and density. PDLC films for different regions have different morphological characteristics as observed in POM images and are dependent on LC droplet shape, size and distribution (Das and Rey, 2004). Influence of PDLC droplets of molecular orientation in the light transmission has been reported in literature (Bloisi et al., 1996).

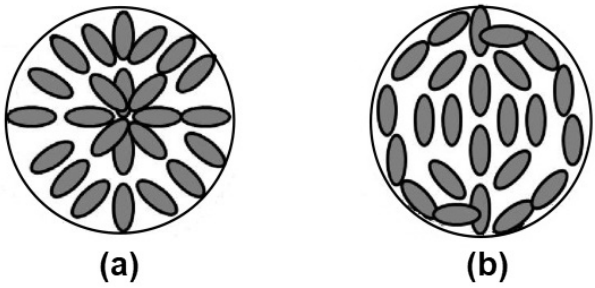

Figure 5. The configurations of molecules (a) radial and (b) bipolar.

The electro-optical properties of the PDLC films also depends on the size and shape of the liquid crystal droplets. In order to evaluate these parameters, the PDLC films were examined by using SEM. Analyses were performed on both the sample surfaces and in cross section. The surface images from SEM were taken for small pieces of the prepared PDLC films. A typical SEM image of the PDLC film is shown in Figure 6. Dark areas in the SEM microphotograph reveal the absence of the liquid crystal material which corresponds to the original liquid crystal domains. Droplet dimensions varies between 2-10 μm in the middle and the centre regions. Liquid crystal droplets are observable along the whole volume, but appear to be interconnected, this means that phase separation process is not fully completed. Droplets dimension increases passing from the upper irradiated surface to the lower one. Droplets mean sizes are always smaller near the surface directly exposed to UV light than near the other surface. Thus, droplets with submicron dimensions can be obtained by a proper choice of curing parameters. For example, low curing time and high UV intensity

lead to droplets which are not well phase-separated from polymer matrix and not uniformly dispersed (Di Bella et al., 1998). On the other hand, morphological changes with increasing cure temperature are associated with a delayed phase separation. SEM studies showed that the PDLC morphology was strongly affected by the LC concentration and the curing temperature. A typical PDLC morphology with isolated LC droplets dispersed in a polymer matrix is only observed at low LC compositions and at low cure temperatures (Han, 2006). In PDLC thin films, and optical and scanning microscopy methods are also used to investigate field molecular reorientation. Strong electric fields are required to reorient the liquid crystals near the polymer interface compared to those required to reorient molecules in the droplet centre. Therefore, different reorientation mechanisms exist along the axis of the liquid crystal droplets (Mei and Higgins, 2000). In the literature fabrication of PDLC flakes has also been reported (Kosc et al., 2005). PDLC flakes suspended in a host fluid can be controlled with an external electric field. The field acts to induce a dipole moment on the flake. The results indicate that the flakes would reorient to align along the electric field.

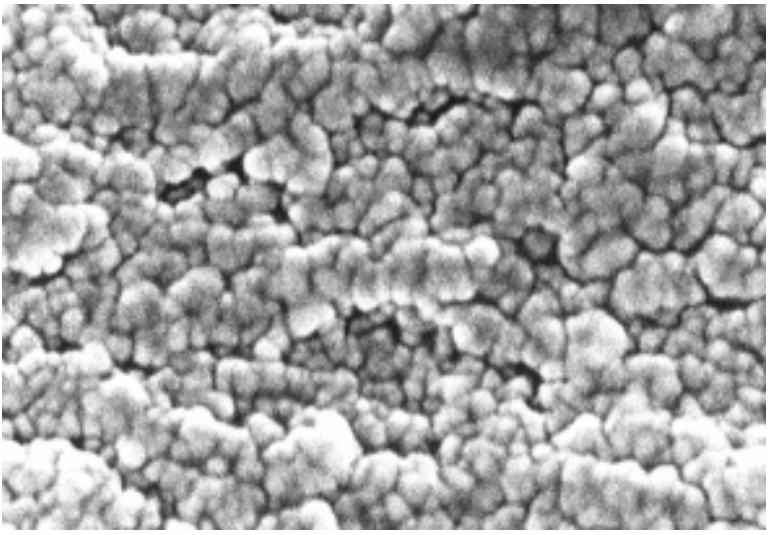

Figure 6. SEM micrograph of the microstructure of polymer matrix.

The optical behaviour of the film was observed by light transmission measurements. A typical transmittance curve as a function of the applied voltage for a PDLC film is shown in Figure 7. Optical transmittance is an important parameter of the performance of the PDLC film. It is a measure of the ability of the film to modulate the incident light. The change in transmittance $\Delta T = (T_{on} - T_{off})$ between the off and on states was about 75% using a light transmission set-up. It is known that incomplete polymerization of the samples leads to higher threshold voltage and a lower clarity state transmission. When the amount of the monomer is too low, the shape of the droplets became irregular which results in larger threshold voltages.

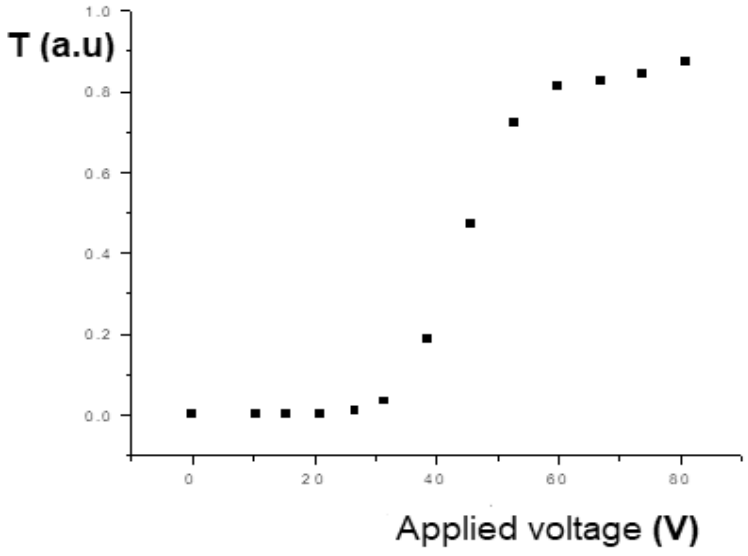

Figure 7. Light transmission as a function of applied voltage.

Optical properties of the PDLC samples can be modulated by changing the polymerization conditions. When the size of the domain decreases it needs high electric field to orient the molecules in a liquid crystal domain. It is clear that in order to use PDLC films in practical applications, such as smart glass for a variable intensity of light, there should be a suitable solution that does not limits the applied voltage or response time. As the dimension of the droplets becomes smaller, the interaction between the polymer and liquid crystal becomes more significant. Because of the higher anchoring of the liquid crystal with the polymer material, a greater electric field-induced torque is necessary to switch the PDLC film. This results in an increase in the threshold voltage. If the size of the liquid crystal is larger, a lower threshold voltage is required because of the anchoring energy at the interface between the liquid crystal droplet and the polymer. That is, threshold voltage depends on the droplet size, droplet shape and anchoring condition of the liquid crystal. In particular, the threshold voltage for the transition to the transparent state is inversely related to size of liquid crystal droplets. The study of reorientation dynamics of the liquid crystal in a PDLC is given by Mucha, and Nastal, (1997).

The response time of a PDLC film is a function of the external applied voltage. Response time can be defined as the period between 10% and 90% of transmitted light intensity. PDLC films showed fast response to applied voltages. As expected theoretically high voltages shorten the response time. Thus, the response times decrease with increasing applied voltages. Response time is also function of temperature. The response time decreases when the temperature increases. The switching behaviour of the PDLC devices is characterized at different voltages using an AC voltage driver

by at specific frequency values. When the droplets are aligned in the direction of the applied field, the PDLC film became transparent. A typical electro-optical response of the PDLC film is shown Figure 8. For frequency of f = 100 Hz and applied voltage V = 40 V, a typical response time is about 3 ms.

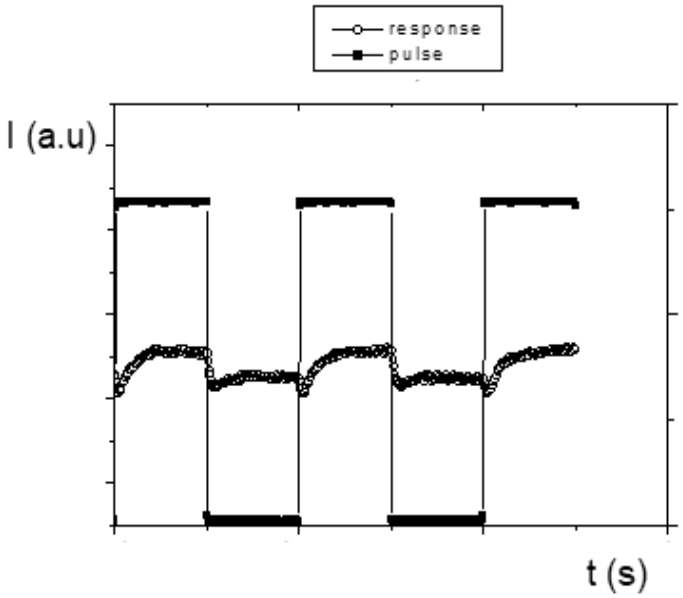

Figure 8. A typical response of the PDLC sample.

The PDLC technology is promising research area and there are new developments in this field. In recent years, significant progress has been made in the preparation, properties and applications of the PDLC films. The electro-optical properties of the PDLC films is optimized by the structural variation of polymer and liquid crystal materials. On the other hand, doping nanoparticles into PDLC films improve the electro-optical performance of the PDLC films. These materials show great potential for application in displays. New applications are related with device components of OLED, sensors, next-generation smart windows, wearable devices (Saeed at al., 2020).

To summarize The PDLC materials are comprised of a polymer matrix sandwiched between two conductive transparent glass substrates. Liquid crystal droplets are randomly dispersed in polymer matrix. The PDLCs can be controlled by an external applied field. In the absence of electrical voltage, liquid crystal molecules show random arrangement and incoming light is strongly scattered by the droplets. Thus, PDLC film appears turbid. When the voltage is applied, molecules align along electric field and PDLC film becomes transparent. The effects of curing parameters on film morphology are analysed by optical microscopy and SEM. Besides, UV intensity has

an important role in the phase separation process. It affects not only size of liquid crystal droplets, but also the morphological uniformity of PDLC films. Film morphology, droplets size and shape affect the electro-optical response of the PDLC film. The ratio between liquid crystal and polymer concentration is also an important parameter in determining the electro-optic properties of the films. The film performance is related with its response to the applied voltage. Fast switching response of a PDLC film is a critical factor in many applications. The switchable PDLCs can be used as privacy optical devices, reflective displays and solar controlled windows.

References

Amundson, K. (1996). Electro-optic properties of a polymer-dispersed liquid crystal film Temperature dependence and phase behaviour, *Physical Review E*, 53(3): 2412-2422.

Bloisi, F. and Vicari, L. (2003). Polymer-dispersed liquid crystals, *Optical Applications of Liquid Crystals:* 148-200.

Bloisi, F., Ruocchio, C. et al. (1996). PDLC: influence of droplet order parameter in light transmittance, *Optics Communications*, 123: 449-452.

Bronnikov, S., Kostromin, S. and Zuev, V. (2013). Polymer-dispersed liquid crystals: Progress in preparation, investigation, and application, *Journal of Macromolecular Science*, Part B, 52: 1718–1735.

Challa, S. R., Wang, S. Q. et al. (1995). Thermal induced phase separation of E7/ PMMA PDLC system, *Journal of Thermal Analysis*, 45(6): 1297-1312.

Chen, K.F., Wang, F.S., et al., (2009). Multicolor polymer disperse microencapsulated liquid crystal displays, *Journal of Display Technology*, 5(6): 184-187.

Coates, D. (2000). Liquid crystal polymers - synthesis, properties and applications, *Rapra Review Reports,* 10(10): 1-3, 5-157.

Crawford, G. P., Jr. Whitehead, J. B. et al. (1998). Optical properties of polymer dispersed liquid crystals, *Optics of Thermotropic Liquid Crystals*, 233-288.

Das, S. K. and Rey, A. D. (2004). Texture formation under phase ordering and phase separation in polymer-liquid crystal mixtures, *Journal of Chemical Physics*, 121(19): 9733-9743.

Di Bella, S., Lucchetti, L. and Simoni, F. (1998). Droplets formation in UV cured polymer dispersed liquid crystals, *Mol. Cryst. Liq. Cryst*., 320: 139-148

Dierking, I. (2000). Polymer network: Stabilized liquid crystals, *Adv. Mater*., 212, 167-181.

Drzaic P.S. (1995). Liquid crystal dispersions. World Scientific. Singapore.

Drzaic, P. S. and Muller, A. (1989). Droplet shape and reorientation fields in nematic droplet/polymer films, *Liquid Crystals*, 5(5): 1467-1475.

Drzaic, P and Drzaic, P.S. (2006). Putting liquid crystal droplets to work: a short history of polymer dispersed liquid crystals*, Liquid Crystals*, 33:11-12, 1281-1296.

Fuh, A. Y. G. and Lin, T.H. (2004). Electrically switchable spatial filter based on polymer-dispersed liquid crystal film, *Journal of Applied Physics*, 96(10): 5402-5404.

Han, J.W. (2006). Morphological studies of polymer dispersed liquid crystal materials, *Journal of the Korean Physical Society*, 49(2): 563-568.

Hakemi H, Pinshow O, Gal-Fuss D. (2019). Evaluation of polymer dispersed liquid crystal (PDLC) for passive rear projection screen application, *Recent Progress in Materials*, 1(3):1-15.

Hakemi H., Hakemi., G. (2019). Eutectic liquid crystal polymer blends for self and thermoplastic reinforcement, *Mol. Cryst. Liq. Cryst.,* 667; 25-35.

Hoppe, C. E., Galante, M. J. et al. (2003). Polymer-dispersed liquid crystals based on polystyrene and EBBA: analysis of phase diagrams and morphologies generated, *Macromolecular Chemistry and Physics*, 204(7): 928-935.

Jamil, M., Farzana, A., J. T. Rhee, J.T. and Jeon, Y.J. (2011). Nanoparticle-doped polymer-dispersed liquid crystal display*, Current Science*, 12 (25): 1544-1552.

Karapinar, R. (1998). Electro-optic response of a polymer dispersed liquid crystal film, *Journal of Physics,* 22, 227-25.

Karapinar, R. and O'Neill, M. (1998). Electro-optic switching properties of a polymer dispersed ferroelectric liquid crystal device, *Journal of Physics D: Applied Physics,* 31: 900-905.

Karapinar, R., Lucchetta, D.E. and Simoni, F. (2009). Electro-optical effect in a nano-sized PDLC film, *10th European Conference on Liquid Crystals,* Colmar, France, 19-24 April

Karapinar, R. (2009). Electro-optical phase shift in a nanosized polymer-dispersed liquid crystal cell, *26. International Physics Congress*, Bodrum/Muğla, Turkey, 24-27 September.

Karapinar, R. (2014). Light modulation by PDLC films, *International Semiconductor Science and Technology Conference (ISSTC-2014),* Istanbul Medeniyet University, Istanbul, Turkey, 13-15 January.

Karapinar, R. (2017). PDLC smart windows for sunlight control, *International Multidisciplinary Studies Congress*, Akdeniz University, Antalya, Turkey, 25-26 November.

Kim, M., Park, K.J., Seok, S. et al. (2015). Fabrication of microcapsules for dye-doped polymer-dispersed liquid crystal-based smart windows, CS Appl. Mater. Interfaces, 7(32): 17904–17909.

Kitzerow H.S. (1994). Polymer-dispersed liquid-crystals from the nematic curvilinear aligned phase to ferroelectric films, *Liquid Crystals*, 16: 1-31.

Klosowicz, S. J. (1994). Poly(methyl methacrylate) based polymer dispersed liquid crystals, Molecular Crystals and Liquid Crystals Science and Technology, Section C: *Molecular Materials*, 4(4): 277-281.

Kosc, T. Z., Jacobs, S. D. and Lambropoulos, J. C. (2005). Polymer cholesteric liquid-cystal flake reorientation in an alternating-current electric field, *Journal of Applied Physics*, 98: 6612-6615.

Liu, J.-H. and Wang, H.-Y. (2002). Optical switching behaviour of polymer-dispersed liquid crystal composite films with various novel azobenzene derivatives, *Journal of Applied Polymer Science*, 91: 789-799.

Lucchetta, D. E., Karapinar, R., Manni, A. and Simoni, F. (2002). Phase-only modulation by nanosized polymer-dispersed liquid crystals, *Journal of Applied Physics*, 91(9): 6060-6065.

Magagnini, P., Paci, M. et al. (1999). Polymer-dispersed liquid-crystal polymers (PDLCPs), Morphology of the LCP droplets. *Polymer Engineering and Science,* 39(10): 1891-1902.

Marin, L. and Karapinar, R. (2016). Polymer dispersed liquid crystal design, Multiphase Polymer Systems: Micro- to Nanostructural Evolution in Advanced Technologies, Edited by A.I. Barzic, S. Ioan, Taylor & Francis, CRC Press, 119-135.

Mei, E., and Higgins, D. A. (2000). Nanometer-scale resolution and depth discrimination in near-field optical microscopy studies of electric-field-induced molecular reorientation Dynamics, *Journal of Chemical Physics*, 112: 7839-7847.

Mucha, M. (2003). Polymer as an important component of blends and composites with liquid crystals, *Progress in Polymer Science*, 28(5): 837-873.

Mucha, M. and Nastal, E. (1997). Complex study of reorientational dynamics of the liquid crystal in PDLC films, *Liquid Crystals*, 23(5): 749-758.

Natarajan, L. V., Sutherland, R. L. et al. (1997). Liquid crystal dispersions in polymers: novel nanostructures, *Polymer Preprints (American Chemical Society, Division of Polymer Chemistry)* 38(2): 634-635.

Olenik, D., Copic, M., Sousa, M. E. and Crawford, G. P. (2006). Optical retardation of in-plane switched polymer-dispersed liquid crystals., *Journal of Applied Physics*, 100, 033515-0033515-7.

Park, N. H., Cho, S. A. et al. (2000). Preparation of polymer-dispersed liquid crystal films containing a small amount of liquid crystalline polymer and their properties, *Journal of Applied Polymer Science*, 77(14): 3178-3188.

Park, S., Kim, H.K. and Hong, J.W. (2010). Investigation of the photopolymerization-induced phase separation process in polymer dispersed liquid crystal, *Polymer Testing*, 29(7): 886-893.

Poniewierski, A. and Sluckin, T. J. (2006). Theory of the nematic-isotropic transition in a restricted geometry, *Liquid Crystals*, 33(11-12): 1260-1280.

Raina, K. K., Kumar, P. and Malik, P. (2006). Morphological control and polarization switching in polymer dispersed liquid crystal materials and devise, *Bulletin of Material Science*, 29(6): 599-603.

Roussel, F., Buisine, J. M. et al. (1998). Photopolymerization kinetics and phase behaviour of acrylatebased polymer dispersed liquid crystals, *Liquid Crystals*, 24(4): 555-561.

Saeed, M.H., Zhang, S. et al. (2020). Recent advances in the polymer dispersed liquid crystal composite and its applications, *Molecules*, 25(5510):1-22.

Simoni, F. (1992). Optical properties of polymer dispersed liquid crystals. Nonlinear optical properties of liquid crystals and polymer dispersed liquid crystals. Singapore, World scientific publishing Co. 2**:** 176-212.

Smith, G. W., and Vaz, N. A. (1988). The relationship between formation kinetics and microdroplet size of epoxy-based polymer-dispersed liquid crystals, *Liquid Crystals*, 3(5): 543-571.

Vaz, N. A. (1989). Polymer-dispersed liquid crystal films: materials and applications, *Proceedings of SPIE-The International Society for Optical Engineering*, 1080: 2-10.

Vaz, N. A., Smith, G. W. et al. (1991). Polymer-dispersed liquid crystal films formed by electron-beam cure, *Molecular Crystals and Liquid Crystals*, 197: 83-101.

Vicari, L., (1997). Electro-optic phase modulation by polymer dispersed liquid crystals, *Journal of Applied Physics*, 81 (10): 6612-6615.

Vorflusev, V. and Kumar, S. (1998). Electro-optical properties of thin PDFLC films prepared by TIPS and PIPS methods, *Ferroelectrics, 213(1-4): 117-124.*

Woo, J.H., Choi, T.H., Jeon, B.G. and Yoon, T.H. (2017). Effects of curing temperature on electro-optical characteristics of a polymer-stabilized in-plane-switching liquid crystal cell, *Crystals*, 7(260): 1-8.

Zhang, C., Wang, D., Cao, H., Song, P., Yang, C., Yang, H., et al. (2013). Preparation and electro-optical properties of polymer dispersed liquid crystal films with relatively low liquid crystal content, *Polym. Adv. Tech*., 24: 453-459.

CHAPTER 5

THE EFFECT OF MOBILE PHASE pH ON CAPACITY FACTOR AND SELECTIVITY IN HIGH PERFORMANCE LIQUID CHROMATOGRAPHY

Murat Soyseven[1] & Burcu Sezgin[2]

[1](Dr.) Anadolu University, e-mail:msoyseven@anadolu.edu.tr

Orcid: 0000-0002-6433-2392

[2](Dr.) Eskişehir Osmangazi University, e-mail:bsezgin@ogu.edu.tr

Orcid: 0000-0003-0279-4839

1. Introduction

High Performance Liquid Chromatography (HPLC) is the most widely used analytical technique for the separation of non-volatile chemical and biological components. HPLC technique is frequently preferred in many fields of science, from drug substance analysis, food analysis, health to agriculture due to its various advantages. With this technique, it is possible to detect quantitatively sensitive, fast and reliable components (pharmaceutical active ingredients, amino acids, sugars, vitamins, antibiotics, pesticides, food additives, food toxins, etc.) in a liquid (Sezgin, Arli, & Can, 2021; Soyseven, Aboul-Enein, & Arli, 2021; Soyseven, Kaynak, Celebier, Aboul-Enein, & Arli, 2020). In addition, the most important advantages of the method include its sensitivity, reproducibility, easy adaptability to quantitative determinations and suitability for the separation of compounds that are non-volatile or easily degraded by temperature (Moldoveanu & David, 2002; Moldoveanu & David, 2013a; Snyder, Kirkland, & Dolan, 2011; Vailaya & Horváth, 1998).

The main parts of an HPLC device are an infusion pump, a column and a column oven, a degasser, a sampler, detectors, a data recording and processing device. In the HPLC method while the mobile phase is polar and the column is apolar, it is called reverse phase chromatography; while the mobile phase is apolar and the column is polar, it is called normal phase chromatography. The most commonly used HPLC method is reversed phase chromatography. The stationary phases used in HPLC systems generally consist of columns with a diameter of 1-5 µm. The liquid phase (mobile phase) passes through the column by means of a pump. The target substance is injected in the mobile phase and passed through the relevant column (Moldoveanu & David, 2013a; Snyder et al., 2011; Snyder, Kirkland, & Glajch, 2012). As the mobile phase flows, substances leaving the column and separated from each other can be detected by various methods. These dissolved molecules are separated by some physicochemical properties (UV-absorption, refractive index, fluorescence, etc.) that

make them detectable. Detection of the compound is performed by obtaining a graphic output called a chromatogram via an electrical signal (Singh, 2013).

Components separated from the mixture are displayed as distinct peaks on the chromatogram and have different retention times (t_R). Each peak on the chromatogram represents a different component in the mixture. An example chromatogram of a mixture is shown in **Figure 1**.

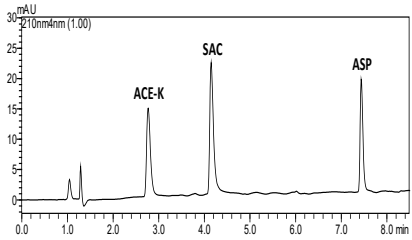

Figure 1. HPLC chromatogram example of various sweeteners with different retention times (Sezgin, Can & Arli, 2016).

In the reverse phase HPLC procedure, the removal of an ionizable compound is dependent on the hydrophobicity and degree of ionization of the substance, which is directly related to the mobile phase pH and the pK_a of the analyte. It is known that the percentage of organic matter in the mobile phase affects these parameters. Therefore, pH control is very important to obtain sensitive, accurate and precise results in HPLC analysis. Each peak belongs to a single molecule only when they are completely separated from each another. In some cases, the components may not be separated from each other at all. There are several parameters that indicate whether the peak separation is excellent or not. Retention factor (k') and selectivity (α) values within certain ranges are among these parameters that are very important in terms of chromatographic separations and analytics (Han et al., 2012; Moldoveanu & David, 2013a, 2013b; Rosés, Canals, Allemann, Siigur, & Bosch, 1996; Subirats, Rosés, & Bosch, 2007).

2. System Suitability Testing (SST)

Before starting the chromatographic separation by HPLC or target sample run, a process called system suitability testing (SST) is performed to ensure the analytical system's suitability during analysis. This process involves checking the system with the reference standard substance and is a very important process for liquid chromatography. In order to be able to say that a good separation has occurred, the SST values must be within the limits specified in **Table 1**. For quantitative analysis, the system suitability testing should provide the relevant values for at least two parameters (USP-United States Pharmacopeial Convention, 2009; Cartwright, 2016; Swartz & Krull, 2018; Engin B., Gümüştaş M., Oktar M., Kurbanoğlu S., Ozkan SA, 2017).

Table 1. Recommended values of System Suitability Testing

SST parameters	Recommended value
Tailing factor (T)	T < 2.00
Resolution (R_s)	R_s > 2.00
Capacity factor (*k'*)	*k'*= 2 - 10
Selectivity (α)	α >1.00
Asymmetry factor (A_s)	A_s= 0.95-1.20
Theoretical plate number (N)	N > 2000

2.1. Capacity Factor (k')

The capacity factor (*k'*) is an expression of the relative retention of substances and is a measure of the retention time of an analyte in a chromatography column. In order to calculate this value, besides the retention times (t_R) of the substances in the column, the dead time called t_0 must also be determined. t_0 represents the retention time of the material that does not adhere to the column. Generally, compounds such as Uracil, potassium bromide (KBr) can be used as a t_0 indicator. The stationary phase (column properties) and mobile phase (percentage of organic phase and pH, etc.) affect the capacity factor value. In general, a value between 2 and 10 is considered ideal. This value is calculated as stated in **Equation 1**;

$$k' = \frac{t_R - t_0}{t_0} \qquad (1)$$

If the capacity factor (*k'*) for a solute is much less than 1, the elution will be so fast that accurate determination of the retention time (t_R) becomes difficult (Skoog, Holler, & Crouch, 2017).

2.2. Selectivity (α)

Selectivity (α), also known as relative retention, refers to the degree to which the two peaks obtained in the chromatogram are separated from each other. Ideally, this value is expected to be α>1. When α=1, the substances do not separate from each other and leave the column at the same time. Factors affecting α are temperature, properties of the mobile and stationary phase. The selectivity factor is calculated as shown in **Equation 2** (Skoog et al., 2017).

$$\alpha = \frac{k_2'}{k_1'} \qquad (2)$$

3. Mobile Phase pH Selection and its Effects on Separation

In all HPLC analyzes, mobile phase selection is a very important step for successful separation. The mobile phases used in HPLC are determined according to the type of

analysis, the nature of the compounds, the properties of the selected stationary phase and also the type of detector. Pure compounds such as water, methanol, acetonitrile, hexane, etc. can be used as the mobile phase, as well as solutions containing various substances such as salts, acids and bases (with low concentrations), which have certain pH and provide ionic strength, prepared by mixing in various proportions. The mobile phase selection is directly related to the retention of the analytes in the column. Especially in the analysis of ionizable compounds, small changes in mobile phase pH can produce dramatic changes in retention times. This also affects the SST parameters such as *k'* and α. Therefore, determining the pH of the mobile phase to be used in the separation has an important place. (Moldoveanu & David, 2013a; Tindall & Dolan, 2002; Tindall & Dolan, 2003; Tindall & Dolan, 2003).

The retention of compounds with different properties (acidic, basic or amphoteric) in HPLC is highly dependent on pH. It is common for compounds to change from neutral to ionized in the 2 pH unit range. So in many HPLC separations, the pH of the mobile phase is used to achieve good separation. The mobile phase pH is usually controlled by buffer solutions. Buffer solutions consist of a mixture of a weak acid and conjugate base or a weak base and conjugate acid. These solutions, which are resistant to pH changes, are used to keep the pH of a solution at a certain level and constant (Skoog, West, Holler, & Crouch, 2013).

pH measurements of solutions are made using modern pH-meters that allow direct reading of pH. Three approaches can be listed that can be used in liquid chromatography applications within the framework of pH measurement procedures defined by IUPAC for organic solvents and aqueous organic solvent mixtures. These;

1) Measurement of pH before mixing the buffer solution with the mobile phase solvent system, using electrodes calibrated with aqueous reference buffer solutions,

2) Measurement of pH after mixing the buffer solution and the mobile phase solvent system, using electrodes calibrated with aqueous reference buffer solutions,

3) Measurement of pH after mixing the buffer solution and the mobile phase solvent system, using electrodes calibrated with reference buffer solutions prepared in the solvent medium used as the mobile phase.

Taking into account the real thermodynamic pK_a values of the analyte in the mobile phase and considering the ease of use, the approach of measuring pH after mixing the buffer solution with the mobile phase solvent system and using electrodes calibrated with aqueous reference buffer solutions is recommended (Canals, Oumada, Rosés, & Bosch, et al. 2001; Inczédy, Lengyel, Ure, Gelencsér & Hulanicki, 1998; Rosés et al., 1996; Tindall & Dolan, 2002).

In acid solutions, in cases where the pK_a value is higher than 2 units, more than 99% ionizes, while the situation is the opposite in bases. In other words, while the bases are ionized below the pK_a value, they are in non-ionized form above the pK_a value. In the non-ionized form, they show a higher retention in reversed phase chromatographic separation due to decreased polarity. In short, for reversed phase systems, acids at low pH and bases at high pH are more retained in the column (Dolan, 2009). The chromatogram obtained in a separation with different mobile phase pH is shown in **Figure 2**. As can be seen from **Figure 2**, *k'* and α values show high sensitivity to small pH changes in the mobile phase.

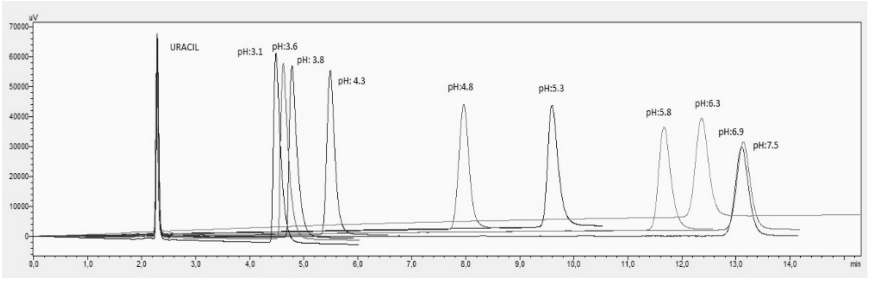

Figure 2. The effect of mobile phase pH on the retention of an ionizable compound (Soyseven, 2021).

In many HPLC methods, the properties of the mobile phase (pH, percentage of organic phase, etc.) affect the separation. It is also very important to know the pK_a values of the compounds in the mixture in order to perform the chromatographic separation processes sensitively and accurately. The pK_a of a weak acid is the pH at which the acid is evenly distributed between its ionized and non-ionized forms. This situation is explained by the Henderson-Hasselbalch equation given in **Equation 3**.

$$pH=pK_a + \log([A^-]/[HA]) \qquad (3)$$

Here $[A^-]$ denotes the molar concentration of the conjugate base and [HA] denotes the concentration of the weak acid. If the weak acid is equally distributed between the two forms, pH = pK_a since $([A^-]/[HA])=1$ and hence $\log([A^-]/[HA])= 0$. In case of unequal pH will be lower or higher than the pK_a of the acid. This directly affects detention (Heinisch & Rocca, 2004; Joseph & Palasota, 2001).

In the separation of ionizable acids or bases, changing the pH of the mobile phase makes it possible to change the α values as desired without major changes in *k'*, resulting in a better separation efficiency. A less used but more effective way to improve α while keeping the *k'* value within the optimum range is to change the chemical composition of the stationary phase (Skoog et al., 2017).

In separation, changes in buffer concentration and buffer type affect retention and selectivity. **Table 2** shows the most commonly used buffers and their properties in HPLC.

Table 2. Some buffer solutions frequently used in HPLC and their properties (Dolan, 2009; Moldoveanu & David, 2013b).

Buffer Solution	**pK_a**	**pH Range**	**UV *cut-off***
Ammonium acetate	4.8;9.2	3.8-5.8; 8.2-10.2	210 nm (50 mM)
Ammonium formate	3.8;4.2	2.8-4.8; 8.2-10.2	210 nm (50 mM)

Potassium formate/formic acid	3.8	2.5-5.0	210 nm (10 mM)
Potassium acetate/acetic acid	4.8	3.8-5.8	210 nm (10 mM)
KH_2PO_4/H_3PO_4	2.12	1.1-3.1	<200 nm (0.1%)
KH_2PO_4/ K_2HPO_4	7.2	6.2-8.2	<200 nm (0.1%)
Trifluoroacetic acid	0.5	1.5-2.5	210 nm (10 mM)
Borate $H_3BO_3/$ $Na_2BO_4O_7.10H_20$	9.24	8.2-10.2	210 nm
Ammonium hydroxide/ ammonium	9.2	8.2-10.2	210 nm (10 mM)
Triethylamine HCl/ triethylamine	11.0	10.0-12.0	210 nm (10 mM)
Diethylamine HCl/ diethylamine	10.5	9.5-11.5	210 nm (10 mM)

The change in the retention of acids and bases with pH change occurs in the opposite way. While acidic substances have good retention at low pH, they show low retention at high pH. Bases are neutral and retain well at high pH, whereas at low pH they are ionized and have low retention. (Singh, 2013).

4. Conclusion

The pH and content of the mobile phase are critical for proper peak separation in HPLC. A successful separation also depends on the degree of acidity or alkalinity of the substances targeted for separation. In reversed phase liquid chromatography, pH control of the mobile phase solvent system is critical for stability of retention and selectivity. The pH of the mobile phase has minimal influence on the retention of neutral compounds, but when ionizable chemicals are present in a sample, pH control is required to stabilize the retention of the substance in the column. During method development, the pH of the mobile phase may be a very potent tool for moving peaks in the chromatogram, but it must be carefully managed during regular analysis to maintain robust separation conditions. Buffer solutions are often preferred to provide this control. To control the mobile phase pH, a buffer solution with a pK_a value within ±1 pH unit of the desired pH should be selected. Otherwise, the buffering capacity may not be sufficient to stabilize the retention.

References

Canals, I., Oumada, F. Z., Rosés, M., & Bosch, E. (2001). Retention of ionizable compounds on HPLC. 6. pH measurements with the glass electrode in methanol–water mixtures. Journal of Chromatography A, 911(2), 191-202.

Cartwright, A. C. (2016). The British pharmacopoeia, 1864 to 2014: medicines, international standards and the state.

Dolan, J. (2009). A guide to HPLC and LC-MS buffer selection. ACE.

Engin B., Gümüştaş M., Oktar M., Kurbanoğlu S., Özkan S. A. (2017). Analitik Yöntem Geçerliliği. Türk Farmakope Dergisi, 2 (1), 74-92.

Han, S.-y., Liang, C., Zou, K., Qiao, J.-q., Lian, H.-z., & Ge, X. (2012). Influence of variation in mobile phase pH and solute pKa with the change of organic modifier fraction on QSRRs of hydrophobicity and RP-HPLC retention of weakly acidic compounds. Talanta, 101, 64-70. doi:https://doi.org/10.1016/j.talanta.2012.08.051

Heinisch, S., & Rocca, J. L. (2004). Effect of mobile phase composition, pH and buffer type on the retention of ionizable compounds in reversed-phase liquid chromatography: application to method development. Journal of Chromatography A, 1048(2), 183-193. doi:https://doi.org/10.1016/j.chroma.2004.07.022

Inczédy, J., Lengyel, T., Ure, A. M., Gelencsér, A., & Hulanicki, A. (1998). Compendium of analytical nomenclature. Hoboken: Blackwell Science.

Joseph, S. M., & Palasota, J. A. (2001). The combined effects of pH and percent methanol on the HPLC separation of benzoic acid and phenol. Journal of Chemical Education, 78(10), 1381.

Moldoveanu, S. C., & David, V. (2002). Sample preparation in chromatography: Elsevier.

Moldoveanu, S. C., & David, V. (2013a). Chapter 1 - Basic Information about HPLC. In S. C. Moldoveanu & V. David (Eds.), Essentials in Modern HPLC Separations (pp. 1-51): Elsevier.

Moldoveanu, S. C., & David, V. (2013b). Chapter 7 - Mobile Phases and Their Properties. In S. C. Moldoveanu & V. David (Eds.), Essentials in Modern HPLC Separations (pp. 363-447): Elsevier.

Rosés, M., Canals, I., Allemann, H., Siigur, K., & Bosch, E. (1996). Retention of Ionizable Compounds on HPLC. 2. Effect of pH, Ionic Strength, and Mobile Phase Composition on the Retention of Weak Acids. Analytical Chemistry, 68(23), 4094-4100. doi:10.1021/ac960105d

Sezgin, B., Arli, G., & Can, N. Ö. (2021). Simultaneous HPLC-DAD determination of seven intense sweeteners in foodstuffs and pharmaceuticals using a core-shell particle column. Journal of Food Composition and Analysis, 97, 103768. doi:https://doi.org/10.1016/j.jfca.2020.103768

Sezgin, B., Can, N. Ö. & Arli, G., (2016, Ekim). Diyabetik Reçellerde Kullanılan Bazı Yoğun Tatlandırıcıların Yüksek Performanslı Sıvı Kromatografisi ile Eş Zamanlı Analizi [Abstract]. Presented at Turkey 12th Food Congress.

Singh, R. (2013). HPLC method development and validation-an overview. Journal of Pharmaceutical Education & Research, 4(1).

Skoog, D. A., Holler, F. J., & Crouch, S. R. (2017). Principles of instrumental analysis: Cengage learning.

Skoog, D. A., West, D. M., Holler, F. J., & Crouch, S. R. (2013). Fundamentals of analytical chemistry: Cengage learning.

Snyder, L. R., Kirkland, J. J., & Dolan, J. W. (2011). Introduction to modern liquid chromatography: John Wiley & Sons.

Snyder, L. R., Kirkland, J. J., & Glajch, J. L. (2012). Practical HPLC method development: John Wiley & Sons.

Soyseven, M., Aboul-Enein, H. Y., & Arli, G. (2021). Development of a HPLC method combined with ultraviolet/diode array detection for determination of monosodium glutamate in various food samples. International Journal of Food Science & Technology, 56(1), 461-467. doi:https://doi.org/10.1111/ijfs.14661

Soyseven, M., Kaynak, M. S., Çelebier, M., Aboul-Enein, H. Y., & Arli, G. (2020). Development of a RP-HPLC method for simultaneous determination of reference markers used for in-situ rat intestinal permeability studies. Journal of Chromatography B, 1147, 122150. doi:https://doi.org/10.1016/j.jchromb.2020.122150

Soyseven, M. (2021, March). Determination of Dissociation Constant of Sildenafil Using an RP-HPLC [Abstract]. Presented at 5th International Academic Studies Conference (UBCAK).

Subirats, X., Rosés, M., & Bosch, E. (2007). On the effect of organic solvent composition on the pH of buffered HPLC mobile phases and the pKa of analytes - A review. Separation and Purification Reviews, 36(3), 231-255. doi:10.1080/15422110701539129

Swartz, M. E., & Krull, I. S. (2018). Analytical method development and validation: CRC press.

Tindall, G. W., & Dolan, J. (2002). Mobile-phase buffers, part I-the interpretation of pH in partially aqueous mobile phases. LCGC North America, 20(11), 1028-1032.

Tindall, G. W., & Dolan, J. (2003). Mobile-phase buffers, part III-Preparation of buffers. LC GC NORTH AMERICA, 21(1), 28-33.

Tindall, G. W., & Dolan, J. W. (2003). Mobile-Phase Buffers, Part II-Buffer Selection and Capacity. LC GC Europe, 16, 10.

USP - United States Pharmacopeial Convention (2009). Chromatography <621>. In The United States Pharmacopeia 32, National Formulary 27 (p. 227). Rockville, MD.

Vailaya, A., & Horváth, C. (1998). Retention in reversed-phase chromatography: partition or adsorption? Journal of Chromatography A, 829(1), 1-27. doi:https://doi.org/10.1016/S0021-9673(98)00727-4

CHAPTER 6

DETERMINATION OF SUCRALOSE IN BEVERAGES BY HPLC-ELSD METHOD

Murat Soyseven[1] & Burcu Sezgin[2]

[1](Dr.) Anadolu University, e-mail:msoyseven@anadolu.edu.tr

Orcid: 0000-0002-6433-2392

[2](Dr.) Eskişehir Osmangazi University, e-mail:bsezgin@ogu.edu.tr

Orcid: 0000-0003-0279-4839

1. Introduction

The sense of taste gives important information about the nutritional value and quality of food. Due to anthropological and medicinal reasons, sweet taste is unquestionably the most significant one among the tastes. (Nelson et al., 2001; Meyers and Brewer, 2008). Despite widespread concerns regarding the safety of non-nutritive sweeteners, there has been a significant growth in their use (Behrens et al., 2011; Swithers, 2013). These sweeteners are commonly used in foods since they do not cause insulin response in the body, dental problems and weight gain. Sucralose (SCL) is one of the most popular non-nutritive sweeteners approved by the Food and Drug Administration and used in about 1500 various products. (Kokotou, Asimakopoulos, and Thomaidis, 2012; Yang, 2010).

SCL (1,6 dichloro-1,6-dideoxy-β-D-fructofuranosyl-4-chloro-4-deoxy-β-D galactopyranoside) is produced from sucrose after a five-step chemical procedure. Chemical structure of SCL is given in **Figure 1**. The sweetness of SCL is 600 times more than sucrose and used synergistically with other non-nutritive sweeteners. Due to its thermal stability, SCL is commonly used in food, beverages and drug industries with the e-code E955. SCL is not metabolized thus calorie intake does not occur. The acceptable daily intake value (ADI) of SCL determined by Joint FAO-WHO Expert Committee Report on Food Additives (JECFA) is 15 mg kg^{-1}. (Grotz and Munro, 2009; Grice and Goldsmith, 2000; Gardner et al.,2012). According to the Turkish Food Codex (TFC), the SCL usage limit in energy-reduced beverages is 300 mg L^{-1} (Turkish Food Codex, 2013).

Studies have shown that SCL is not carcinogenic and genotoxic. However, there are some studies in the literature showing that SCL triggers migraine pain. There are scientists who argue that SCL is responsible for the increased incidence of inflammatory colon disease in Canadians by reducing gut bacteria (Brusick et al., 2010; Shankar, Ahuja and Sriram, 2013; Whitehouse, Boullata and McCauley, 2008).

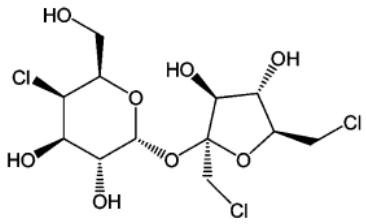

Figure 1. Chemical structure of SCL (Yang & Chen, 2009).

Liquid chromatographic methods are frequently used in the analysis of foods and beverages (Sezgin, Arli, & Can, 2021; Soyseven, Aboul-Enein, & Arli, 2021). Since the sucralose has no strong chromophore, UV analysis is not sensitive enough (Yan et al., 2016). Therefore, methods using mass spectrometry and evaporative light scattering detectors are preferred for SCL determinations. Several analytical techniques have been reported in the literature for determination SCL including liquid chromatography/time-of-flight mass spectrometry (LC/TOF-MS) (Ferrer & Thurman, 2010), UHPLC-MS/MS (Wu et al., 2014), high-performance thin-layer chromatography (Morlock, Schuele & Grashorn, 2011), high temperature liquid chromatography–tandem mass spectrometry (Ordoñez et al., 2015), HPLC-MS/MS (Lim et al., 2013), LC/MS (Chang & Yeh, 2014), HPLC coupled with electrospray ionization mass spectrometric detection (ESI-MS) (Yang & Chen, 2009), HPLC and evaporative light scattering detection (HPLC-ELSD) (Wasik, McCourt, & Buchgraber, 2007).

HPLC-ELSD is superior to other methods because it does not require a derivatization step, uncomplicated sample preparation steps, short analysis time, sensitive detection at low temperatures and applicability to non-chromophoric substances (Troubleshooting, 2003; Young & Dolan, 2004; Yan et al., 2016; Koh et al., 2018).

In this study, an HPLC-ELSD method was optimized and validated for the analysis of SCL in beverages. The method has been successfully applied to various beverage samples and SCL contents were evaluated according to TFC.

2. Materials and Method

2.1. Chemicals and reagents

USP Reference standard of SCL (> 99% purity and analytical grade) and acetonitrile (ACN) were purchased from Sigma-Aldrich (Germany). Ultra-pure HPLC water (Aq_{DD}: <0,55 µS/cm) was supplied from Stakpure (Germany) ultra-pure water system was used for the preparation of the standard solutions and mobile phases. Analytical purity nitrogen gas was used whole analysis. Prior to injection into the HPLC-ELSD system, non-sterile polyvinylidene fluoride (PVDF) syringe filters with a 13 mm id and a 0.2 m pore size were used to filter all solutions.

2.2. Apparatus

HPLC – ELSD analysis was carried out using a Shimadzu, Nexera-i, LC-2040C 3D Model liquid chromatograph system consisting of a binary pump, a degasser, an autosampler, a thermo-stated column compartment combined with a Shimadzu Evaporative Light Scattering Detector (ELSD LT-II Model) (Tokyo, Japan). For vortex Heidolph Vortex (Schwabach, Germany) was used. Lab Companion ultrasonic cleaner CS-10 (Seoul, Korea) was used to sonicate the whole standards solutions and beverages. Ohaus analytical balance system (USA) was used for all preparation steps. LabSolution Shimadzu Corporation software was used for monitoring all analysis. (Japan).

2.3. HPLC-ELSD Conditions

The separations were carried out on a SVEA C18 column (5 µm particle size, 150 mm x 4.6 mm id.) with isocratic elution of (Water:ACN) (85:15, v/v). Prior to use, the mobile phase was vacuum filtered through a 0.2 µm filter and sonicated for 20 min. The column oven temperature was set at 30 ºC. Separation was carried out at a flow rate of 1 mL min^{-1} in 8 min run time at ambient temperature. The injection volume was chosen 10 µL. The temperature of the evaporate drift tube was set to 35°C, the nitrogen pressure was set to 350 kPa, and the Gain and Filter values on the ELSD system were set to 5 and 10, respectively with sampling time of 10 Hz.

2.4. Standards and Samples Preparations

Standard stock solutions of SCL were prepared in HPLC grade water as the final concentration to be 1 mg mL^{-1}. The stock solution was kept at -18 ºC in fridge. All working solutions were freshly prepared by diluting stock standard solution with the HPLC grade water. A total of five beverages samples were collected from supermarkets. HPLC grade water was preferred for extraction of SCL from beverages samples. All solutions and beverages samples were sonicated for 15 min and filtered through syringe PVDF filter prior to injection. Supernatant was transferred to the HPLC vial after the filtration. All solutions kept away from daylight.

2.5. Method Validation

HPLC-ELSD method was validated according to the International Conference on Harmonization guidelines ICH Q2(R1) to evaluate the quality of the analytical method (ICH, 2005). The method was validated for the linearity, LOD, LOQ, accuracy, precision, specificity and robustness.

2.6. Statistical Analysis

LabSolution software (Shimadzu Corporation) was used to monitor and integrate all of the chromatograms. The results of the analyses were given as mean ± standard deviation for three replicates of samples. (n=3). For data analysis, MS Excel 2007 was used for data analysis (Microsoft Corporation, USA).

3. Result and Discussion

3.1. Method Optimization

400 µg mL^{-1} SCL was injected during the optimization studies. (Water:ACN) (85:15, v/v). mixture was chosen as the mobile phase, because of its lower viscosity, higher separation efficiency, suitability for ELSD systems due to its high volatility, and show low system pressure. Obtained 400 ppm SCL standard chromatogram is shown in **Figure 2**.

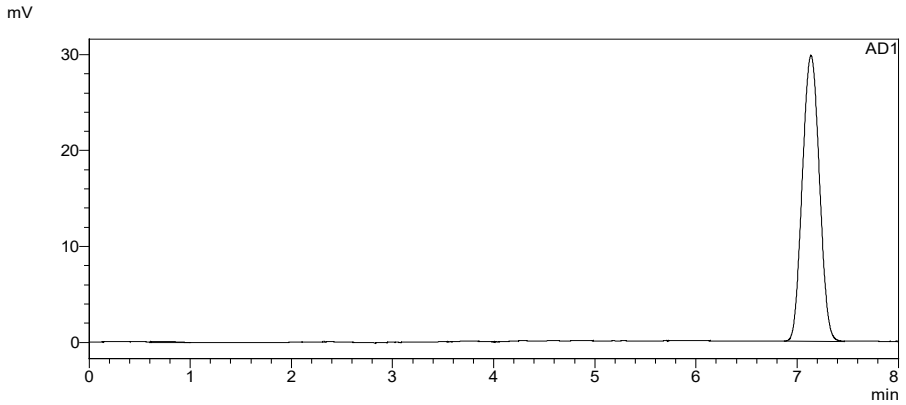

Figure 2. Obtained 400 µg mL^{-1} SCL chromatogram using HPLC-ELSD

System suitability testing (SST) (including resolution (Rs), tailing factor (T), asymmetry factor, capacity factor (*k'*), selectivity (α) and theoretical plate number (N) were examined and used for optimal conditions to be decided under mentioned the HPLC-ELSD section. Obtained SST results was shown in **Table 1**.

Table 1. System suitability testing results of 400 µg mL^{-1} SCL (*n=5*)

Parameters	**Observed value**	**Recommended value**
Retention time (min)	7.13	-----
Tailing factor (T)	1.03	T < 2.00
Resolution (R_s)	17.3	R_s > 2.00
Capacity factor (*k'*)	8.26	*k'* > 2.00
Asymmetry factor (A_s)	1.02	A_s = 0.95-1.20
Theoretical plate number (N)	8312	N > 2000
RSD% of Retention Time	0.11	RSD% < 1.0

As a result, determined analytical parameters were carried out for validation procedure of the HPLC-ELSD method. The SCL was separated under 8 min. Obtained 20-1000 µg mL-1 SCL chromatogram is shown in **Figure 3**.

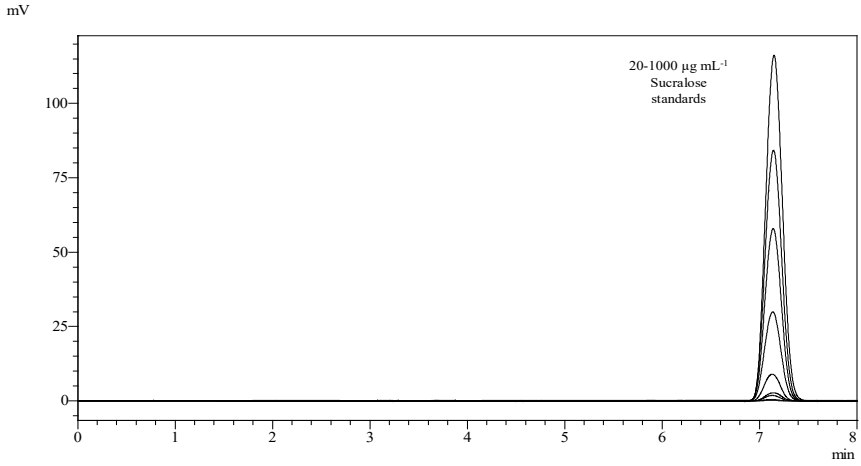

Figure 3. Obtained HPLC-ELSD chromatogram of 20-1000 µg mL^{-1} of SCL

3. 2. Validation

3.2.1. Linearity, LOD and LOQ

The HPLC-ELSD method's linearity was assessed using nine-point calibration curves within the range of 20-1000 µg mL^{-1}. Three calibration sets were tested in triplicate for SCL standards. Since the ELSD is not a direct linear response detector (**Figure 4a)**, the calibration curve was drawn by plotting the logarithm of the chromatogram peak areas versus the logarithm of the SCL standard solutions. It is used to construct a linear calibration curve. (Troubleshooting, 2003). The obtained regression equation showed good linear relationship (R^2 = 0.9992) (**Figure 4b**).

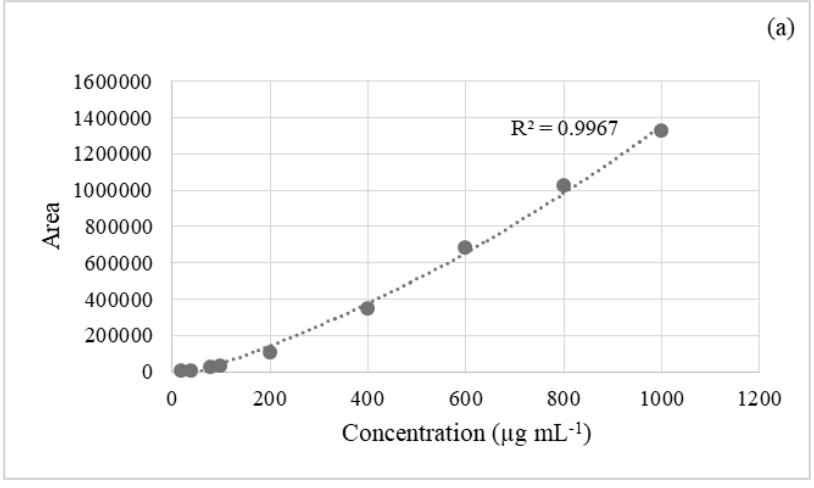

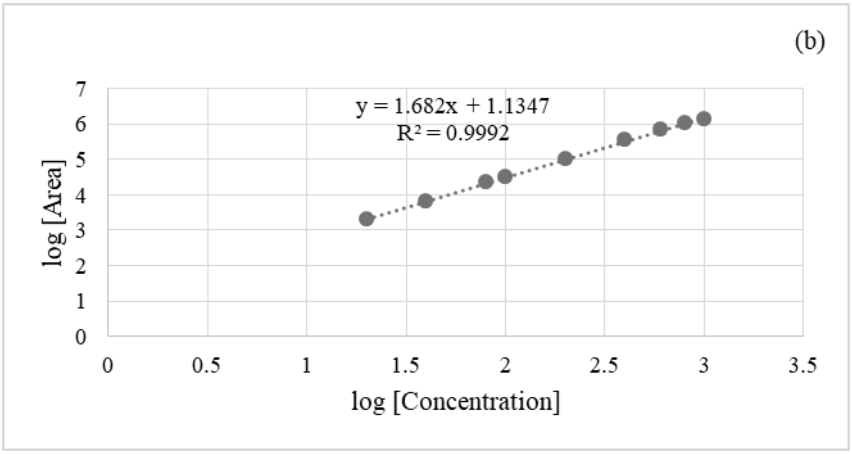

Figure 4. a) Obtained ELSD area response versus SCL concentrations **b)** Obtained ELSD log [area response] versus log [SCL concentration]

LOD present the lowest concentration of a target compound. LOQ is the lowest analyte level determined with an appropriate precision and accuracy. The lowest concentration of analyte in a sample that can be quantitatively determined with proper precision and accuracy is referred to as the LOQ. In accordance with ICH guidelines. The HPLC-ELSD method's LOD and LOQ were determined using the 3.3 and 10 standard deviation (SD) of the observed detector response (σ) to slope of the calibration curve (m), respectively. " σ " was calculated using the standard deviation of regression lines' y-intercepts (**Table 2**). According to the results, there was no peak interference.

Table 2. Linearity, range, LOD, LOQ, correlation coefficient and regression equation data for SCL.

Compound	**Range (µg mL-1)**	**Regression equation**	***R*²**	**LOD (µg mL-1)**	**LOQ (µg mL-1)**
Sucralose	20-1000	*y=1.682x+1.1347*	0.9992	0.10	0.30

R^2: coefficient of determination, LOD: limit of detection, LOQ: limit of quantification

3.2.2. Accuracy and Precision

The accuracy of the method was evaluated with recovery test which is obtained by comparing the theoretical concentration of the compounds with that of the experimental concentration. Three different concentration of SCL samples (80, 200 and 600 µg mL^{-1}) were prepared and each was analyzed triplicate in same day.

Recovery was calculated by comparing the theoretical concentration (*X*) of SCL with observed concentration (*C*) from the **Eq (1)**.

$$Recovery\ (\%) = (X) / (C) \times 100 \quad Eq\ (1)$$

In order to show precision of the HPLC-ELSD method *intra-day* and *inter-day* variability were investigated. The precision data was expressed via relative standard deviation (RSD%) and calculated with **Eq (2)**.

$$RSD\% = SD / Mean \times 100 \quad Eq\ (2)$$

SCL solutions at the concentration of 80, 200 and 600 µg mL^{-1} were analyzed three times on the same day and, three successive days. The method was found accurate according to the recovery values (94.4-100.3%). RSD% was found between 0.10-0.44 (< 1%). Results showed that a good accuracy and precision values are achieved (**Table 3** and **Table 4**).

Table 3. Accuracy results of HPLC-ELSD method

	Accuracy				
Compound	**Main value (µg mL-1)**	**Found value (µg mL-1)**			
		1st	***2nd***	***3rd***	**Mean Recovery (%)**
Sucralose	80	75.51	76.69	74.34	94.4
	200	201.7	200.3	199.9	100.3
	600	601.0	595.4	596.8	99.63

Table 4. Precision results of HPLC-ELSD method

Precision			
***Intra-day* (n=3) (RSD%)**			***Inter-day* (n=9) (RSD%)**
1st	***2nd***	***3rd***	**Whole day**
0.58	0.62	0.12	0.44
0.05	0.04	0.21	0.10
0.11	0.11	0.06	0.10

RSD: Relative standard deviation.

3.3. Application on Beverages Samples

The validated chromatographic HPLC-ELSD method was carried out the beverages samples and the obtained results are given in **Table 5**. SCL contents are given with SD values which are derived by each sample 3 times analyzed. A representative chromatogram of a sample is given in **Figure 5**.

Table 5. Content of SCL in beverages samples.

No	Sample name	Sucralose content (µg mL-1) ± SD (*n = 3*)
1	Beverage sample 1	20.46 ±0.02
2	Beverage sample 2	33.04 ± 0.02
3	Beverage sample 3	90.75 ± 0.32
4	Beverage sample 4	277.16± 0.14
5	Beverage sample 5	178.46± 0.32

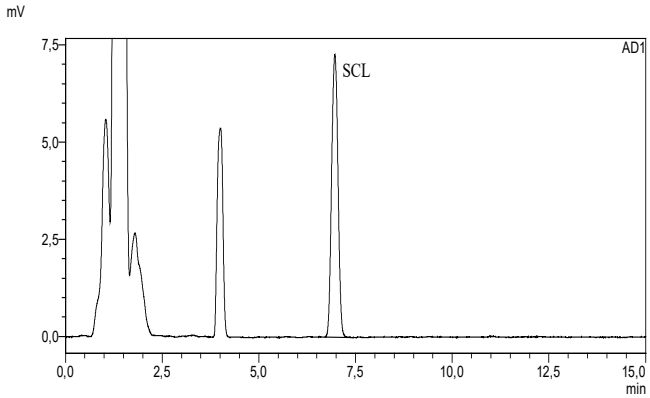

Figure 5. Representative chromatogram of a beverage sample

4. Conclusion

Due to aesthetic, medical and dental concerns, the use of SCL in food, beverage and personal care products is increasing. Since SCL shows poor UV absorption, chromatographic SCL determinations require the use of a detector such as ELSD. It has been shown that SCL determinations in beverages can be made successfully with the HPLC-ELSD method. All beverage samples were found to comply with the TFC.

References

Behrens, M., Meyerhof, W., Hellfritsch, C., & Hofmann, T. (2011). Sweet and umami taste: natural products, their chemosensory targets, and beyond. Angewandte Chemie International Edition, 50(10), 2220-2242. doi:https://doi.org/10.1002/anie.201002094.

Brusick, D., Grotz, V. L., Slesinski, R., Kruger, C. L., & Hayes, A. W. (2010). The absence of genotoxicity of sucralose. Food and Chemical Toxicology, 48(11), 3067-3072. doi:https://doi.org/10.1016/j.fct.2010.07.047.

Chang, C.-S., & Yeh, T. S. (2014). Detection of 10 sweeteners in various foods by liquid chromatography/tandem mass spectrometry. Journal of Food and Drug Analysis, 22(3), 318-328. https://doi.org/https://doi.org/10.1016/j.jfda.2014.01.024.

Ferrer, I., & Thurman, E. M. (2010). Analysis of sucralose and other sweeteners in water and beverage samples by liquid chromatography/time-of-flight mass spectrometry. Journal of Chromatography A, 1217(25), 4127-4134. https://doi.org/https://doi.org/10.1016/j.chroma.2010.02.020.

Gardner, C., Wylie-Rosett, J., Gidding, S. S., Steffen, L. M., Johnson, R. K., Reader, D., & Lichtenstein, A. H. (2012). Nonnutritive sweeteners: current use and health perspectives: a scientific statement from the American Heart Association and the American Diabetes Association. Circulation, 126(4), 509-519. doi: https://doi.org/10.1161/CIR.0b013e31825c42ee.

Grice, H. C., & Goldsmith, L. A. (2000). Sucralose-an overview of the toxicity data. Food and Chemical Toxicology, 38(suppl 2). doi: https://doi.org/10.1016/S0278-6915(00)00023-5.

Grotz, V. L., & Munro, I. C. (2009). An overview of the safety of sucralose. Regulatory toxicology and pharmacology, 55(1), 1-5. doi: https://doi.org/10.1016/j.yrtph.2009.05.011.

ICH - International Conference on Harmonisation of Technical Requirements for Registration of Pharmaceuticals for Human Use (2005). Validation of Analytical Procedures: Text and Methodology Q2(R1). In ICH Expert Working Group, ICH Harmonised Tripartite Guideline, Geneva, pp. 1–17.

Koh, D. W., Park, J. W., Lim, J. H., Yea, M. J., & Bang, D. Y. (2018). A rapid method for simultaneous quantification of 13 sugars and sugar alcohols in food products by UPLC-ELSD. Food chemistry, 240, 694-700. doi: https://doi.org/10.1016/j.foodchem.2017.07.142.

Kokotou, M. G., Asimakopoulos, A. G., & Thomaidis, N. S. (2012). Artificial sweeteners as emerging pollutants in the environment: analytical methodologies and environmental impact. Analytical Methods, 4(10), 3057-3070. doi:https://doi.org/10.1039/C2AY05950A.

Lim, H.-S., Park, S.-K., Kwak, I.-S., Kim, H.-I., Sung, J.-H., Jang, S.-J., Kim, S.-H. (2013). HPLC-MS/MS analysis of 9 artificial sweeteners in imported foods. Food Science and Biotechnology, 22(1), 233-240.doi: 10.1007/s10068-013-0072-2

Meyers, B., & Brewer, M. S. (2008). Sweet taste in man: a review. Journal of food science, 73(6), R81-R90. doi:https://doi.org/10.1111/j.1750-3841.2008.00832.x.

Morlock, G. E., Schuele, L., & Grashorn, S. (2011). Development of a quantitative high-performance thin-layer chromatographic method for sucralose in sewage effluent, surface water, and drinking water. Journal of Chromatography A, 1218(19), 2745-2753. https://doi.org/https://doi.org/10.1016/j.chroma.2010.11.063.

Nelson, G., Hoon, M. A., Chandrashekar, J., Zhang, Y., Ryba, N. J., & Zuker, C. S. (2001). Mammalian sweet taste receptors. Cell, 106(3), 381-390. doi:https://doi.org/10.1016/S0092-8674(01)00451-2.

Ordoñez, E. Y., Rodil, R., Quintana, J. B., & Cela, R. (2015). Determination of artificial sweeteners in beverages with green mobile phases and high temperature liquid chromatography–tandem mass spectrometry. Food Chemistry, 169, 162-168. https://doi.org/https://doi.org/10.1016/j.foodchem.2014.07.132.

Sezgin, B., Arli, G., & Can, N. Ö. (2021). Simultaneous HPLC-DAD determination of seven intense sweeteners in foodstuffs and pharmaceuticals using a core-shell particle column. Journal of Food Composition and Analysis, 97, 103768. doi:https://doi.org/10.1016/j.jfca.2020.103768.

Shankar, P., Ahuja, S., & Sriram, K. (2013). Non-nutritive sweeteners: review and update. Nutrition, 29(11-12), 1293-1299. doi: https://doi.org/10.1016/j.nut.2013.03.024.

Soyseven, M., Aboul-Enein, H. Y., & Arli, G. (2021). Development of a HPLC method combined with ultraviolet/diode array detection for determination of monosodium glutamate in various food samples. International Journal of Food Science & Technology, 56(1), 461-467. doi:https://doi.org/10.1111/ijfs.14661

Swithers, S. E. (2013). Artificial sweeteners produce the counterintuitive effect of inducing metabolic derangements. Trends in Endocrinology & Metabolism, 24(9), 431-441. doi: https://doi.org/10.1016/j.tem.2013.05.005.

Troubleshooting, L. (2003). Success with evaporative light-scattering detection. LC-GC Europe, 2.

Turkish Food Codex. (2013). Türk Gıda Kodeksi Gıda Katkı Maddeleri Yönetmeliği. [cited 2021 Nov 24]. https://www.mevzuat.gov.tr/mevzuat?MevzuatNo=18532&MevzuatTur=7&MevzuatTertip=5

USP - United States Pharmacopeial Convention (2009). Chromatography <621>. In The United States Pharmacopeia 32, National Formulary 27 (p. 227). Rockville, MD.

Wasik, A., McCourt, J., & Buchgraber, M. (2007). Simultaneous determination of nine intense sweeteners in foodstuffs by high performance liquid chromatography and evaporative light scattering detection—development and single-laboratory validation. Journal of Chromatography A, 1157(1-2), 187-196. doi:https://doi.org/10.1016/j.chroma.2007.04.068

Wu, M., Qian, Y., Boyd, J. M., Hrudey, S. E., Le, X. C., & Li, X.-F. (2014). Direct large volume injection ultra-high performance liquid chromatography-tandem mass spectrometry determination of artificial sweeteners sucralose

and acesulfame in well water. Journal of Chromatography A, 1359, 156-161. https://doi.org/https://doi.org/10.1016/j.chroma.2014.07.035.

Whitehouse, C. R., Boullata, J., & McCauley, L. A. (2008). The potential toxicity of artificial sweeteners. Aaohn Journal, 56(6), 251-261. doi: https://doi.org/10.1177%2F216507990805600604.

Yan, W., Wang, N., Zhang, P., Zhang, J., Wu, S., & Zhu, Y. (2016). Simultaneous determination of sucralose and related compounds by high-performance liquid chromatography with evaporative light scattering detection. Food Chemistry, 204, 358-364. https://doi.org/https://doi.org/10.1016/j.foodchem.2016.02.099.

Yang, D. J., & Chen, B. (2009). Simultaneous determination of nonnutritive sweeteners in foods by HPLC/ESI-MS. Journal of agricultural and food chemistry, 57(8), 3022-3027. doi:https://doi.org/10.1021/jf803988u.

Yang, Q. (2010). Gain weight by "going diet?" Artificial sweeteners and the neurobiology of sugar cravings: Neuroscience 2010. The Yale journal of biology and medicine, 83(2), 101.

Young, C. S., & Dolan, J. W. (2004). Success with evaporative light-scattering detection, part II: Tips and techniques. LC/GC North Am, 22, 244-250.

CHAPTER 7

SYNTHESIS AND SPECTRAL CHARACTERIZATION OF THE BENZYLIDENEAMINO-PYRIMIDIN-2(1*H*)-ONE/-THIONE DERIVATIVES

Zülbiye Kökbudak[1] & Halime Güzin Aslan[2]

[1]*(Prof.Dr.) Erciyes University, e-mail: zulbiye@erciyes.edu.tr*

Orcid: 0000-0003-2413-9595

[2]*(Asst. Prof. Dr.) Erciyes University, e-mail: guzina@erciyes.edu.tr*

Orcid: 0000-0002-2759-6583

1. Introduction

Furan-2,3-dione compounds are highly active compounds. Therefore, they are used as the starting material for obtaining many new heterocyclic compounds [(Kollenz, 1972: 947), (Altural & Kollenz, 1998: 677)]. The reaction of furan-2,3-dions with carbazones gives pyrimidine derivatives. The pyrimidine ring and its related activities comprise many specific chemical or physical properties. This ring system's synthesis and reactivity are numerous and diverse [(Kachroo et al., 2014: 352)]. Pyrimidine derivatives show various interesting biological and pharmacological properties. Pyrimidine derivatives have been reported as antitubercular [(Siddiqui et al., (2014: 1493)], anti-microbial [(Kaur et al., 2012: 199)], anti-inflammatory [(Goudar et al., 2012: 3100)], antibacterial [(David et al., 2014: 2278)], anti-cancer [(Ma et al., 2015: 1124)], anti-HCV [(Shakya et al., 2014: 1407)], anti-malarial [(Singh et al., 2013: 314)], and antioxidant agents [(Farag, 2019: 304)].

Systems containing pyrimidine rings have chemical priority due to their biological activity. The pyrimidine ring is a vital DNA biomolecule and a structural component of essential drugs [(Sahu et al., (2016: 8)]. **Scheme 1** shows the open structures of some critical drugs with a pyrimidine ring.

Schiff-based ligands and metal complexes have various applications; they are widely used for industrial purposes and have high biological activity values. Multiple studies have proven that Schiff bases have a wide range of biological activities [(Gomathi & Selvameena, 2013: 94), (Shivakumar et al., 2008: 2274)]. Many of the Schiff bases have biological significance and applications in various fields.

The present study synthesized new Schiff bases containing pyrimidine rings, and made characterizations using spectroscopic methods. In addition, ESP maps of the molecules were produced using the Gaussian program. Studies showing significant catalytic activity and anticancer properties of Schiff bases and complexes synthesized from N-aminopyrimidine derivatives have been reported previously [(Aslan et al.,

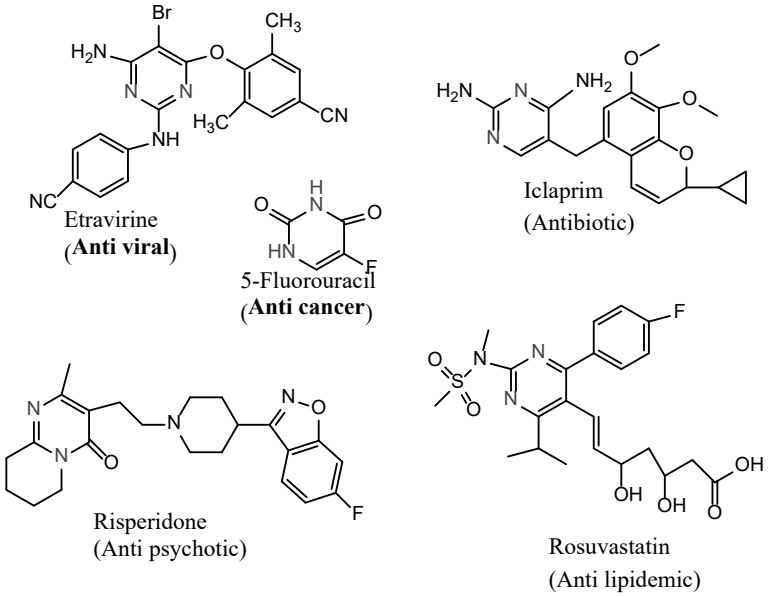

Scheme 1. Structures of some compounds containing pyrimidine nucleus. (Marketed drugs having pyrimidine pharmacophore).

2017: 2263), (Aslan et al., 2018: 145), (Aslan et al., (2020: 111), (Çimen et al., 2018: 1), (Aslan & Önal 2014: 2596), (Kökbudak et al., 2020: 440)].

In this study, the compounds **(1, 2)** were synthesized from 4-benzoyl-5-phenylfuran-2,3-dione and acetophenon semicarbazone/-thiosemicarbazone in benzene or toluene [(Kökbudak et al., 2020: 440)]. Then, a series of Schiff bases bearing pyrimidine rings **(3, 4)** were prepared from the reactions of compounds (**1 and 2**) with the various aromatic aldehyde derivatives under reflux conditions. The synthesized compounds **(3, 4)** are shown in (**Scheme 2**). FT-IR was first applied to confirm the chemical structures of the new compounds. Nuclear magnetic resonance analyses were performed when the expected spectrum was obtained, and elemental analysis was performed. Optimization was completed with the help of the Gaussian program, and ESP maps were drawn.

2. Experimental

All instruments used are the same as they were stated in our earlier studies (Çimen et al., 2018: 1).

3. Synthesis of Schiff Bases

According to the following procedure, the Schiff base derivatives **(3, 4)** were synthesized by a condensation method. (1 mmol) of Compounds **(1, 2)** was dissolved in ethanol (30 mL) and added to a solution of (1.2 mmol) of biphenyl-4-carboxaldehyde

or 3,4-dimethoxybenzaldehyde in the same solvent. The mixture was boiled for five to eight hours, and was then stirred for one day at room temperature. Ethyl alcohol was removed, and diethyl ether was added to the solid portion. It was stirred for 24 hours and filtered. The resulting solid was crystallized twice with ethyl alcohol. The structures of Schiff bases **(3, 4)** were explained with the help of spectroscopic methods.

3.1. 1-(([1,1'-Biphenyl]-4-ylmethylene)amino)-5-benzoyl-4 phenylpyrimidin-2(1H)-one (3)

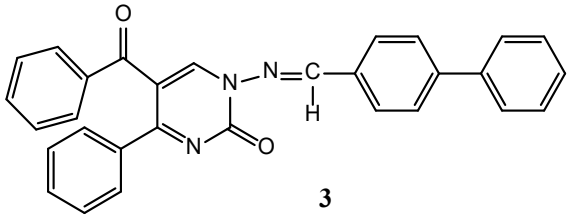

3

A mixture of compound **1** (1 mmol, 0.291 g) and biphenyl-4-carboxaldehyde (1.2 mmol, 0.218 g) in 30 mL of ethanol and *p*-toluene sulfonic acid was boiled for four hours. The solvent was evaporated with the evaporator and diethyl ether was added onto the remaining solid. It was mixed for one day, filtered and dried, and **3** was purified with ethyl alcohol. Yield: (70%); m.p.: 200-201 °C; color: yellow. FT-IR: υ = 3054 (arom. C-H), 2919 (aliph. C-H), 1681, 1645 (C=O), 1601 (C=N), 1568 (C=C), 760-727 cm^{-1} (pyrim. ring). ^{1}H NMR (400 MHz, DMSO-d_6) δ (ppm) = 9.30 (s, 1H, N=CH), 8.79 (s, 1H, CH in pyrimidine ring), 8.71-7.23 (m, 19H, Ar-H). ^{13}C NMR (100 MHz, DMSO-d_6) δ (ppm) = 192.06 (Ph-C=O), 171.17, 166.15, 151.62, 149.23, 144.65, 139.31, 137.33, 137.27, 133.90, 131.53, 130.65, 130.19, 129.60, 129.15, 128.88, 128.71, 128.57, 127.83, 127.72, 127.59, 127.37 and 116.10. Anal. Calcd. for $C_{30}H_{21}N_3O_2$ (455.50 g/mol): C, 79.10; H, 4.65; N, 9.22. Found: C, 78.90; H, 4.75; N, 9.15.

3.2. (1-((3,4-Dimethoxybenzylidene)amino)-4-phenyl-2-thioxo-1,2-dihydropyrimidin-5-yl)(phenyl)methanone (4)

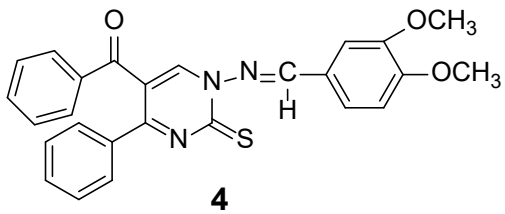

4

Compound **2** (1 mmol, 0.307 g) and 3,4-dimethoxybenzaldehyde (1.2 mmol, 0.199 g) in 30 mL of ethanol was refluxed for eight hours. *p*-Toluene sulfonic acid was added as a catalyst. After this reaction time, the solvent was removed. The residue was stirred with dry diethyl ether for one day and filtered. This obtained Schiff base was

purified in ethyl alcohol. Yield: (61%); m.p.: 180-181 °C; color: white. FT-IR: υ = 3054 (aromatic C-H), 2930 (aliphatic C-H), 1652 (C=O), 1587 (C=N), 1565 (C=C), 740-695 cm^{-1} (pyrim. ring). ^{1}H NMR (400 MHz, DMSO-d_6): δ (ppm) = 8.90 (s, 1H, N=CH), 8.80 (s, 1H, -CH in pyrimidine ring), 7.88-7.14 (m, 13H, Ar-H), 3.86 and 3.82 (s, 6H, 2x-OCH_3). ^{13}C NMR (400 MHz, DMSO-d_6): δ (ppm) = 192.21 (Ph-C=O), 169.72, 163.86, 153.69, 146.74, 136.72, 134.31, 131.36, 130.30, 129.35, 129.23, 128.89, 125.72, 120.43, 111.99, (Ar-C), 56.27 and 56.03 (2x-OCH_3). Anal. Calcd. for $C_{26}H_{21}N_3O_3S$ (455.52 g/mol): C.68.55; H, 4.65; N, 9.22; S, 7.04. Found: C, 68.50; H, 4.75; N, 9.22; S, 7.15.

4. Results and Discussion

In this study, the compound **(1, 2)** was synthesized in two steps from furan-2,3-dione derivatives according to the procedures in the literature [(Kollenz, 1972: 947), (Altural & Kollenz, 1998: 677)]. The new Schiff bases **(3, 4)** were prepared from the reactions of biphenyl-4-carboxaldehyde and 3,4-dimethoxybenzaldehyde with compounds **(1, 2)** in good yields such as 61-70% **(Scheme 2).** All compounds were purified by recrystallization. The carbonyl groups represent the electrophilic site in aldehydes derivatives to interact with nucleophiles **(Scheme 2)**. The synthesis of Schiff bases is usually carried out through the reaction of amines with carbonyl compounds through addition and elimination steps. In the IR spectrum of these compounds, characteristic stretch bands of carbonyl (C=O) groups are observed. In the ^{1}H NMR spectra of the compounds, the most striking peak belongs to the azomethine proton. [(Toledo et al., 2015: 106), (Ngan et al., 2011: 2922)].

Compound **3** was synthesized from the reaction of compound **1** and biphenyl-4-carboxaldehyde in a 70% yield. In the IR spectrum, the two C=O absorption bands were observed at 1681 and 1645 cm^{-1}. In the ^{1}H NMR spectrum, the N=CH proton was resonated in the downfield area at δ 9.30 ppm. The proton peaks of -N=CH bond of Shiff bases in the range of 8.96-9.94 ppm confirm the formation of azomethine bond between compounds **1** and **2** with aromatic aldehydes [21-22]. The proton signal for -CH in the pyrimidine ring for **3** was detected singlet at δ8.79 ppm. Aromatic protons were observed as multiplet between δ 8.71 and 7.23 ppm. In the ^{13}C NMR spectrum, benzoyl carbon's signal was observed at δ192.06 ppm. Other carbons of the molecule were obtained between δ 171.17-116.10 ppm.

Compound **4** was synthesized in a 61% yield. In the IR spectrum, C=O stretch bands were observed at 1652 cm^{-1}. In the 1H NMR spectrum, aromatic protons were detected in the range of 7.88-7.14 ppm. Peaks of N=CH proton at 8.90 ppm and -CH proton in the pyrimidine ring at 8.80 ppm were marked. Also, methoxy protons were observed singly at 3.86 and 3.82 ppm, respectively. The ^{1}H NMR spectrum confirms the predicted structure of the Schiff base. (Figure 4, Supplementary Data). In the ^{13}C NMR spectrum, the signal of the benzoyl carbon for **4** was observed at 192 ppm, and the aromatic carbons were between 169-111 ppm. The data obtained because of the analyses fully confirmed the structure of Schiff bases. All analysis results are included in the supplementary data section. The synthesis scheme of compounds **3, 4** is given in Table 1.

Table 1. A synthesis scheme of compounds **3** and **4**.

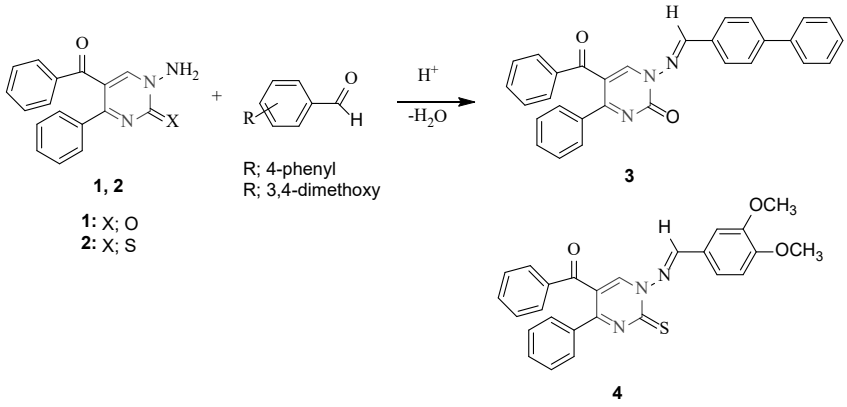

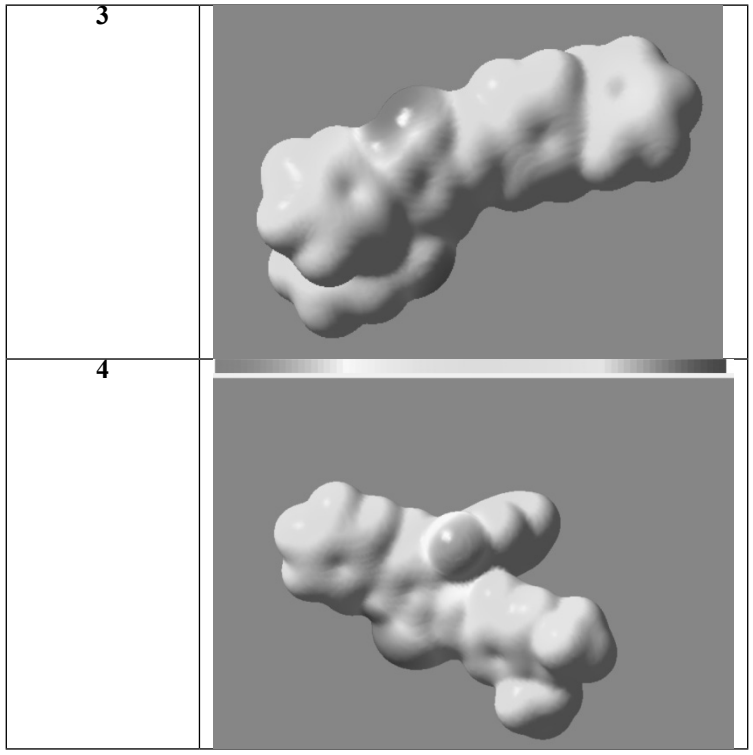

Figure 1. ESP Map of **(3)** and **(4).**

4.1. ESP Maps of 3 And 4

ESP maps provide information about the chemical activity sites and charge density of a molecule. Different colors give molecular surface electrostatic potentials. Red:

high electron density (largest solvent-dissociation interaction); blue: (low electron density)-characterizes areas suitable for nucleophilic attacks. When the ESP maps of the molecules are examined, it is seen that the electron density in the **3** molecule is concentrated on the -C=O groups. In the **4** molecule, there is a density above -C=O and -C=S. It can be concluded that the probability of chemical interaction of molecules through these areas is high. ESP maps of molecules are given in **Figure 1.**

5. Conclusions

As a result of these studies, a new series of pyrimidin-2(1H)-one/-thione derivatives **(3 and 4)** were synthesized, starting from **(1 and 2)**. Experimental techniques were extensively used to determine the structures of the novel compounds **(3 and 4)**. It was concluded that the probability of chemical interaction is high on the -C=O groups in the **3**rd molecule and on the -C=O and -C=S in the **4**th molecule.

References

Kollenz, G. (1972). Uber Reaktionen mit Cyclischen Oxalyverbindungen. *Monatshefte für Chemie*, 103: 947-950.

Altural, B., & Kollenz, G. (1998). Reactions of cyclic oxalyl compounds, Part 30:Some Reactions with N-Amino-pyrimidine Derivatives. *Monatshefte für Chemie*, 121: 677-682.

Kachroo M., Panda, R., & Yadav, Y. (2014). Synthesis and biological activities of some new pyrimidine derivatives from chalcones. *Der Pharma Chemica,* 6 (2):352-359.

Siddiqui, A. B., Trivedi, A. R., Kataria, V. B., & Shah, V.H. (2014). 4,5-Dihydro-1H-pyrazolo[3,4-d]pyrimidine containing phenothiazines as antitubercular agents. *Bioorganic & Medicinal Chemistry Letters,* 15;24:1493-1495.

Kaur, N., Aggarwal, A.K., Sharma, N., & Choudhary, B. (2012). Synthesis and *in-vitro* antimicrobial activity of pyrimidine *derivatives*. International Journal of Pharmaceutical Sciences and Drug Research, 4(3):199-204.

Goudar, V., Rashmi, P., Shantharam, U., Hazra, K., & Nargund L.G. (2012). Synthesis of novel thienopyrimidines and evaluation for their anti-inflammatory activity. *Journal* of *Chemical* and *Pharmaceutical Research*, 4(6):3100-3106.

David, V. B., Babu, V. H., & Reddy, V. M. (2014). Synthesis of novel 4,6-disubstituted-2-amino pyrimidines as antibacterial agents. *International Journal* of *Pharma* and *Chemical Research*, 3(1):2278-8700.

Ma, L., Wang, B., Pang, L., Zhang , M., Wang, S., Zheng, Y., *et al.* (2015). Design and synthesis of novel 1,2,3-triazole–pyrimidine–urea hybrids as potential anticancer agents. *Bioorganic & Medicinal Chemistry Letters,* 25:1124–1128.

Shakya, N., Vedi, S., Liang, C., Yang, F., Agrawal, B., Kumar, R., *et al.* (2014). 4'-Substituted pyrimidine nucleosides lacking 5'-hydroxylfunction as potential anti-HCV agents. *Bioorganic & Medicinal Chemistry Letters*, 24:1407–1409.

Singh, K., Kaur, H., Chibale, K., & Balzarini, J. (2013). Synthesis of 4-aminoquinoline-pyrimidine hybridsaspotent antimalarials and their mode of action studies. *European Journal of Medicinal Chemistry*, 66:314-323.

Farag, A. M., & Fahim, A. M. (2019). Synthesis, biological evaluation and DFTcalculation of novel pyrazole and pyrimidine derivatives. *Journal of Molecular Structure*, vol. 1179, 304-314.

Sahu, M., & Sıddıquı, N. (2016). A Review On Biological Importance of Pyrimidines In The New Era. *International Journal Of Pharmacy And Pharmaceutical Sciences,* 8(5), 8-21.

Gomathi, V., & Selvameena, R. (2013). Synthesis, characterization and biological studies of complexes of 3D transition metals and with Schiff base derived from sulfadiazine and 2-acetylnaphthalene. *International Journal* of *Recent Scientific Research,* 4:94-97.

Shivakumar, K., Shashidhar, P., Vithal, R. P., & Halli, M. B. (2008). Synthesis, spectral characterization and biological activity of benzofuran Schiff bases with Co(II), Ni(II), Cu (II), Zn (II), Cd (II) and Hg (II) complexes. *Journal of Coordination Chemistry,* 61:2274-2287.

Aslan, H. G., Akkoç, S. Kökbudak, Z., & Aydın, L. (2017). Synthesis, characterization, and antimicrobial and catalytic activity of a new Schiff base and its metal (II) complexes. *Journal of the Iranian Chemical Society,* 14(7), 2263-2273.

Aslan, G., Akkoç, S., Akkurt, M., Özdemir, N., & Kökbudak, Z. (2018). Synthesis, spectroscopic characterization and catalytic activity of 1-(2-hydroxybenzylideneamino)-5-(4-methylbenzoyl)-4-(4-methylphenylpyrimidin)-2(1*H*)-one. *Journal of the Chinese Advanced Materials Society,* 6(2), 145-155.

Aslan, G. Akkoç, S., & Kökbudak, Z. (2020). Anticancer activities of various new metal complexes prepared from a Schiff base on A549 cell line. *Inorganic Chemistry Communications,* 111, 107645.

Çimen, Z., Akkoç, S., & Kökbudak, Z. (2018). Reactions of Amino Pyrimidine Derivatives with Chloroacetyl and Isophthaloyl Chlorides. *Heteroatom Chemistry,* 21458, 1-6.

Aslan, G., & Önal, Z. (2014). Novel Metal Complexes, Their Spectrophotometric and QSAR Studies. *Medicinal Chemistry Research,* 23, 2596-2607.

Kökbudak, Z., Aslan, G., & Akkoç, S. (2020). New Schiff Bases Based on 1-Aminopyrimidine-2-(1*H*)-one: Design, Synthesis, Characterization and Theoretical Calculations. *Heterocycles,* 100 (3), 440-449.

Toledo, T. A., Pizani, P. S., da Silva, L. E., Teixeira, A. M. R., & Freire, P. T. C. (2015). Spectroscopy studies on Schiff base N,N'-bis(salicylidene)-1,2-phenylenediamine by NMR, infrared, Raman and DFT calculations. *Journal of Molecular Structure*, 1097: 106–111.

Ngan, N. K., Lo, K. M., & Wong, C. S. R. (2011). Synthesis, structure studies and electrochemistry of molybdenum (VI) Schiff base complexes in the presence of different donor solvent molecules. *Polyhedron*, 30(17):2922–2932.

CHAPTER 8

THE RELATIONSHIP BETWEEN GEOMETRIC DISTRIBUTION, MOMENT GENERATING FUNCTION AND PASCAL TRIANGLE APPROACH

Ege Kor[1] & Sıddık Keskin[2]

[1](Bachelor Student), Bilkent University, e-mail: ege.kor@ug.bilkent.edu.tr

[2](Prof. Dr.), Van Yuzuncu Yil University, e-mail: skeskin@yyu.edu.tr

Orcid: 0000-0001-9355-6558

1. Introduction

In daily life, determining possible outcomes of natural events and calculating their probabilities play a crucial role to reach successful or desired results in terms of controlling or directing of the events to desired way. The possibility of events is directly related to the probability distributions. In statistics, the distribution can be defined as the demonstration of scatter diagram of observed numeric values about any event and its expression with proper functions. The occurrence or outcome of these observations or numerical values can be expressed as 'probability distribution'. Probability distributions are used directly or indirectly in decision process in many areas, especially, governments, businesses and families. Probability distributions provide to obtain statistical models showing all the possible results of a certain event and the possibilities of being observed statistically for each result of the event. These models help to make scientific and conscious decisions rather than subjective decisions during the making decision process. Furthermore, in statistics, determining the distribution of data helps to determine the appropriate approaches in the analyses of data. This is because the descriptive and inferential statistic methods implemented to data having different distributions are also different. In general, the distributions are dived into two groups called discrete and continuous distributions based on whether the data are discrete or continuous. Moreover, based on these distributions, probability functions are also expressed as continuous or discrete probability functions. Discrete probability function includes many finite or countable distinct results obtained from sample space. On the other hand, continuous possibility function includes many infinite and indistinct results obtained from sample space. Whereas the distributions such as Poisson, Binomial, Negative Binomial, Geometric, and Hypergeometric are discrete distributions, Normal distribution is the most used and known continuous distribution. When the events in the nature are expressed with a variable, although creating or defining a new specialized distribution for many variables is hard or impossible, approaching one of the known distributions is likely to be possible.

Defining the distribution plays an important role in the operations regarding the distributions. Moments, characteristic functions, and cumulative distributions are used to calculate the most important two representative properties of the distribution which are expected values and variance.

In this study, general information regarding geometric distribution is given and the approach that can be used to calculate expected value and variance of the geometric distribution when the outcome variables are 3 or more (k different possible outcomes when k is a positive integer greater than 3) cases, is explained and a new method is expressed to find the result of moment generating function for geometric distribution.

2. Geometric Distribution

In the nature, the events whose possible outcomes can only represent with two categories such as 'yes-no', 'healthy-patient', 'success-failure', 'alive-dead' and 'head-tail' are named as binary outcome. When we trial those cases just for one time, this experiment is called as Bernoulli process. With regarding this, the experiment of tossing a coin has two possible outcomes which are head and tail, thus, tossing a coin just one time is named as Bernoulli trial. In order to separate these two possible outcomes from each other, one of these results is named as 'success' whereas the other one is called as 'failure'. Which case or result is named as 'success' is the prefer of the researcher.

Geometric distribution which is in the group of discrete distributions is directly related to Bernoulli distribution and experiment (Bulut, 2020). In Geometric distribution, there are two possible outcome categories too, or the number of categories can be reduced to two categories in case of more than two. Geometric distribution computes the probability of observing the first success in n^{th} trials. The probabilities of 'success' and 'failure' are 'p' and '(1-p)' or 'q', respectively. Thus, $p + q = 1$ due to Bernoulli trial (Anonymous, (2021a)

When the probability of observing the first success in the n^{th} trial is calculated, this means that all first 'n-1' trials result in failure. According to this assumption, '$q^{n-1}p$' represent the probability of the first 'success' result occurs in the n^{th} trial. This representation is slightly different from Binomial representation because it has no combination operation before the expression. This is because all first 'n-1' tries are clearly failure and there is no change in ordering of these cases.

Apart from the last 'success' trial, there are one or more Bernoulli trials resulted in failure. In other words, the researcher continues to trial until reaching the first success. After reaching the first success, the experiment is ended. Theoretically, there must be at least one trial to reach "success" however the number of trial can be infinitely. Each trial is independent from each other and the probability of 'success' is 'p' and failure is 'q' is constant for each trial and they do not change from trial to trial.

Geometric distribution can be expressed as the distribution of the probability of obtaining the first 'success' in X different Bernoulli trials, or it can be expressed as the distribution of probability of the fact that the number of failure Y=X-1 before obtaining the first success.

If the probability of getting 'success' for each trial is 'p', the probability of obtaining success in k^{th} trials is written as;

Pr (X=k)= $\llbracket(1\text{-}p)^{k\text{-}1}p$ [k = 1, 2, 3, …, n]

For the random variable, X showing Geometric distribution, the expected value is $E(X) = \frac{1}{p} E(X) = \frac{1}{p}$ and the variance is $Var(X) = \frac{1-p}{p^2} Var(X) = \frac{1-p}{p^2}$ (Anonymous, (2021b)

When the researcher assumes that he or she plays a game of tossing a coin and ends the game when he or she gets heads for the first time, or when a family continues to make a child until reaching a girl, or when a company continues to bore until reaching petrol, or when a firm continues to dig until finding mine, the expected value and variance calculation can be expressed as seen below.

Let us assume that 'H' represents 'success' (Head for tossing coin trial), and 'T' represents 'failure' (Tail for tossing coin trial). P_k represents the probability of obtaining the 'success' for the first time in the k^{th} trial.

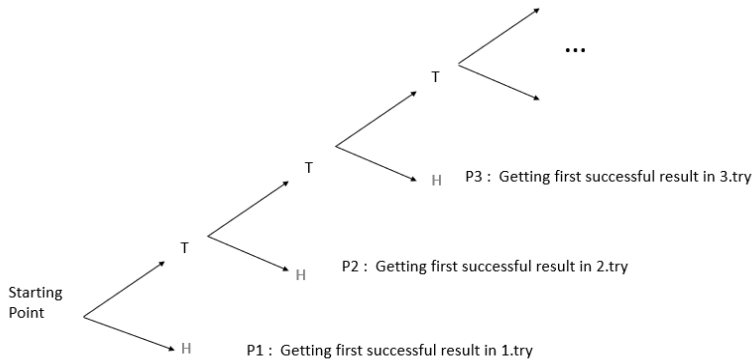

$$P1 = \frac{1}{2}$$

$$P2 = \frac{1}{2} \times \frac{1}{2}$$

$$P3 = \frac{1}{2} \times \frac{1}{2} \times \frac{1}{2}$$

$$\dots$$

$$P_k = \frac{1}{2^k}$$

In this case, expected value and the variance can be computed as follows:

$$E[x] = \sum_{k=1}^{\infty} k \times P_k = \sum_{k=1}^{\infty} \frac{k}{2^k} = K_1 = 2$$

$$Var(x) = E[x^2] - E[x]^2 = \sum_{k=1}^{\infty} \frac{k^2}{2^k} - 4 = K_2 - 4 = 6 - 4 = 2$$

If the number of possible different results become 3 (not 2 like in the previous example), and the probability of success (p) is constant for each trial, the calculations for the probability of observing the success (case number 1 in this example) in k^{th} trial can be performed as follows:

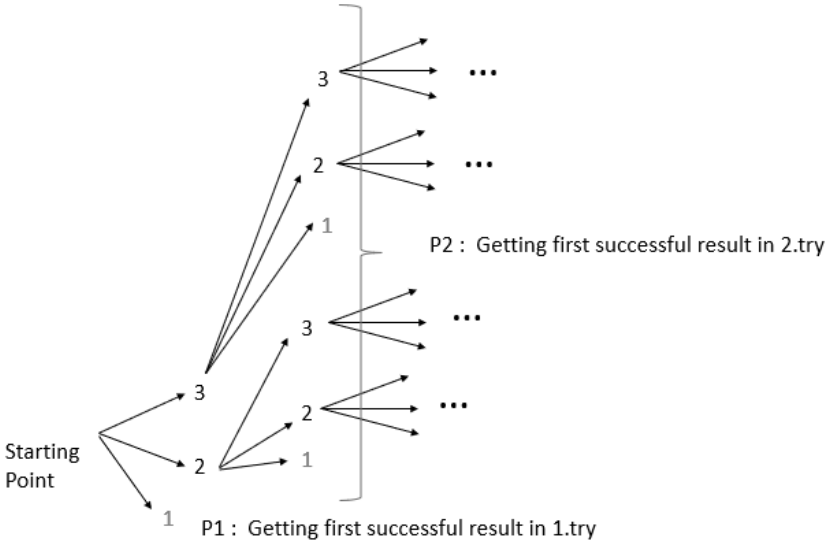

$$P1 = \frac{1}{3}$$

$$P2 = 2 \times \left(\frac{1}{3} \times \frac{1}{3}\right)$$

...

$$P_k = \frac{1}{2} \times \left(\frac{2}{3}\right)^k$$

In this example, there is a recursive relation among infinitely many cases and the addition of their probability is required. In the previous examples, for the expected value and variance calculations, it is required to write the multiplication of P_k and k or k^2 in the summation symbol, sigma. However, for some cases, the question of the term multiplied with P_k be k^n may considered. Under this condition, moment can be used however this requires to know some calculus knowledge integral and derivative. The relationship among calculation steps can also be represented by using the Pascal Triangle and a recursive relationship can be set among steps. In order to organize this new relationship among calculation steps, we need a new variable called K_n as seen below.

$$K_n = \sum_{k=1}^{\infty} \frac{k^n}{2^k}$$

As mentioned before, in order to reach more generalized case as represented in the example with 3 possible results, when a second variable is defined called 'p' such that 0<p≤ 1≤ 1, it represents the probability of 'success'.

$$K_n = \sum_{k=1}^{\infty} k^n p^k$$

When we consider the Pascal Triangle and the variables defined above, we can set a simple system without using integral or derivative in order to find the values of these variables. Let us observe this idea with p = $\frac{1}{2}\frac{1}{2}$ at first.

$K_0 = \sum_{k=1}^{\infty} \frac{1}{2^k} = \frac{1}{2} \cdot \frac{1}{1-\frac{1}{2}} = 1$

Thus, $K_0 = 1$

$K_1 = \sum_{k=1}^{\infty} \frac{k}{2^k}$

$$\sum_{k=1}^{\infty} \frac{k}{2^k} = \frac{1}{2} + \sum_{k=2}^{\infty} \frac{k}{2^k} = \frac{1}{2} + \sum_{k=1}^{\infty} \frac{k+1}{2^{k+1}}$$

$$= \frac{1}{2} + \frac{1}{2}\sum_{k=1}^{\infty} \frac{k}{2^k} + \frac{1}{2}\sum_{k=1}^{\infty} \frac{1}{2^k} = 1 + \frac{1}{2}\sum_{k=1}^{\infty} \frac{k}{2^k}$$

$$\rightarrow \sum_{k=1}^{\infty} \frac{k}{2^k} = 2$$

Thus, $K_1 = 2$ $K_2 = \sum_{k=1}^{\infty} \frac{k^2}{2^k}$

$$\sum_{k=1}^{\infty} \frac{k^2}{2^k} = \frac{1}{2} + \sum_{k=2}^{\infty} \frac{k^2}{2^k} = \frac{1}{2} + \sum_{k=1}^{\infty} \frac{(k+1)^2}{2^{k+1}} = \frac{1}{2} + \frac{1}{2}\sum_{k=1}^{\infty} \frac{k^2+2k+1}{2^k}$$

$$= \frac{1}{2} + \frac{1}{2}\sum_{k=1}^{\infty} \frac{k^2}{2^k} + \frac{1}{2}\sum_{k=1}^{\infty} \frac{2k}{2^k} + \frac{1}{2}\sum_{k=1}^{\infty} \frac{1}{2^k}$$

Let say $A = \sum_{k=1}^{\infty} \frac{k^2}{2^k}$, then

$$A = \frac{1}{2} + \frac{A}{2} + 2 + \frac{1}{2} \rightarrow A = 6 \rightarrow \sum_{k=1}^{\infty} \frac{k^2}{2^k} = 6$$

Thus, $K_2 = 6$

Let's define $K_n = \sum_{k=1}^{\infty} \frac{k^n}{2^k}$, then;

$$K_n = \sum_{k=1}^{\infty} \frac{k^n}{2^k} = \frac{1}{2} + \sum_{k=1}^{\infty} \frac{(k+1)^n}{2^{k+1}} = \frac{1}{2} + \frac{1}{2}\sum_{k=1}^{\infty} \frac{(k+1)^n}{2^k}$$

$$= \frac{1}{2} + \frac{1}{2}\sum_{k=1}^{\infty} \frac{\binom{n}{n}k^n + \binom{n}{n-1}k^{n-1} + \cdots + \binom{n}{1}k^1 + \binom{n}{0}k^0}{2^k}$$

$$= \frac{1}{2} + \frac{1}{2}\left(\binom{n}{n}K_n + \binom{n}{n-1}K_{n-1} + \cdots + \binom{n}{1}K_1 + \binom{n}{0}K_0\right)$$

$$K_n = 1 + \binom{n}{n-1}K_{n-1} + \cdots + \binom{n}{1}K_1 + \binom{n}{0}K_0$$

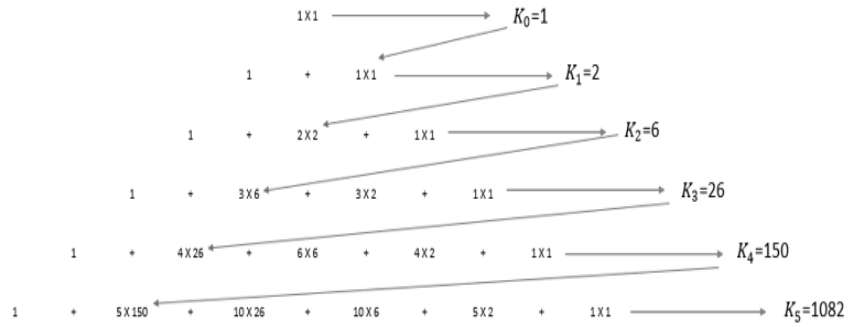

After calculating the values of K_n variables for n = 0, 1, 2, 3, 4, and 5, we can find the following values.

$K_0 = 1$, $K_1 = 2$, $K_2 = 6$, $K_3 = 26$, $K_4 = 150$, $K_5 = 1082$

Let us say $K_n = \sum_{k=1}^{\infty} k^n p^k$ such that $0 \leq p < 1$, then;

$$K_n = \sum_{k=1}^{\infty} k^n p^k = 1^n p^1 + \sum_{k=2}^{\infty} k^n p^k = p + \sum_{k=1}^{\infty} (k+1)^n p^{k+1}$$

$$= p + p\sum_{k=1}^{\infty} p^k (k+1)^n$$

$$= p + p\left(\sum_{k=1}^{\infty}\binom{n}{n}k^n p^k + \sum_{k=1}^{\infty}\binom{n}{n-1}k^{n-1}p^k + \cdots + \sum_{k=1}^{\infty}\binom{n}{0}k^0 p^k\right)$$

$$K_n = p + p\left(\binom{n}{n}K_n + \binom{n}{n-1}K_{n-1} + \cdots + \binom{n}{1}K_1 + \binom{n}{0}K_0\right)$$

$$K_n = \frac{p}{1-p} + \frac{p}{1-p}\left(\binom{n}{n-1}K_{n-1} + \cdots + \binom{n}{1}K_1 + \binom{n}{0}K_0\right)$$

$$K_n = \frac{p}{1-p}\left(1 + \sum_{i=1}^{n}\binom{n}{i-1}K_{i-1}\right) \quad for\ n \geq 1\ and\ K_0 = \sum_{k=1}^{\infty} p^k$$

$$= \frac{p}{1-p}$$

$$K_1 = \frac{p}{1-p}\left(1 + \binom{1}{0}K_0\right) = \frac{p}{1-p}\left(1 + \frac{p}{1-p}\right)$$

$$= \frac{p}{1-p} + \frac{p^2}{(1-p)^2}$$

$$K_2 = \frac{p}{1-p}\left(1 + \binom{2}{1}K_1 + \binom{2}{0}K_0\right)$$

$$= \frac{p}{1-p}\left(1 + \frac{2p}{1-p} + \frac{2p^2}{(1-p)^2} + \frac{p}{1-p}\right)$$

$$= \frac{p}{1-p} + \frac{3p^2}{(1-p)^2} + \frac{2p^3}{(1-p)^3}$$

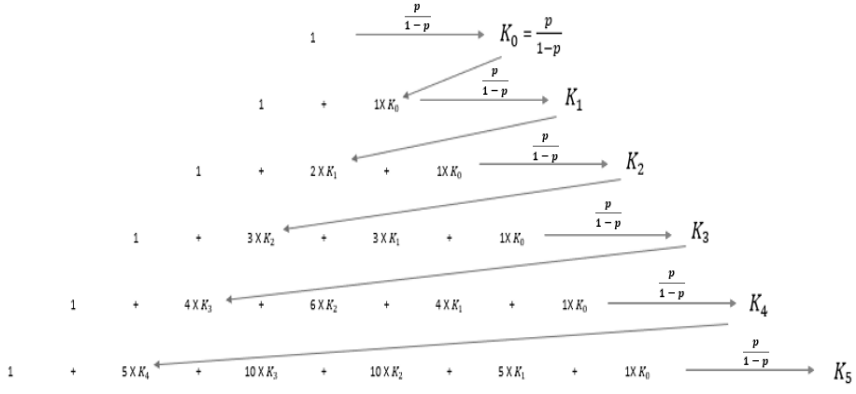

3. Pascal Triangle Approach (PTA)

The transform associated with a random variable X that can also be named as associated moment generating function, is a function shown as $M_X(s)$ This function is of a scalar parameter s and it is defined by using expectation.

$$M_X(s) = E[e^{sX}]$$

By using simpler notation;

$$M(s) = \sum_x e^{sx} p_X(x)$$

While in the continuous case, the equation changes slightly.

$$M(s) = \int_{-\infty}^{\infty} e^{sx} f_X(x)\, dx$$

The moment is defined by using transform concept. This is because the transform is called as moment generating function. The n^{th} moment refers to $E[X^n]E[X^n]$, thus the moment can be calculated as follows:

$$\frac{d^n}{ds^n} M(s)|_{s=0} = \int_{-\infty}^{\infty} x^n f_X(x)\, dx = E[X^n]$$

More generally, also for discrete cases, the moment can be defined as following.

$$\frac{d^n}{ds^n} M(s)|_{s=0} = E[X^n]$$

When we consider the Geometric distribution, if the possibility is defined as $p_X(k) = p(1-p)^{k-1} p_X(k) = p(1-p)^{k-1}$ where k =1, 2, … then the moment generating function is defined as the following;

$$M_X(s) = \frac{pe^s}{1-(1-p)e^s}$$

In order to figure out the relation between our approach clarified in this article and the moment concept, firstly, let us assume that the probabilities of 'success' and "failure" are "(1-p)" and "p", respectively. There are two possible outcomes for each trial, then, the probability can be calculated by $p_X(k)=p^{k-1}(1-p)$. Thus, the expected value of k^n is defined as shown below.

$$E[k^n] = \sum_{k=1}^{\infty} k^n p^{k-1}(1-p) = \frac{1-p}{p} \sum_{k=1}^{\infty} k^n p^k$$

Thus, the moment generating function is defined as;

$$M_k(s) = \frac{(1-p)e^s}{1-pe^s}$$

By using the moment generating function, moment definition and the variable we defined previously called K_n, we can see the relation among them as shown below [4]. In order to figure out the relation, we assume that the probability of the 'success' is p for K_n calculations and "1-p" for moment calculations with two possible results in each trial for both cases.

$$K_n = \sum_{k=1}^{\infty} k^n p^k = \frac{p}{1-p} E[k^n] = \frac{p}{1-p} \frac{d^n}{ds^n} M_k(s)|_{s=0}$$

Thus, K_n can also be defined by using n^{th} derivative as follows:

$$K_n = p \frac{d^n}{ds^n}\left(\frac{e^s}{1-pe^s}\right)|_{s=0}$$

When we compare the approach clarified in this article with the method using moment generating function, there are some points taking attention. First of all, the method of moment generating function requires taking n times derivative and, in each step, taking derivative with hand becomes harder compared to the previous step.

For example, to find K_2;

If we use the method using moment generating function;

$$\begin{aligned}\frac{d^2}{ds^2}\left(\frac{e^s}{1-pe^s}\right) &= \frac{d}{ds}\left(\frac{e^s}{1-pe^s} + pe^{2s}(1-pe^s)^{-2}\right) \\ &= \left(\frac{e^s}{1-pe^s} + pe^{2s}(1-pe^s)^{-2}\right. \\ &\quad \left. + 2pe^{2s}(1-pe^s)^{-2} + 2p^2e^{3s}(1-pe^s)^{-3}\right) \\ &= \frac{e^s}{1-pe^s} + 3pe^{2s}(1-pe^s)^{-2} \\ &\quad + 2p^2e^{3s}(1-pe^s)^{-3} \\ &= \frac{e^s}{1-pe^s} + 3p\left(\frac{e^s}{1-pe^s}\right)^2 + 2p^2\left(\frac{e^s}{1-pe^s}\right)^3\end{aligned}$$

$$K_2 = p \frac{d^2}{ds^2}\left(\frac{e^s}{1-pe^s}\right)|_{s=0} = \frac{p}{1-p} + \frac{3p^2}{(1-p)^2} + \frac{2p^3}{(1-p)^3}$$

(Bertsekas and Tsitsiklis, 2008).

On the other hand, by using Pascal Triangle Approach (PTA);

$$K_0 = \frac{p}{1-p} \times 1 \rightarrow K_1 = \frac{p}{1-p}\left(1 + \binom{1}{0}K_0\right)$$
$$= \frac{p}{1-p} + \frac{p^2}{(1-p)^2}$$
$$K_2 = \frac{p}{1-p}\left(1 + \binom{2}{1}K_1 + \binom{2}{0}K_0\right)$$
$$= \frac{p}{1-p}\left(1 + \frac{2p}{1-p} + \frac{2p^2}{(1-p)^2} + \frac{p}{1-p}\right)$$
$$= \frac{p}{1-p} + \frac{3p^2}{(1-p)^2} + \frac{2p^3}{(1-p)^3}$$

Even finding K_2, it can be seen that using Pascal Triangle is shorter and easier method compared to the method using moment generating function. When we consider K_n values for greater n values like 4, 5 or 6, the method using moment generating function becomes harder and harder. Moreover, it requires taking derivatives in 4, 5 or 6^{th} order that means it is likely to calculation errors if the calculations are made by hand. Furthermore, the method using moment generating function requires calculus knowledge for taking high derivatives with exponential equations. On the other hand, Pascal Triangle Approach (PTA) just uses addition operator. It becomes considerably shorter for greater values of n. Furthermore, it does not include exponential equations. The method using moment generating function takes n^{th} order derivate and it does not finish yet. After finishing taking derivatives, it takes s = 0 and it makes some calculations. In the final step it multiplies the expression with p. However, Pascal Triangle Approach (PTA) does not include any equations, or variables. It only includes p representing the possibility. Thus, it just makes simple calculations because there is not any equation using variables in Pascal Triangle Approach (PTA).

4. Conclusion

When we consider the speed and easiness of Pascal Triangle Approach (PTA), this method can be preferred to the method using moment generating functions while finding K_n. Additionally, finding the moments, by using Pascal Triangle Approach (PTA) is also possible. K_n is found at first by using Pascal Triangle Approach (PTA), then by using the relation between K_n and the n^{th} moment, $\frac{1-p}{p}K_n = E[k^n]$ $\frac{1-p}{p}K_n = E[k^n]$, the moment can also be calculated easily, without taking any derivative thanks to Pascal Triangle Approach (PTA). Thus, Pascal Triangle Approach (PTA) is faster and easier method compared to the method using moment generating function and it can also help to find moments in an easier and faster way.

References

Anonymous, (2021a) "Geometric Distribution Introduction to Statistics" *courses.lumenlearning.com*. https://courses.lumenlearning.com/introstats1/chapter/geometric-distribution/ (accessed Sep. 14, 2021).

Anonymous, (2021b) "Geometric Distribution | Brilliant Math & Science Wiki," *brilliant.org*. https://brilliant.org/wiki/geometric-distribution/.

Bertsekas, D.P. & Tsitsiklis, J.N., (2008). *Introduction to probability*. Belmont, Mass.: Athena Scientific, Athena, Greece.

Bulut, T (2020) "Geometrik Olasılık Dağılımı Üzerine Bir Vaka Çalışması: A Case Study on Geometric Probability Distribution," , Aug. 25, 2020. https://tevfikbulut.com/2020/08/25/geometrik-olasilik-dagilimi-uzerine-bir-vaka-calismasi-a-case-study-on-geometric-probability-distribution/ (accessed Sep. 14, 2021).